The Neural Correlates of Vection: an fMRI study

Ramy Kirollos

A Thesis Submitted to the Faculty of Graduate Studies In Partial Fulfillment of the Requirements for the Degree of Master of Arts

Graduate Program in Psychology

York University

Toronto, Ontario

November 2014

©Ramy Kirollos, 2014

Abstract

Vection is an illusion of visually-induced self-motion in a stationary observer. I used different types of vection stimuli in a functional magnetic resonance imaging (fMRI) study to determine the interaction between cortical visual regions and cortical vestibular regions during vection. My findings suggest that the cingulate sulcus visual area is heavily involved in self-motion processing. The parieto-insular vestibular cortex, showed a significant change in blood oxygenation level dependent signal activity during vection but to a lesser extent than CSv. Behavioural data correlated with the neuroimaging data (in CSv and PIVC) as both show a significant difference when comparing the radial oscillating condition to the radial smooth condition in CSv and PIVC - suggesting a neural correlate of the jitter effect. My results suggest that the brain region of primary importance in the self-motion debate is CSv - a region that has received little attention in the vection literature to date.

Keywords: Vection; optic flow; fMRI; BOLD; visual-vestibular integration; CSv; PIVC; MT; VIP; Pc; V6; jitter

Acknowledgements

I would like to thank the many people involved in this project that have assisted me in the various phases of this Master's thesis. Namely, Dr. Rob Allison my thesis supervisor, for his expertise, mentorship and encouragement, Dr. Keith Schneider, Aman Ish Goyle, and Joy Williams for their expertise and unwavering assistance in the research design, data analysis and MRI operation throughout the project, Dr. Steve Palmisano who served as a mentor and proof-read my document numerous times to provide critical feed-back, importantly my wife, parents and friends who encouraged me during this time period, my defense committee members Dr. Laurence Harris and Dr. Minas Spitsakis for their participation and feedback, the research assistants that facilitated this project; Mariam Sardar, Carly Hylton and Suzette Fernandez and the late Dr. Ian Howard for always serving as inspiration. I would also like to thank NSERC for funding this project through the CREATE program for applications in vision science and York U for providing me with pilot hours in the MRI and supplemented funding.

Table of Contents

List of Tables

List of Figures

List of Acronyms

BOLD Blood oxygenation level-dependent

CSv Cingulate sulcus visual area

CV Circular vection

EC Egomotion-compatible

EEG Electroencephalography

EI Egomotion-incompatible

EV Explanatory variable

fMRI Functional magnetic resonance imaging

FOV Field of view

FWHM Full-width half maximum

GLM General linear model

GVS Galvanic vestibular stimulation

HRF Hemodynamic response function

LIP Lateral intraparietal region

ME Magnitude estimation

MEG Magnetoencephalography

MIP Medial intraparietal region

MNI Montreal neurological institute

MST+ Medial superior temporal complex

MT+ Medial temporal complex

Pc Precuneus (referred to as precuneus visual area)

PET Positron emission tomography

PIVC Parieto-insular vestibular cortex

POs Parieto-occipital sulcus

RFT Random field theory

ROI Region of interest

SCC Semi-circular canal

TE Echo time

TMS Transcranial magnetic stimulation

TR Repetition time

VEP Visually evoked potential

VIP Ventral intraparietal region

1. Introduction

1.1 - Introduction to Vection

We receive many cues that make us constantly aware of our active or passive self-motions through the environment. These include visual cues such as the global optic flow during self-motion (Helmholtz, 1867/1925; Gibson, 1964), vestibular cues that indicate direction of passive and active acceleration of the head (Howard, 1982), as well as proprioception/somatosensory cues (Lishman and Lee, 1973) and kinesthesia.

Vection is an illusion of visually-induced self-motion in a stationary observer. An example of vection is when an individual on a stationary train watches an adjacent train moving past them but feels as though he/she is moving (Mach, 1875). Vection occurs because the optic flow sensed when a stationary individual observes a moving adjacent train is similar to real self-motion past a stationary adjacent train.

In this illusion there is a conflict between the visual system receiving stimulation indicating self-motion and other sensory systems indicating one is not moving (Reason, 1978). It is important to understand the sensitivity of the sensory systems involved in processing self-motion, particularly the visual and vestibular systems as these are the most critical for self-motion processing. The visual system is most sensitive in processing constant velocity self and object motion (Previc, 2003). On the other hand, the vestibular system is sensitive to passive and active acceleration of the head (Howard, 1982). Unlike the visual system, the vestibular system is unable to differentiate constant velocity motion from being stationary (Lishman and Lee, 1973). The strengths and weaknesses of both these systems reflect their anatomical and physiological properties.

1.2 – Anatomical and Physiological Properties of Visual and Vestibular Systems in Relation to Optic Flow, Object Motion, and Self-Motion

The Visual System

In humans, visual motion signals begin to be processed cortically in V1, the most posterior region of the occipital cortex and are relayed to higher-level visual processing regions of the occipital, parietal, and temporal lobes specialized for egomotion/self-motion and coherent motion processing. These brain regions include but are not limited to the medial temporal gyrus (MT/V5), medial superior temporal region (MST+), V6, cingulate sulcus visual area (CSv), precuneus motion area (Pc) as well as parieto-occipital regions parieto-insular vestibular cortex (PIVC) and ventral intraparietal region (VIP). The relative motion pattern produced by a moving observer is known as the optic flow (Gibson, 1964). During forward self-motion, the images of objects in the scene radiate from the focus of expansion which lies in the direction of the travel, assuming no rotation.

The Vestibular Peripheral System

The peripheral vestibular apparatus is located in the bony labyrinth of the inner ear. The vestibular apparatus has two main structures that detect acceleration. These structures are the otolith organs and the semi-circular canals (SCCs). The otolith organs of each ear consist of two separate sensors - the saccule and the utricle. These respond to linear acceleration from translational self-motion and gravity. The semi-circular canals respond to angular acceleration. The three orthogonal canals and the pair of otolith

organs in each inner ear create a 3-dimensional configuration that permits detection of head acceleration with six degrees of freedom.

The SCCs are filled with endolymph fluid and are blocked by the cupular membrane in which hair cells are embedded. When the head moves, the endolymph fluid lags, causing mechanical pressure/movement of the cupula sensed by the hairs cells in the sensory endothelium. Bending of the stereocilia causes K+, Ca++ and Cl- graded ion channel currents. Once there is a strong enough graded response from the ion channel currents, the vestibulocochlear (8^{th}) cranial nerve is stimulated, signaling head motion (Cohen and Raphan, 2004). In the otolith organs, the otoconia are salt crystals that move when the head moves.

Vestibular signals are cortically processed in the parietoinsular vestibular cortex (PIVC) and ventral intraparietal region (VIP). Recently these areas have been identified in imaging experiments during stimulation of the peripheral vestibular system. To stimulate PIVC, methods such as caloric stimulation, which stimulates the semicircular canals with thermal gradients, and galvanic vestibular stimulation (GVS), which uses electric currents to stimulate the 8th nerve, have been employed. According to Fasold et al.(2002), GVS does not allow distinct and clear stimulation of vestibular organs independently, instead the entire vestibular apparatus is activated simultaneously. This creates neural noise and increased variability in corresponding BOLD signals during fMRI. Alternatively, caloric irrigation permits clear and direct stimulation of the horizontal semicircular canals independently when in the supine posture.

Fasold and colleagues (2002) located PIVC in the posterior insula, and reported that posterior insular BOLD signal increases were significant when caloric stimulation

evoked disorientation. Insular BOLD increases were stronger in the right hemisphere. This asymmetry in BOLD signal change in the insular gyrus replicated findings of Suzuki and colleagues (2001). An important point to note is that these two caloric irrigation studies in fMRI stimulated different regions in the insula. Additionally, Fasold et al., reported that insular stimulation by caloric irrigation results indicated that many independent clusters in the insular gyrus were stimulated.

1.3 – Cortical Regions Related to Vection

Medial Temporal Complex (MT+)

Area MT+ is the cortical region most widely accepted as being involved in processing general visual coherent motion. Many studies have reported its preference for coherent motion compared with incoherent motion or static stimulus displays in both humans and monkeys. Studies on visual motion processing in monkeys' area MT (Rodman, 1989) were extended to humans by Zeki and colleagues (1991) and Watson et al. (1993). They observed a visual motion sensitive region homologous to monkeys V5/MT using PET in humans. Zeki found that V5/MT prefers motion over stationary stimuli. Tootell et al., (1995) replicated the findings of Zeki on area MT in fMRI and confirmed the same spatial coordinates for MT as Zeki.

Importantly, in an fMRI Morrone et al. (2000) reported that V5/MT is activated by changes in optic flow, and to continuous translation. Huk and Heger (2001) concluded that MT in humans has pattern motion cells that prefer perceived coherent motion compared with incoherent motion, but did not specify the spatial coordinates of this region in their study in fMRI. Similar to Morrone et al., Pitzalis et al (2013) reported

greater activity in MT+ for translational, and looming egomotion displays than for spiraling egomotion displays.

Medial Superior Temporal Region (MST+)

MST+ (see Figure 1), a subregion of MT+, has neurons with larger receptive fields than the rest of MT+, (Pitzalis et al., 2013). In attempt to functionally localize MST+, Pitzalis and colleagues argued that a stimulus that restricts optic flow to an aperture in the left or right hemifield should show increased BOLD activity in the contralateral hemifield only for area MT+, but for both the contralateral and ipsilateral hemifields for area MST+ because of the neurons in this region have larger receptive fields. To test this hypothesis, Pitzalis et al. developed a hemifield-specific stimulus. As hypothesized, they found higher activation in MST+ for ipsilateral displays than in MT+, whereas MT+ only responded to motion in the contralateral hemifield. Thus, MST+ responds to visual motion in both contralateral and ipsilateral hemifields, whereas MT+ is sensitive only to motion in the contralateral hemifield. This finding suggests that MST+ is functionally and anatomically defined independently within the wider MT+ complex.

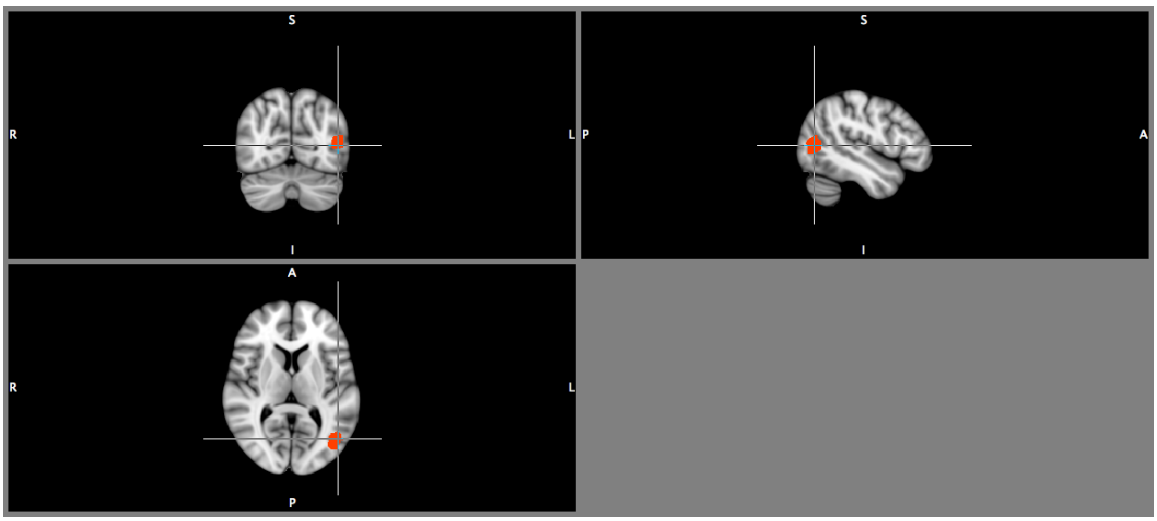

Figure 1. MST+ is shown in orange in coronal (top-left), sagittal (top-right) and axial (bottom-left) slices of the right hemisphere in an MNI standard brain. Coordinates are based on findings of Pitzalis et al., (2013).

Precuneus Motion Area (Pc)

The precuneus is located in the posterior, medial region of the parietal lobe (see Figure 2). Cavanna and Timble (2006) reported precuneus involvement in cognitive functions related to consciousness, episodic memory and visuo-spatial imagery. In relation to vection, Wolbers et al., (2007) conducted an fMRI study in which they reported heightened BOLD signal in Pc during path-integration - a cognitive task that may require self-orientation updating. In a later study, Wolbers et al., (2008) expanded on the functional role of Pc during vection and concluded that Pc is involved in subserving spatial updating. Later studies also show increased BOLD activity in Pc during egomotion-compatible, and decreased BOLD activity with egomotion-incompatible stimuli (Cardin and Smith, 2010; Billington et al., 2013) and report roughly the same spatial coordinates. Therefore, it seems likely that Pc is not explicitly involved in perceiving self-motion, but rather higher-level cognitive aspects of vection processing.

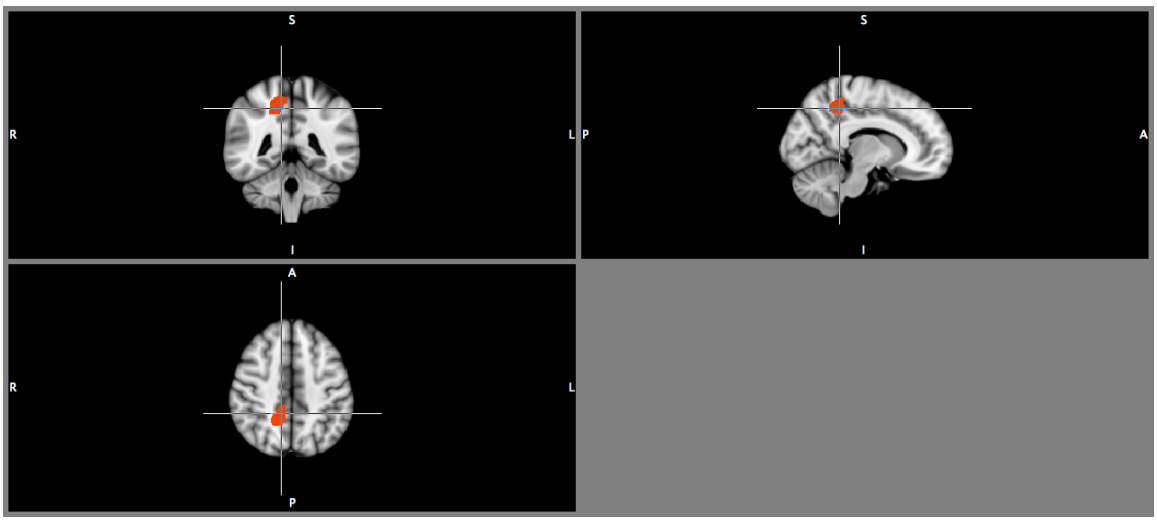

Figure 2. MNI standard image of Pc in left hemisphere. Coordinates based on Wolbers et al., (2008)

V6

Pitzalis and colleagues confirmed that the human homologue to monkey V6 is located posterior to the dorsal end of the parieto-occipital sulcus (see Figure 3; POs; Pitzalis et al., 2013). There is variability in explaining the precise functional role of V6 as some studies show that V6 is sensitive to translational egomotion and is thought to be involved in visually-guided motor control and distinguishing visually-induced self-motion from object motion (Pitzalis et al., 2010). Other studies have suggested that it is involved in obstacle avoidance (Cardin et al., 2012) and others still reporting its importance for estimating egomotion (Pitzalis et al., 2013). Pitzalis and colleagues (2013) compared BOLD response to five types of optic flow; translational, circular, radial, spiral, as well as random motion and static dots. They found that % BOLD signal change in V6 was largest for translational optic flow displays compared to circular, radial, spiral, random motion, or static dots.

A functional difference distinguishing MT+ from V6 is that MT+ prefers flow in the center of fixation, whereas V6 is preferentially activated by wide-field stimulation (Pitzalis, et al., 2006). Another difference between MT+ and V6 is that V6 is believed to be retinopically organized while MT+ is not. However, there is still disagreement on this point (Pitzalis et al., 2013). Research comparing V6 function to MT+ (VonPfostl et al., 2009; Ciavarro, M., 2013) suggests that V6 may be involved in motor activity linked to obstacle avoidance or grasping near-by objects. This hypothesis is supported by the fact that area V1 and V6 seem to show almost identical BOLD activity onset times to visual motion stimuli. This lends support to the notion that V6 is involved in 'online' processing of visually guided behaviour (Galetti et al, 2001). Alternatively, the time course of a visually evoked potential (VEP) in electroencephalography (EEG) signal change to visual motion stimuli in both MT and V6 are very similar during obstacle avoidance tasks (Pitzalis et al., 2013). This suggests that MT is also involved in obstacle avoidance, or that neither V6 nor MT are involved in obstacle avoidance.

Although V6's function is not yet clearly defined, the dominant view is that it is involved in 1) processing wide-field visual stimulation, 2) disambiguating different types of optic flow, and 3) visually-guiding motor control. Moreover, there is a functional distinction made between V6, and neighbouring V6a in which activity is driven by pointing and reaching and is located in the anterior bank of the parieto-occipital lobe (Pitzalis et al., 2013).

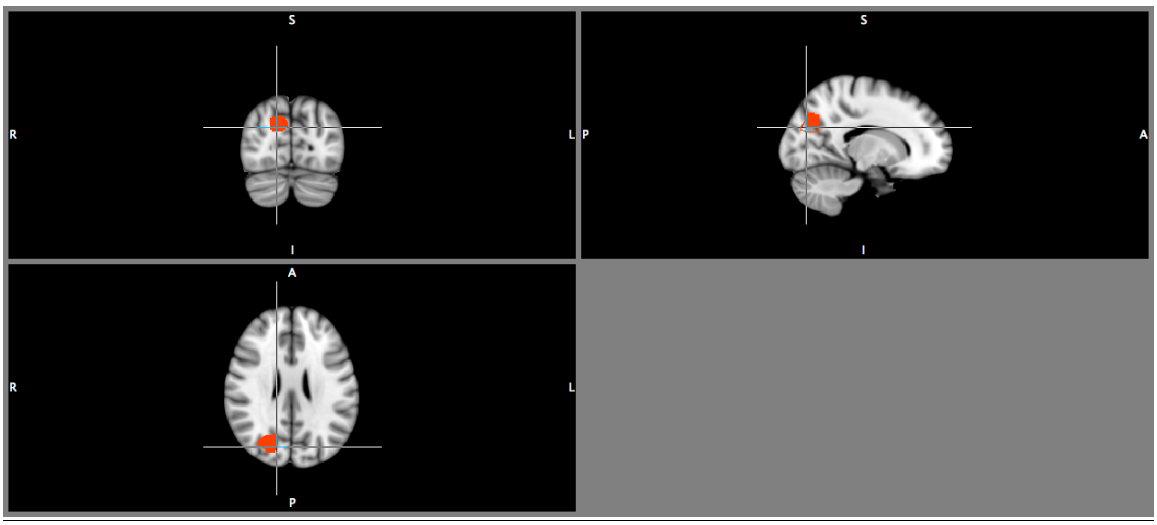

Figure 3. V6 displayed in MNI standard space in the left hemisphere. Coordinates taken from Wall and Smith (2012).

VIP

The ventral intraparietal region (VIP) in macaques is regarded as a polysensory region because it responds to visual, (see Figure 4; Shaafsma and Duysens, 1996) vestibular and somatosensory stimuli (Duhamel et al., 1998). In a fMRI study, Bremmer et al., (2001) functionally localized VIP visually, using optic flow in the frontal plane. Later studies also confirmed visual sensitivity of VIP (Cardin and Smith, 2010; Smith et al., 2012), but reported slightly different coordinates for this region. Vestibular stimulation during fMRI in humans suggests that VIP is not a vestibular processing region (Fasold et al., 2002). Notably, Fasold's group (2002) functionally localized vestibular regions in humans by stimulating the inner ear with cold nitrogen calorics in fMRI. Fasold and colleagues' results point to strong involvement of PIVC in vestibular processing of caloric stimulation, but not VIP. Similarly in an fMRI study, Eickhoff and colleagues (2006) showed a significant change in BOLD activity compared to baseline in

the parieto-insular cortex (approximating PIVC), but not in VIP, during galvanic vestibular stimulation.

In sum, VIP in humans does not seem to be directly activated by vestibular stimulation (Fasold, et al., 2002; Eickhoff et al., 2006; Pitzalis et al., 2013). Therefore, rather than a general polysensory integration area for self-motion signals, VIP could be principally involved in visually-guided obstacle avoidance.

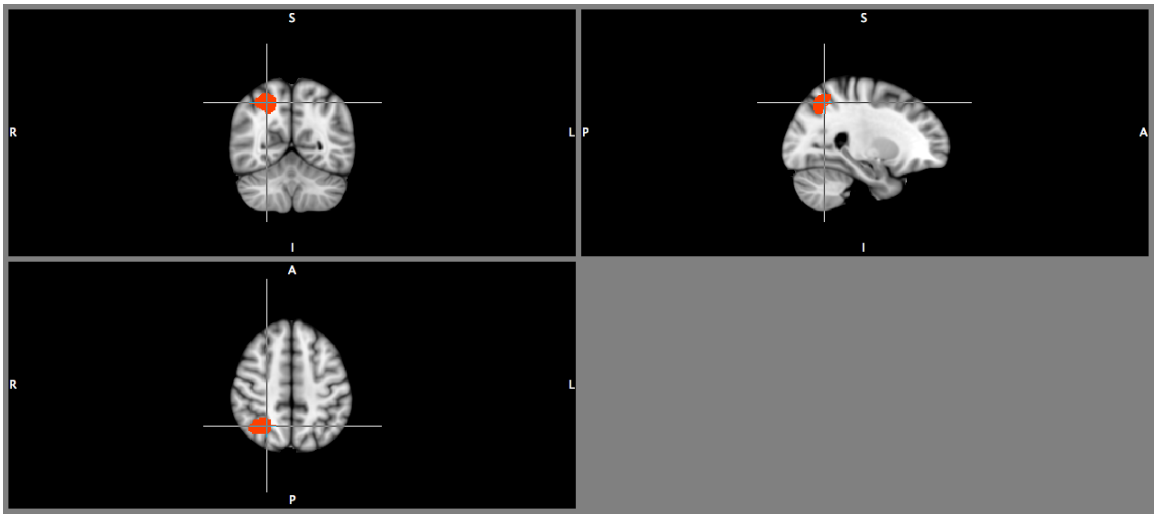

Figure 4. Area VIP highlighted using coordinates from Cardin and Smith (2010) in MNI standard brain.

Cingulate Sulcus Visual Area (CSv)

CSv is the cortical region reported to be involved in heading estimation and anatomically separates the boundaries of the parietal and occipital lobes (see Figure 5). Wall and Smith (2008) reported that BOLD activity in CSv was greater with a full-field stimulus signaling self-motion than during a stimulus containing 9 smaller patches of the same display. According to Furlan et al.,(2013) activity in CSv seems to be correlated

with activity in VIP. Smith (2014) argues that CSv is involved in motor planning, as opposed to motion perception, based on its anatomical and functional connectivity.

Furlan et al. (2013) noted that CSv responds particularly well to changes of heading compared with other visual motion processing regions such as MST+ and V6. In contrast, MST+ responds better to continuous heading than to changes of heading. Fischer et al. (2012) demonstrated the importance of CSv for processing visual self-motion during eye movements, compared with other known visual motion sensitive cortical regions and argued that CSv integrates eye movements with retinal motion during self-motion displays. In sum these features suggest that CSv plays a role in estimating heading direction.

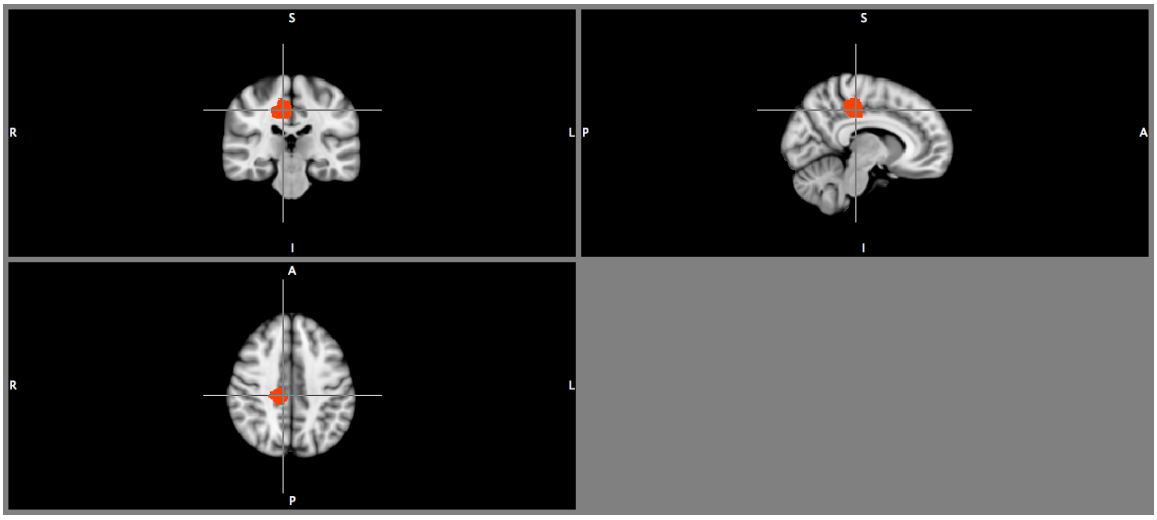

Figure 5. Area CSv illustrated in a MNI standard brain.

PIVC

PIVC is widely accepted as a polysensory region in both non-human (see Figure 6; Guldin and Grusser, 1998) and human (Fasold et al., 2002) primates and is known to be primarily involved in vestibular signal processing. For instance, in PET studies,

caloric irrigation has been used to localize PIVC (Bottini et al., 1994) and in fMRI, PIVC was functionally localized using GVS (Bense et al., 2001; Eickhoff et al., 2006). There have been reports of functionally localizing PIVC both with vestibular stimulation and visual stimulation separately.

Cardin and Smith (2010) reported increased PIVC activity during a visual stimulus signaling egomotion. In their experiment, they contrasted an 'egomotion-compatible (EC)' display, with an 'egomotion-incompatible (EI)' display. Their EC stimuli were wide-field optic flow displays that lasted 3s, and therefore were unlikely to induce vection because vection takes time to build (see section 3.1). Furthermore, the authors did not measure vection and the display was not consistent with real motion through a stable environment. Cardin and Smith found a significant change in activity for EC compared to EI stimuli in PIVC. In line with this finding, Antal et al. (2008) reported that coherent optic flow displays activate similar insular areas to PIVC in a human fMRI study. Similar to Cardin and Smith, Antal et al. did not record participant vection experience. However, there are fMRI studies that measured vection and reported increased PIVC activity during vection (Beer et al., 2002; Kovacs et al., 2008; Indovina et al., 2013). As such, PIVC may not be spatially well defined, but there is convincing evidence of insular cortex activation during visual stimulation of this region.

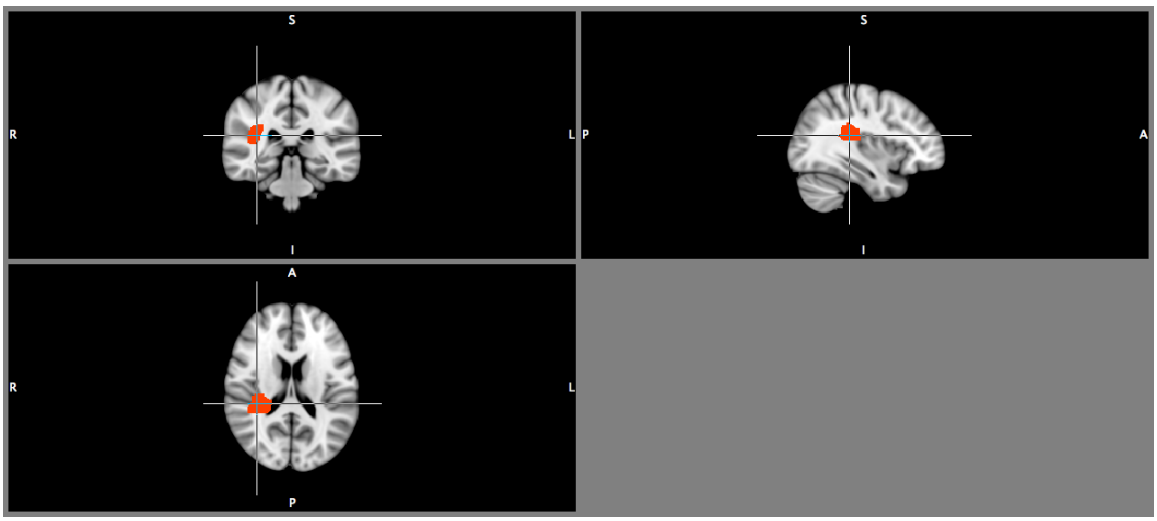

Figure 6. Parieto-insular vestibular cortex (PIVC). Coordinates taken from Cardin and Smith (2010).

1.4 - Vestibular Facilitation and Vestibular Inhibition During Vection

A large amount of the vection literature focuses on the sensory integration of the visual system with the vestibular system. This is because the visual and vestibular systems often undergo significant conflict during vection (Reason, 1978; Oman 1982). Specifically, during vection the visual system receives input consistent with self-motion but vestibular self-motion signals indicate no change in motion. An expected, but absent vestibular signal consistent with the visual signal causes a conflict between the two systems. Moreover, the degree and duration of the conflict depend on whether the visually simulated self-motion is of a smooth (low conflict) or accelerating (high conflict) scene (Palmisano et al., 2011).

Visual and vestibular signals are integrated at the earliest sites of central processing in the primate brainstem (Waspe & Henn, 1977). Early studies reported that almost all units responded to both vestibular and visual signals although a recent study suggests that

not all cells are visually responsive (Bryan & Angelaki, 2009). These visual signals are processed by the same circuitry which drives vestibular responses and thus visual and vestibular self-motion signals share a common and synergistic representation at this level of the brainstem (Robinson, 1977). Thus, we might expect analogous synergistic representation of visual signals at higher levels of the visual system, for example in vestibular cortical regions. In this case visual self-motion signals would also be represented in vestibular cortex increasing neural activity in these areas.

From a neuroimaging standpoint, one might expect that during vection, there would be increased blood flow in visual and non-visual cortical regions involved in processing self-motion stimuli. Increased blood flow can be represented as BOLD signals in fMRI, $H_2{}^{15}O$-bolus levels in positron emission tomography (PET) or magnetic fields in magnetoencephalography (MEG). An increase blood flow in a specified brain region during a vection display compared to a non-vection display would presumably reflect these regions' sensitivity to processing vection, or some component of vection such as optic flow, or coherent motion. However, it is unclear if any change in blood flow during vection displays occurs in vestibularly sensitive cortical regions. Alternatively, it is plausible to assume a suppression of vestibular cortical activity during vection because it is a visual illusion. These two possibilities are discussed in detail below as I evaluate the potential involvement of cortical vestibular regions PIVC and VIP during vection.

Vestibular Facilitation

Because visual self-motion generally occurs during real motion, vection should induce an expectation of concomitant signals from other senses. Moreover, self-motion

perception may require multi-modal integration and processing (Palmisano et al., 2011). Thus, vestibular regions in the cortex could be involved in processing and updating this expected self-motion information which would result in higher blood flow during vection. This would be due to visually evoked signals induced in vestibular regions that produce the expected activation corresponding to real self-motion, despite the vestibular system not actually receiving input.

In a MEG study by Nishiike et al., (2002) participants sat upright and visual stimuli were displayed in complete darkness. Researchers used two egomotion-compatible conditions. One condition was a baseline with a set of concentric circles centered on the display that expanded at a constant rate. The other condition was experimental and had concentric rectangles that expanded at a faster rate than in the control condition. The stimuli randomly changed from the baseline to the experimental condition. Because condition 1 and condition 2 had different rates of expansion, this created stepwise acceleration in the optic flow when conditions spontaneously switched. Subjects were instructed to discriminate stimulus change from 'circle' to 'rectangle' by raising their index finger as quickly as possible. Authors reported that subjects experienced vection when the stimulus changed from the control condition to the experimental condition, but only a vague vection measurement technique was described. In this study Nishiike and colleagues reported increased activation in posterior-insular regions (qualifying as vestibular cortical areas) during vection and therefore provided support for a vestibular facilitation hypothesis.

Despite Nishiike's group (2002) not explicitly measuring vection, their vestibular facilitation finding is consistent with previous studies that explicitly measured vection.

Previc (2000) used Positron Emission Tomography (PET) a technique that measures regional cerebral blood flow (rCBF) by injecting a tracer that measures $H_2{}^{15}O$-bolus activity in the brain in a vection experiment. Previc reported an increase of $H_2{}^{15}O$-bolus tracer signal in the insula during wide-field circular vection (CV) displays consisting of clock-wise or counter-clockwise moving dots, coherently moving dot display compared with incoherent dot motion displays. Similarly, Cardin and Smith (2010) reported increased parieto-insular vestibular cortex (PIVC) BOLD signal when participants viewed an egomotion-compatible stimulus in an fMRI experiment. Additionally, Kovacs and colleagues (2008) reported heightened BOLD signal in vestibular regions during stimuli that produced vection in depth versus object motion stimuli that did not produce vection in an fMRI study. In addition, Beer et al. (2002) report increased right insular activity in a PET study comparing coherent motion displays with incoherent motion displays. Based on all these studies, it appears that vection correlates with increased cerebral blood flow in vestibular regions of the brain, supporting the vestibular facilitation hypothesis. On the other hand, there are many studies supporting a decrease in blood flow in vestibular regions during vection (Brandt et al., 1998).

Vestibular Inhibition

According to Brandt and colleagues (1998), an alternative way to deal with visual-vestibular conflict during vection would be to inhibit vestibular processing by visual dominance. Visual dominance is the strong activation of visual areas that simultaneously drive a decrease in activity, or inhibition of blood flow to vestibular cortical regions. Brandt and colleagues' reciprocal visual-vestibular inhibition hypothesis suggests that the

deep insular cortex (including PIVC) becomes deactivated from blood flow during constant-velocity circular vection even as visual cortical self-motion centers increase in blood flow.

In Brandt and colleagues' PET experiment (1998), participants laid in a supine posture, and viewed a circular vection (CV) stimulus through a head-mounted display. There were 3 relevant conditions. 1) A static grey square on a black background; 2) a non-vection condition in which randomly-moving red dots were overlaid on the baseline display; and 3) a clockwise vection condition where the red dots move coherently. To measure vection, the researchers asked participants to rank their feeling of self-motion on a 1-5 scale after each trial. They found heightened $H_2{}^{15}O$-bolus levels in visual regions and a reduction of $H_2{}^{15}O$-bolus in vestibular regions during condition 3 (the vection condition) compared with the non-vection conditions.

Brandt's inhibition hypothesis (1998) has been supported in follow-up studies from the same laboratory (Dietrich et al., 1998, Brandt et al., 2002, Deutshlander et al., 2002, Dietrich et al., 2003, Deutshlander et al., 2004), and others. Deutschlander and colleagues' (2004) PET study is notable for two reasons. First, this experiment replicated the findings of Brandt et al. (1998) suggesting an inhibitory interaction between visual and vestibular cortical regions represented by decreased blood flow in parieto-insular regions when viewing CV displays. Second, responses during CV and looming vection displays were compared in order to investigate how both types of vection displays activated brain regions. They reported similar activation patterns during both types of vection displays in parieto-insular regions.

In Nishiike and colleagues (2002) the authors discuss the discrepancy in their vestibular facilitation results compared to Brandt et al. (1998) vestibular inhibition results. Nishiike and colleagues note that first, circular vection, and looming vection may be processed differently in the brain, particularly in vestibular regions. However, Deutshlander et al's. (2004) study (mentioned above) discounts this argument because they reported similar activation for CV and for looming vection in their PET study. Second, Brandt hypothesized that an increase in blood flow in both visual and vestibular regions could occur if the stimulus display possessed 'unexpected transitions'. According to Nishiike, in this case the change of rate of expansion of the circular/rectangular stimulus to the other's rate of expansion could qualify as an unexpected transition, explaining their observed increase in vestibular activation.

Cardin and Smith (2010) also noted that their finding of increased PIVC activity during egomotion-compatible (EC) displays conflicts with Brandt's reciprocal vestibular inhibition hypothesis. Cardin and Smith did not measure vection and the short duration stimulus was unlikely to have induced vection. However, other studies that did measure vection reported facilitation of vestibularly-sensitive areas during vection (Kovacs et al., 2008; Indovina et al., 2013; Beer et al.,2002; Previc et al., 2000).

The inconsistent findings between Nishiike (2002) and Brandt et al., (1998) are likely due to three important differences. First, characteristics of the stimuli used in each experiment differ. Stimuli signaling circular vection, arguably appear different and produce different percepts than stimuli inducing looming vection, making the studies difficult to compare. Second, behavioural vection measurements were made differently in both studies. Finally, the studies used different brain imaging techniques (PET vs.

MEG) which differ in imaging parameters, specifications, as well as spatial and temporal resolution capabilities. Taken together, the sizeable amount of research on brain activity in vestibular regions during vection is difficult to reconcile due to limitations in defining and measuring vection. As a result, the functional role of vestibular cortical regions during vection remains unclear.

1.5 – Hypotheses and Contributions

The neuroimaging literature on vection is polarized by the vestibular inhibition/facilitation debate (Brandt et al., 1998, Nishiike et al., 2002, Deuthschlander et al., 2004, Cadrin and Smith, 2010; Indovina et al., 2013). Furthermore, because MRI research capable of localizing brain regions involved in vection is relatively new, there is a fair amount of disagreement on exact visual regions involved and in their specific role during vection. Moreover, I use a unique set of displays that are hypothesized to induce different levels of vection and are presumed to induce different levels of sensory conflict (Palmisano et al., 2011). In all, the goal of this thesis is threefold. 1) To identify those brain regions responsive to vection stimuli. 2) To clarify the vestibular inhibition/facilitation debate by understanding the function of vestibular cortical regions during vection. 3) To determine if there is neurophysiological data that parallels behavioural data of vection strength sensation.

Hypotheses

I hypothesize that the two radial conditions will induce vection and that the two scrambled conditions will not induce vection (See Methods).

Second, I hypothesize that vection ratings made in the fMRI experiment will be consistent with vection ratings obtained in the psychophysical lab experiments, supporting that the visual displays are equivalent.

Third, I hypothesize that there will be a significant difference in vection rating between the two vection displays (a radial smooth condition, and a radial oscillating condition), with the radial oscillating condition predicted to be rated significantly higher. This hypothesis is based on a phenomenon known as the jitter effect (Palmisano et al., 2000) which can be defined as a stronger perception of vection created by up/down oscillation or jitter in a scene. I hypothesize that stronger vection (behavioural measure) will be reflected in cortical activity (neurophysiological measure).

Assuming that visual-vestibular conflict is related to vestibular facilitation, my fourth hypothesis is that vestibular facilitation will occur during radial oscillating vection displays, but not in radial smooth vection displays. This is because the oscillating radial display is conceptually similar to Nishiike et al's (2002) in that both use variable speeds, and therefore, our result will be similar.

Contributions

The novelty in my thesis is that I am comparing vection inducing-stimuli with non-vection inducing stimuli while holding other elements of my stimuli constant, limiting unwanted artifacts. In addition one of my stimuli has an acceleration component (radial oscillation) that will allow me to compare varying levels of sensory conflict during

vection (ie. radial oscillating condition compared with radial smooth condition). Second, I have used a replicated and reliable vection measurement technique (Stevens, 1959; Allison et al., 2012) and ensured that all participants understood what vection is and how to express their sensation of the illusion accurately. Third, I have conducted my main fMRI experiment under unvarying protocols and scanning parameters, facilitating comparisons between conditions. This methodical research design, allowed me to isolate my questions of interest – what is the role of visual and vestibular regions during vection, and how are they integrated?

2. Methods

2.1. Experiment 1 – fMRI Vection

Apparatus and Scanning Parameters

I used a Siemens 3-Tesla Magnetom MRI Scanner (Erlangen, Germany) for two of the three experiments in this thesis. This scanner was equipped with a 32-channel radio-frequency head coil that maximizes signal-to-noise ratio to acquire anatomical and functional images. An Avotec projector inside the magnet room displayed images onto a screen inside the scanner bore. The projector had a 1024 by 768 pixel resolution and 60 Hz refresh rate. The screen was 25 cm wide and 18.8 cm long. To view the display, which was placed above the observers' heads, a mirror was angled at 45º to the face. The displayed images subtended 36˚ horizontally and 27˚ vertically at the 38 cm optical distance. Stimuli were generated by a T61 Lenovo ThinkPad equipped with an Intel Core 2 Duo processor and a NVidia Quadro FX 570M graphics processor. Scanner configuration is displayed below in figure 7.

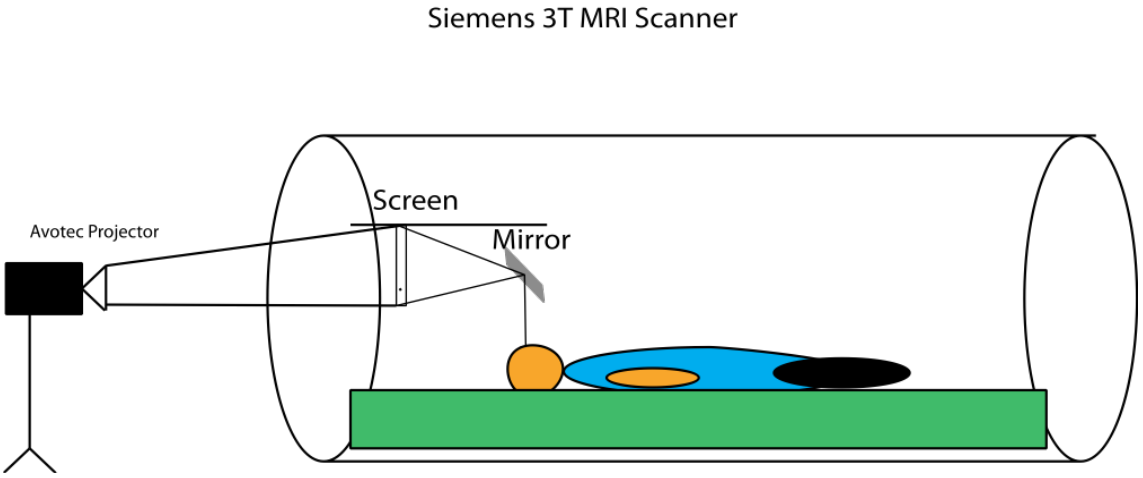

Figure 7. Experiment 1 setup.

A high-resolution T1-weighted MPRAGE sequence anatomical scan was obtained for each participant to which all subsequent functional images were registered. For the high-resolution anatomical scans, voxel size was 1.0 x 1.0 x 0.95 mm, TR=1900 ms, TE=2.52 ms, flip angle of 9˚ and FOV=256 mm. Functional runs all shared the following parameters: T_2*-weighted, voxel size=3.0 x 3.0 x 3.5 mm, TR=2000 ms, TE=30ms, flip angle of 90˚ and FOV of 240 mm.

Data Preprocessing

A general linear model (GLM) was run in Fossil's (FSL) (5.0.1) FEAT functional MRI tool (v6.00). General linear model (GLM) is the modeling method used in FSL's FEAT. GLM allows users to model the behavior of a voxel in a given time course and fit it to the real data. Z-tests are then automatically implemented by FEAT. The GLM in FEAT has many robust regressors built in to cancel noise created by head motion, physiological changes and magnetic properties of the scanner. For my manipulation, I created 6 explanatory variables (EVs). These were the modulus stimulus (explained in the 'Stimuli and Conditions' section on page 35), 4 experimental conditions (1 EV each) and 1 EV for response intervals in which participants rated their sensation of vection after each trial. Static periods of each stimulus were used as the baseline in the GLM. EVs were represented in a raw text file making up the event-related design for the experiment. Conditions were labeled as 'ON' phases and static periods before the motion of stimuli began were treated as the 'OFF' phases/baseline.

All data were spatially smoothed using estimates from random-field theory (RFT) at the full-width half maximum (FWHM) value of 5 mm of the Gaussian kernel

smoothing process applied prior to processing the functional localizer data (Worseley et al., 1992). Participants remained stationary throughout the experiment. However, brain images were motion corrected using the MCFLIRT tool set in FEAT to reduce the effect of any minor participant head motion (ie. resulting from respiration). Non-brain tissue was filtered from the images using the BET brain extraction tool also built into FEAT. Functional data were overlaid on a standard 1mm MNI brain, as well as each subject's structural image which also had a voxel size of 1mm x 1mm x 1mm, and corrected for accidental head motion in 12 degrees of freedom. All data were modeled using a double-gamma hemodynamic response function (HRF) that takes into account the late onset of the BOLD signal (typically estimated to be approximately a 5-6 s lag) as well as the late undershoot known to follow stimulus presentation.

Participants

Eight members of the York University community participated in the study (6 males and 2 females). The mean age of participants was M=31.5 and SD=8.4. Six participants were right-handed and two participants were left-handed. All participants reported no history of abnormal vestibular function. Seven participants had normal or corrected to normal vision with aided vision. One participant did not wear his habitual eyeglasses but could see the stimuli clearly at the near distance.

Five subjects had previously participated in vection experiments, using similar stimuli. The three participants that had never been in a vection experiment underwent several practice runs to ensure that they understood what vection was, experienced clear vection and understood the task. Prior to the experiment, participants provided their

informed consent in accordance with a protocol approved by York University's Ethics Committee. Subjects participated on a voluntary basis.

Stimuli and Conditions

The 4 conditions were 1) Smooth radial optic flow. In this condition, all elements in the display move coherently in a radially expanding flow pattern (velocity of elements depended on their simulated distance as well) simulating smooth, forward self-motion (Figure 8). 2) Radial optic flow with spinal-axis oscillation. This is similar to condition 1 with the addition of simulated coherent, spinal-axis oscillating motion of the computer graphics camera used to render the scene (Figure 9). 3) Smooth local optic flow. This display is identical to condition 1, but the coherent display is evenly segmented into six panels (3 panels in the top half of the screen and 3 panels in the bottom half), which are reordered (scrambled) to scramble the radial optic flow (Figure 10) and no longer simulated forward self-motion. Condition 4 - spinal-axis, oscillating, local optic flow. This condition is identical to condition 2, but is segmented into a scrambled 6-panel arrangement (Figure 11) and should also no longer simulated forward self-motion. All displays included a centered stationary green fixation dot. Displays began with a 5-second static frame of the scene before simulated motion began. Simulated motion of objects in the scene lasted 20 seconds each.

Condition 1

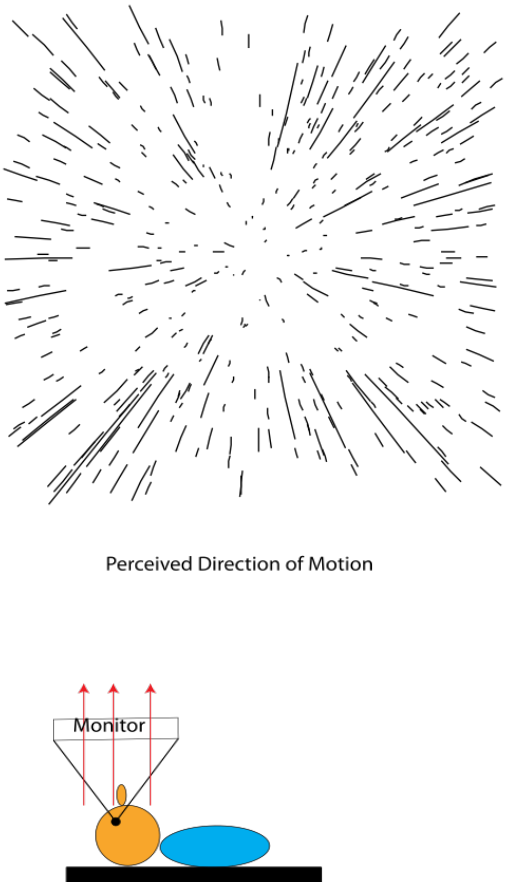

Figure 8. Illustrations of all 4 conditions are adapted from Palmisano et al., (2011). Condition 1 - Smooth Global Motion: Note that the red arrows indicate smooth global self-motion is in the forward direction opposite to the simulated motion of the elements in the display.

Condition 2

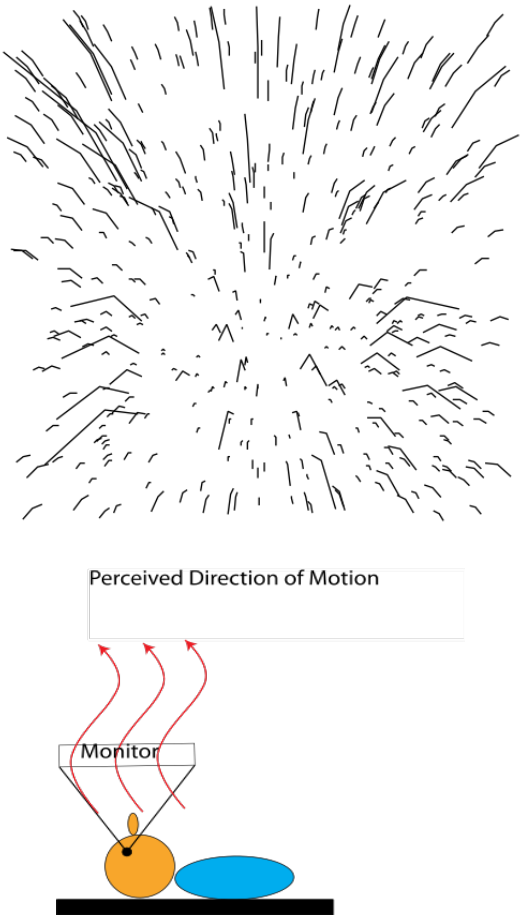

Figure 9. Condition 2 - Oscillating Global Motion: The top image illustrates a view of the stimulus at the highest virtual amplitude. The red arrows indicate spinal-axis oscillation in the forward direction.

Condition 3

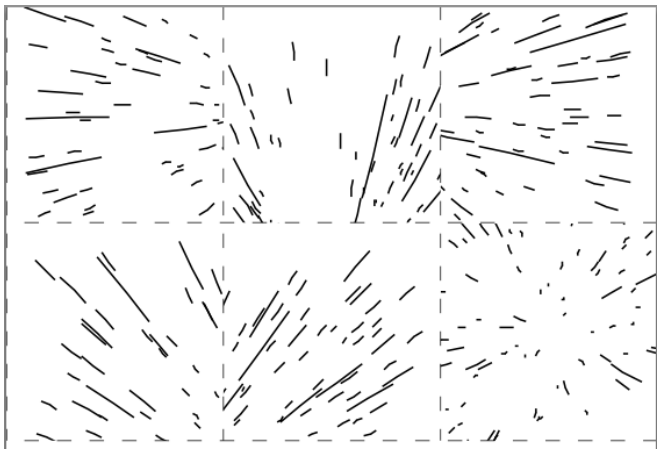

Figure 10. Condition 3 - Smooth Local Motion

Condition 4

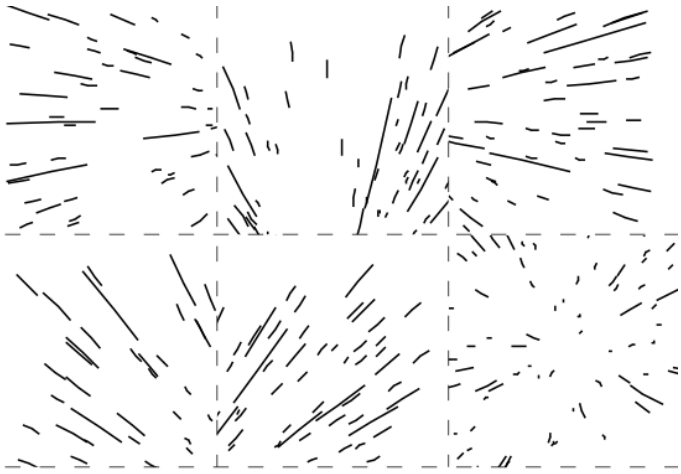

Figure 11. Condition 4 - Oscillating Local Motion.

Stimuli were developed in Pyglet, rendering a virtual world 15 m wide, 15 m high, and 40 m deep. The computer graphics were rendered with a perspective projection appropriate for the distance and size of the display. In this virtual world there were 7000 evenly distributed textured blue spheres (diameter 15 cm) each. All spheres moved at a

speed of 0.08 meters per frame (60Hz) in the virtual world. Sphere size, density, and velocity in the image varied as a function of simulated distance from the viewer according to perspective projection. Spheres were not placed within 28 cm of the path of the camera to prevent collisions with the face. As each sphere passed behind the observer it was replaced by a new sphere at the far end of the simulated volume. Soft fog simulated in the environment caused contrast to decrease in the distance which made their reappearance less distracting. Oscillation in conditions 2 and 4 was given by the formula $0.16 \times \sin(2\pi f t)$ in which 0.16 m/s is the peak speed in the up/down direction of the virtual camera, f = 1.2 is the oscillation frequency and t is the time since the start of the motion (time progresses on each frame, that is, in discrete steps of 1/60 s). In conditions 3 and 4, the local motion conditions, identical images to conditions 1 and 2 respectively were presented in scrambled order. Therefore, sphere size, speed, density, velocity, frequency and amplitude remained the same as in the global motion conditions, but scrambled into 6 panels creating the local motion displays. Luminance values for conditions 1 and 2 were calculated using a photometer positioned slightly to the right of the center of the projected display and had a value of 0.24 cd/m^2. Scrambled conditions had a luminance value of 0.29cd/m^2.

Procedure

Each session consisted of 37 trials in which the first trial was a 'standard display' (modulus). Subjects were told to monitor their sensation of vection during this standard and to assign its strength a value of '50' on a 0-100 scale. The standard display was identical to condition 1. Subjects were to rate all subsequent trials relative to the vection

perception experienced on this standard trial (Stevens, 1959) such that on a subsequent trial, if a participant experienced half the strength of vection, he/she would rate that '25'. Subjects gave ratings verbally after each trial. They viewed 12 repeats of Condition 1, 12 repeats of Condition 2, 6 repeats of Condition 3, and 6 repeats of Condition 4. These were pseudo-randomized in blocks of 6. Subjects were instructed to stay fixated on the centered green sphere throughout all trials.

2.2. Experiment 2 - Functional Localizer Scans

I used the same projector, MRI scanner, scanning parameters, and high-resolution, T1-weighted images from Experiment 1 in this experiment. Stimuli were generated on an iMac equipped with a 3.2 GHz Intel Core i3 processor and Radeon HD 5670, 512 MB graphics card.

Data Preprocessing

I conducted a series of localizer tests in which seven participants watched video clips that functionally localized regions MT, MST+ and V6 individually. Functional data were analyzed in FEAT. Stimuli were modeled with a square wave function for V6, MST+, and MT+ localizers. For V6 and MT+ stimuli, the static periods were used as the baseline, and stimulus motion was used as the ON period. For the MST+ stimulus, static periods were the baseline, but leftward motion, and rightward motion were modeled separately and contrasted against one another to investigate the reported effects of larger receptive fields in the ipsilateral hemifield of MST+ (Pitzalis et al., 2013). Localizer data for V6 and MT+ were collected in a single run, and therefore were only analyzed in a first-level analysis. Data collected for the MST+ contrasts were recorded in two four-minute scanner runs. This was done to allow for equal amounts of repetitions for right ON (moving), right OFF (static), left ON (moving), and left OFF (static) periods with reasonable run durations and were analyzed in a second-level analysis. All localizer data were thresholded with a minimum Z-score value of 2.3 at the $p<0.05$ corrected confidence level. In other words, BOLD data was only deemed significant if greater than $Z=2.3$ at the $p<0.05$ two-tailed alpha level. A cluster threshold was implemented as a

permutation method to correct for multiple comparisons (for details see Winkler et al., 2014).

Participants

7 of the 8 participants in Experiment 1 took part in Experiment 2. One participant was unavailable during the time period in which we were conducting Experiment 2. Thus, we had n=7 participants with an average age of M=29.7 and SD=7.5.

Stimuli and Conditions

MT+ Localizer

To functionally isolate the MT+ complex, we used the low-contrast Radial Rings display used by Pitzalis and colleagues (2010). This display features light grey concentric rings overlaid on a darker grey background, with a small, red fixation cross in the center. In order to better isolate MT from the wider MT+ complex, we set a 1.5% luminance contrast between the background and rings (Tootell et al., 1995). Average luminance was 8 cd/m^2. This was much brighter (gray and white) than our experimental stimuli (black and dark blue) and therefore had a much larger luminance value.

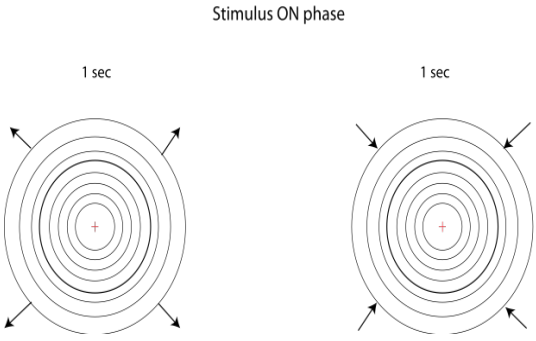

Figure 12. Radial Rings Stimulus - during the ON phase, the display alternated between 1 sec outward motion (left) and 1 sec inward motion (right) of the concentric rings.

The stimulus consisted of eight 'ON' sequences alternating with eight 'OFF' sequences. ON sequences were 16-second periods in which the concentric rings alternatively expanded for 1 second and contracted for 1 second. This was done to minimize motion adaptation effects. OFF sequences were 16-second periods of a static image of the concentric rings. Participants were instructed to fixate the centered red cross throughout. This display lasted a total of 4 minutes and 16 seconds.

MST+ localizer

We replicated Pitzalis et al's. (2013) display designed to differentiate MT from MST+ using a patch of an expanding or contracting optic flow field. This display featured white dots on a black background in a circular window located either to the left or right of a centered, blue fixation cross. The visual angle of the display was identical to that of the vection display (36˚ horizontally, 27˚ vertically) and eccentricity of the circular window was scaled to this display, as Pitzalis' study did not give an indication of the visual angle of their native display[1]. These dots moved in the right or left hemifield in a way that simulated forward or backward looming motion through a volume of dots. Motion of the dots emanated from the center of the display, rather than from the center of the circular window. The dots alternated between moving and static on both the right and left of the centered blue fixation cross. Motion periods on the right and left side of the centered fixation cross were coded as the ON phases. These lasted 16 s each and consisted of alternations of 2 s inward looming motion with 2 s outward looming motion. There were eight repeats of these ON phases in one run. (4 displayed on left, 4 displayed

[1] It is highly probable that this discrepancy in MST+ size and eccentricity of our display accounts for its ineffectiveness in functionally localizing MST+ in subjects in the Results section.

on right). OFF phases were 8 repeats of a static shot of the display (4 on left, 4 on right). The stimulus lasted a total of 4 min 16 sec. We repeated this display in a second run for each participant in order to obtain 8 phases of right-hemifield motion and 8 phases of left-hemifield motion.

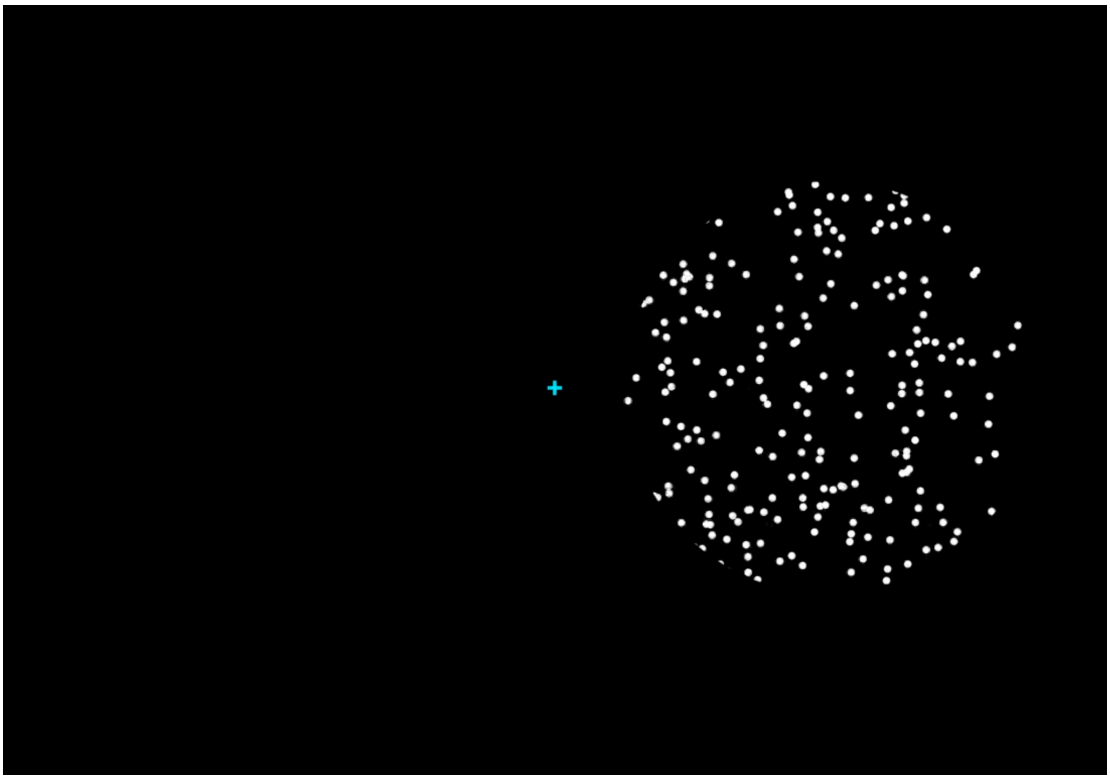

Figure 13. MST+ localizer – right hemifield motion. Participants fixated on center cross at all times. Motion alternated in the forward and backward direction in the left and right hemifields. Motion emanated from the center of the display.

V6 localizer

We used Pitzalis et al's' (2013) 'flow fields' stimulus to functionally localize V6 as they have found this display to induce strong activity in V6. This display was composed of white dots set on a black background with a centered, red fixation cross. During the ON phase, the display presented spiral motion optic flow display continuously varying from pure radial to spiral to pure rotational optic flow in black and white with a

red fixation cross. These dynamic elements of the display simulated self-motion. During the OFF phases the white dots moved randomly and incoherently on the black background with the red fixation cross still present. Thus, this OFF phase possessed only local motion/object motion components and should not have induced the perception of self-motion. The display consisted of 8, 16-sec ON phases alternated with 8, 16-sec OFF phases, and lasted 4 minutes and 16 seconds in total. Participants were instructed to stay fixated on the red cross at all times during the display.

Anatomical Localizers for PIVC, VIP, CSv

Anatomical localizers were used in identifying PIVC, VIP, and CSv because these are more difficult to isolate with functional techniques such as by visual stimulus presentation. Therefore, spatial coordinates of these areas from various sources were collected (Cardin and Smith, 2010; Bremmer et al., 2001). Subsequently, we used our experimental vection stimuli to identify if these regions became functionally activated by our display. Our vection displays from Experiment 1 were successful in identifying these regions because coordinates that matched those previously reported were found.

Procedure

At the beginning of the experiment, participants were informed that they would view a series of visual motion displays. Before each stimulus we described the display they were about to see and the length of the stimulus. They were instructed to stay fixated. The entire experiment consisted of approximately 30 minutes of scanning, but

took almost an hour with set up time and occasional unforeseen circumstances (for example coughing or sneezing which required rerunning a localizer).

2.3. Experiment 3 - Psychophysical Vection Experiment

Experiment 3 was a behavioural, laboratory experiment that took place before Experiment 1 to determine if vection could be induced under identical conditions of the MRI configuration. Experiment 3 mimicked important characteristics of the MRI/Experiment 1 such as the supine posture, the visual angle of the MRI display, the experimental stimuli and instructions for the participants. All participants of Experiment 1 were in Experiment 3 to ensure that participants understood the task and that they all experienced vection. Two participants that took part in Experiment 3 were excluded from the study because they did not experience vection. We excluded these participants as the experience of vection is an important precondition in assessing BOLD signals in Experiment 1, therefore only participants that experienced vection were included in the study.

Apparatus

Participants held a gamepad and laid supine on a massage table and viewed the display of a T61 Lenovo ThinkPad, identical to the computer used to produce the vection displays in the fMRI scanner. The display of the computer was frontal at a distance of 38 cm from the participant's eyes. This configuration replicated the distance, and visual masking was used to match the visual angle in the scanner (Figure 14). The computer was clamped onto a metal plate held by two upright posts. Participants viewed the

display through thick goggle frames with no lenses. These frames were used to approximate the occlusions caused when the head coil is installed over a participant's face in the MRI.

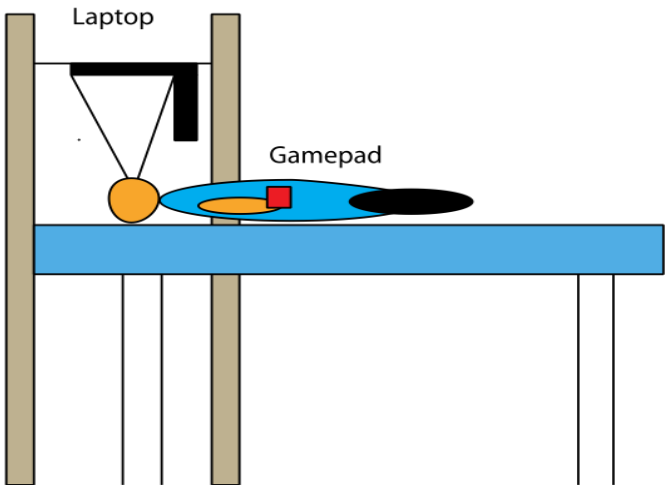

Figure 14. Setup of Experiment 3. Setup mimics that of Experiment 1.

Procedure

Experiment 3 allowed me to measure vection duration time and onset time in addition to vection magnitude rating by using a gamepad. Participants were told to press and hold the right shoulder button on the gamepad when they experienced vection, and to release this button when they did not experience vection. Therefore vection onset times were calculated as the time from the start of the trial when the button was not pressed until the participant pressed the shoulder button the first time. Vection duration time was calculated by summing of the total amount of time the shoulder button was pressed during each trial. Vection ratings were calculated by participant input after each trial. They used 'up' and 'down' buttons to navigate on the 0-100 rating scale. As in

Experiment 1, a magnitude estimation scale from 0-100 was used by participants to rate vection of a trial in relation to the standard trial.

3. Results & Discussion

3.1 – Psychophysics of Vection

Magnitude Estimation Ratings for Laboratory Experiment and MRI Experiment

Bar plot representations of mean magnitude estimation (ME) ratings of vection across participants in the psychophysics experiment and in the MRI vection experiment are displayed in Figure 15. The bar plots show that the scrambled smooth condition produced the smallest vection ratings followed by the scrambled oscillating condition. Figure 1 shows that radial smooth and radial oscillating conditions were rated much higher. Consistent with my third hypothesis, strong vection is experienced during radial smooth flow as well as radial oscillating flow. Little vection, if any, is experienced in the scrambled versions of these radial conditions consistent with my first hypothesis.

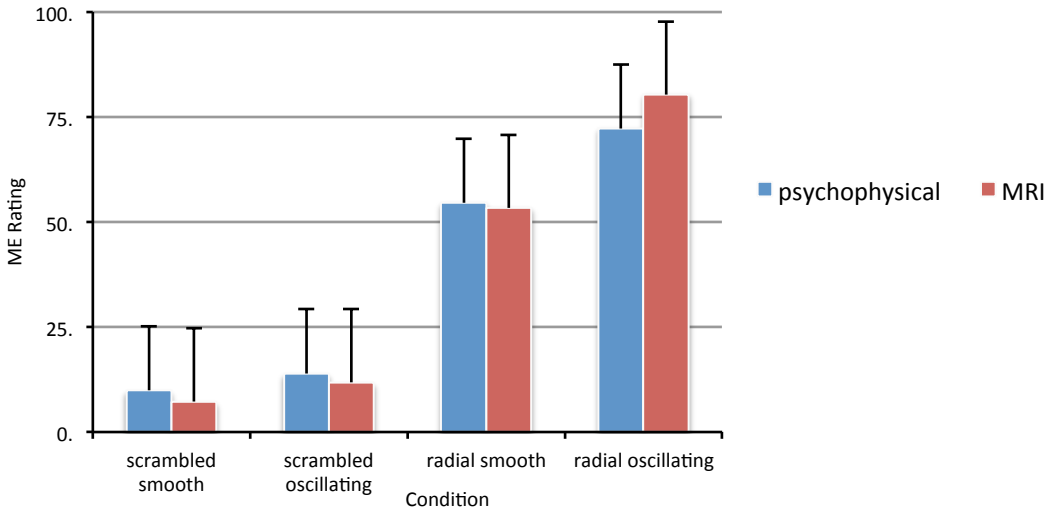

Figure 15. Bar plot representation of magnitude estimation rating for sensation of vection in each condition for psychophyiscal vection experiment and MRI vection experiment. Error bars indicate standard error of the mean.

Figure 15 demonstrates that there is a higher vection rating for radial oscillating than for radial smooth trials and that vection ratings in the psychophysical study are

similar to ratings in the MRI study. This is consistent with hypothesis two. First there was no significant difference between ratings made in Experiment 1 and ratings made in Experiment 3. Second, as I hypothesized, we can observe a jitter effect in our rating data because vection ratings are significantly higher with radial oscillating stimuli than with radial smooth stimuli.

I conducted a repeated-measures one factor ANOVA in which the 4 conditions were the independent variables, and the rating scores within participants were the dependent variables. This analysis revealed a significant effect of the 4 conditions on vection magnitude rating scores with an effect size of R^2=0.77. Pairwise post-hoc comparisons were calculated with the Bonferonni correction used to correct for multiple comparisons and therefore to avoid a Type 1 error. Pairwise post-hoc comparisons showed that all conditions were significantly different with the exception of the Scrambled Smooth > Scrambled Oscillating comparison (Table 1). Of major importance were the contrasts comparing radial (vection-inducing) and scrambled (non vection-inducing) conditions.

Hypothesis 3 states that there would be significant differences between radial and scrambled conditions because the former were designed to elicit vection and the latter were not. My results are consistent with this hypothesis because post-hoc comparisons using t-tests show that for the radial oscillating > scrambled smooth comparison t=-32.94, SE=2.07 and $p<.05$ two-tailed. For the radial smooth > scrambled smooth contrast t=-21.09, SE=2.07 and $p<.05$ two-tailed (Table 1).

Another hypothesis was that I would find a significant difference for vection rating during the radial oscillating condition compared with radial smooth condition.

Post-hoc comparisons confirmed that vection magnitude was larger in the radial oscillating condition compared to the radial smooth condition ($t=9.74$, $SE=2.03$ and $p<0.05$) when comparing these two conditions. There were no significant differences when comparing the two scrambled conditions which both produced low vection sensation.

For the fMRI vection rating data, a repeated-measures one factor ANOVA was conducted as in the psychophysical vection experiment. I found a significant difference in vection ratings between conditions ($F=485.26$, (degrees of freedom) $df=3$ $p<0.05$, $R^2=0.84$ using a two-tailed alpha-level). Table 1 shows post-hoc pairwise comparisons for the ANOVA with Bonferonni correction. Note that unlike contrasts for the psychophysical analysis, all contrasts in the MRI vection experiment showed a significant difference. This includes the scrambled oscillating > scrambled smooth contrast which was not significant in the psychophysical study, however this was a small effect. A significant difference between scrambled oscillating and scrambled smooth conditions is caused by the higher vection ratings for scrambled oscillation. Such is the case because only the forward optic flow was scrambled in the scrambled oscillating condition. However, the up-down oscillation of the display remained coherent, despite it signaling flow in scrambled directions.

Table 1. Post-hoc contrasts for one-factor repeated-measures ANOVA in fMRI Vection Experiment calculated using Bonferonni correction.

Contrast	t-value	SE	p-value
Radial Smooth - Scrambled Oscillating	-16.67	2.07	<.0001

Radial Smooth - Scrambled Smooth	-21.09	2.07	<.0001
Radial Oscillating - Scrambled Smooth	-32.94	2.07	<.0001
Radial Oscillating - Scrambled Oscillating	-28.52	2.07	<.0001
Radial Oscillating - Scrambled Oscillating	-14.51	1.69	<.0001
Scrambled Smooth - Scrambled Oscillating	-3.83	2.40	<.0010

Vection onset and duration measurements from vection psychophysics experiment

An important characteristic of vection is that it takes time to build. The average onset of vection is approximately 3-5 seconds after the start of the radial displays (Figure 16). Data for vection duration are displayed in figure 17.

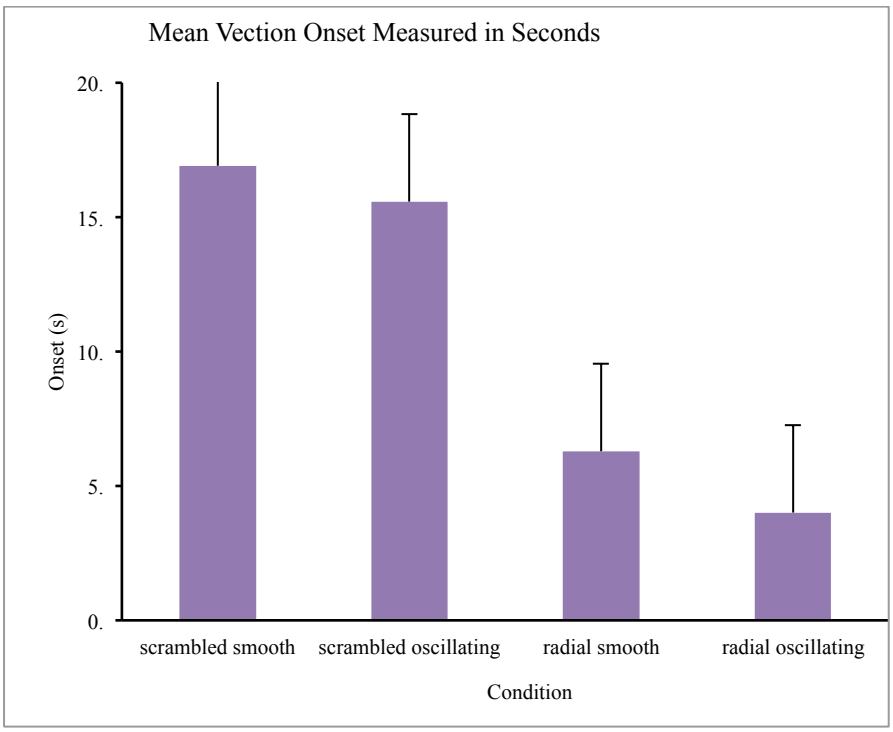

Figure 16. Vection onset times recorded during psychophysical vection experiment.

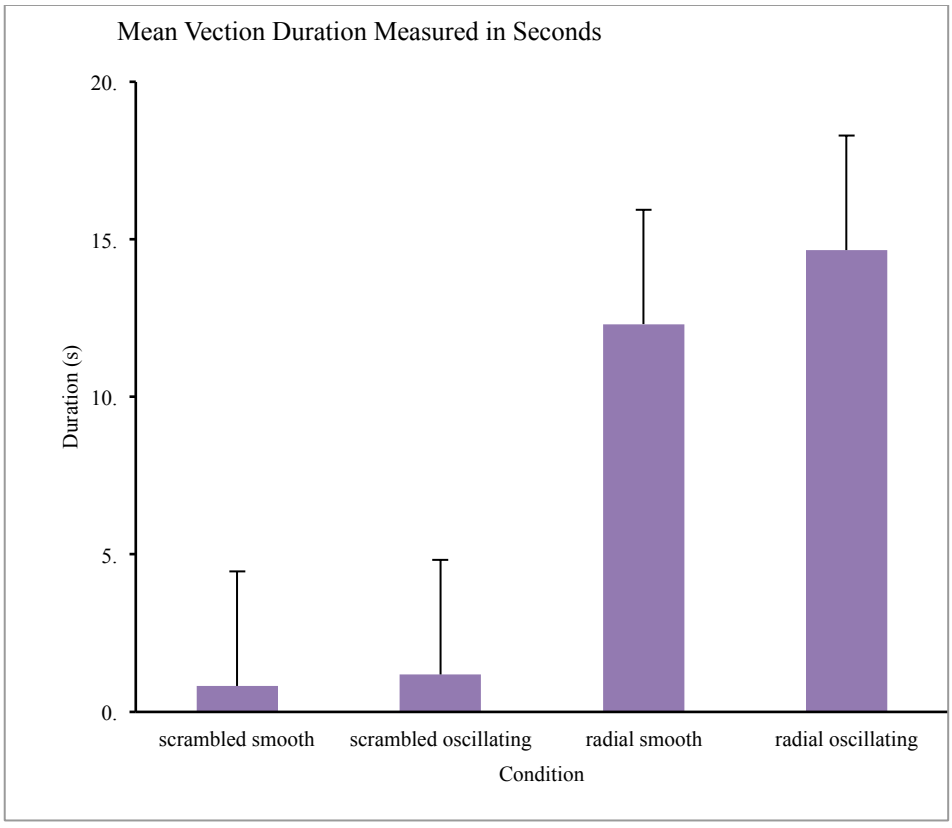

Figure 17. Vection duration recorded during psychophysical vection experiment.

The scrambled smooth condition had the longest onset on average, lasting approximately 20s, or the duration of the stimulus. In contrast, onset times for the radial conditions were much shorter indicating that participants experienced vection early into these trials.

Vection duration is shown in Figure 17. Figure 17 indicates that duration of vection on average for the scrambled conditions was very short. In contrast, vection was experienced for much longer intervals for the radial conditions.

Onset and duration are negatively correlated dependent variables. That is, when onset time increases, duration generally decreases and vice versa. However, this relationship between onset and duration is not perfect, because of vection 'drop-outs'. These are periods where a participant releases the button and then presses it again later within the same trial. Despite this, a longer duration generally results in shorter onset time, and longer onsets generally result in shorter durations.

I conducted a repeated measures ANOVA for vection duration and found that there was a significant difference between conditions at the two-tailed $p<.05$ cut-off ($F=135.83$, $df= 3$ and $p<0.05$). Post-hoc comparisons adjusted for multiple comparisons by the Bonferronni procedure revealed that there was a significant difference for vection duration between all conditions, with the exception of the scrambled oscillating > scrambled smooth comparison (Table 2).

Table 2. One Factor Within-Subjects repeated measures ANOVA for Vection Duration during vection psychophysics experiment.

Contrast	t-value	SE	p-value
Radial Smooth - Scrambled Oscillating	12.67	2.07	<.0001

Radial Smooth - Scrambled Smooth	12.78	0.87	<.0001
Radial Oscillating - Scrambled Smooth	15.50	0.87	<.0001
Radial Oscillating - Scrambled Oscillating	15.37	0.87	<.0001
Radial Oscillating - Scrambled Oscillating	3.27	0.72	<.0072
Scrambled Smooth - Scrambled Oscillating	0.02	1.00	1.0

Vection onset data are presented in Table 3. As expected, they are complementary to the findings for vection duration. Repeated-measures ANOVA shows a significant difference between onset times of vection between conditions ($F=94.13$, $df=3$ and $p<0.05$ using a two-tailed alpha-level). Post-hoc pairwise contrasts reveal that there is a significant difference for start time between all conditions with the exception of the two scrambled conditions (Table 3).

Table 3. One Factor Within-Subjects repeated measures ANOVA for Vection Onset during vection psychophysics experiment.

Contrast	t-value	SE	p-value
Radial Smooth - Scrambled Oscillating	9.77	0.95	<.0001
Radial Smooth - Scrambled Smooth	11.18	0.95	<.0001

Radial Oscillating - Scrambled Smooth	13.56	0.95	<.0001
Radial Oscillating - Scrambled Oscillating	12.16	0.95	<.0001
Radial Oscillating - Scrambled Oscillating	2.92	0.78	<.02
Scrambled Smooth - Scrambled Oscillating	1.21	1.10	1.00

3.2 - Localizer Experiment

V6

The V6 localizer showed bilateral activity in the typically reported region of V6 for 12 of 14 cerebral hemispheres. Across subjects in the left hemisphere, mean coordinates in MNI space were x = -20, y = -83, z = 29 and occupied 3994 voxels. Mean Z-score = 8.34 at the $p< 0.05$ corrected confidence level. In the right hemisphere, mean coordinates were x = 25, y = -78, z = 31 and occupied 3952 voxels with a mean Z-stat = 11.0. Detailed results for each participant are shown in table 4a for left hemisphere data, and 4b for right hemisphere.

MT+

The radial rings display, intended to localize area MT+, activated 11 of 14 hemispheres bilaterally in the hypothesized MT+ region. Mean coordinates in the left hemisphere were x = -40, y = -73, and z = 10 at 2186 voxels and a Z-stat = 9.93. In the right hemisphere, mean coordinates were x = 46, y = -67, z = 9 for 1921 voxels and Z-stat = 10.26 (Supplementary data is in Tables 4a and 4b).

MST+

Using the same contrast method as Pitzalis et al., (2013), MST+ was localized in only 4 of the 14 hemispheres. No participants showed bilateral activation elicited by the MST+ localizer in MST+. Rather, MST+ was active in the right hemisphere for 3 of the 4 hemispheres in separate subjects. In the left hemisphere, MST+ was only activated in one participant. The coordinates for MST+ in the left hemisphere, based on the 1 hemisphere showing activation, is x = -36, y = -67, z = 11 and Z-stat = 11.8. In the right hemisphere, MST+ is located at x = 57, y = -57, z = 8, and a Z-stat = 5.06. Interestingly, 3 of the 4 activations of supposed region MST+ occurred in the opposite hemifield. Meaning that in the left hemisphere, activity occurred when contrasting right versus left activity, but not in both hemispheres simultaneously. Similarly, in the right hemisphere, 2 of the 3 localizations of MST+ occurred when contrasting left versus right activity. This is opposite to the findings of Pitzalis et al's reports because my findings suggest that there is increased contralateral activity in MST+. However, in all, localization of MST+ was not robust in our experiment as we had predicted, as only 4 of 14 hemispheres

showed activation in this region. Eccentricity of patches in our displays are different than those used by Pitzalis, probably accounting for our differing findings.

To recap, the contrast for the V6 localizer was spiral motion vs. random motion, for MST+ left hemifield motion vs. static, for MT+ radial ring motion vs. static. However, MST+ ON phases were right hemifield motion vs. right hemifield static periods. Figures 18 a, b and c display each of these three brain regions in a standard brain. Average coordinates and voxel sizes are taken from each participant based on activations of each respective functional localizer in Figure 18.

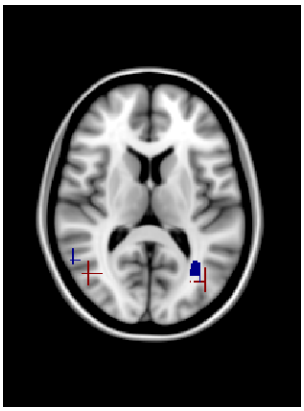

Figure 18a MST+ shown in blue

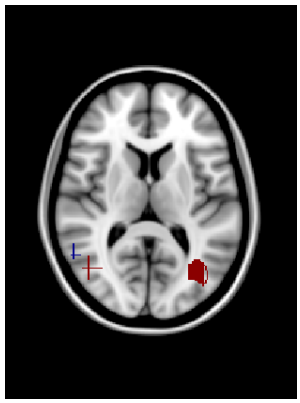

Figure 18b MT shown in burgundy

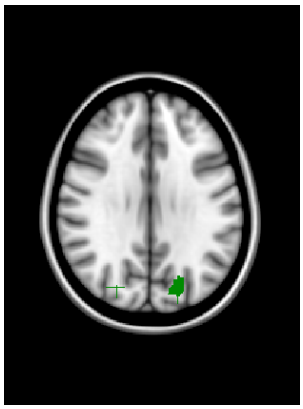

Figure 18c V6 shown in green

3.3 - Vection MRI Experiment – Z-score data

In the FEAT analysis, I set up all possible combinations of contrasts comparing all 4 conditions to each other. These contrasts allowed me to identify those that yielded a significant difference in BOLD activity, given by z-scores. Before running these contrasts, I made masks for brain regions of interest for each subject using brain atlases in FSL View, a drawing/viewing tool in the FSL brain imaging software package. Masks covered larger regions than brain regions of interest. This was done for two reasons. First, the coordinate-space of regions of interest (ROIs) varies across individuals.

Second, exact location of ROIs are not well defined in the literature. Despite these loose masks, using a mask based on an atlas is more statistically conservative than a whole-brain analysis because the GLM runs fewer comparisons, therefore requiring fewer corrections.

Masks were created by registering a subject's brain with a 1-mm MNI standard brain. The combination of subject brain space with standard brain permits for the use of generalized brain atlases in FSL View. This would not be possible if using only the subject's brain. I selected the Talairach Daemon Label Atlas in making the masks. Below is a table showing the mask used for a given ROI.

Table 4. The left column contains specific brain regions of interest for our study. The right column shows the corresponding larger masks used in FSL in which our ROIs are found.

Brain Region of Interest	Talairach Daemon Label Mask Used
Medial Temporal Gyrus	Medial Temporal Region
Precuneus Motion Area	Precuneus
V6	Cuneus
Cingulate Sulcus Visual Area	Cingulate Gyrus
Parieto-insular vestibular cortex	Insula
Ventral Intraparietal Region	Superior Parietal Lobe

A drawback of using loose masks that covered larger regions than our ROIs was that some brain regions that were not of interest within these loose masks showed significant activity. However, regions that had coordinates that were vastly different from previous reports of our ROIs were excluded from my report.

PIVC Activity

PIVC showed significant activity for one of our contrasts of interest - Radial Oscillating > Radial Smooth. Results shown in Figures 19 and 20 indicate that in this contrast 5 of 8 participants show more PIVC activity during radial oscillating than in radial smooth. A Z-score test was calculated in the FEAT analysis for each subject. In the left hemisphere, Z=5.07, p<0.04 and occupied 2712 voxels at x=44, y=-28.8, and z=17.5 on average. In the right hemisphere, Z=5.01, p<0.045 and represented 837 voxels at x=51.7, y=-35 and z=20 on average.

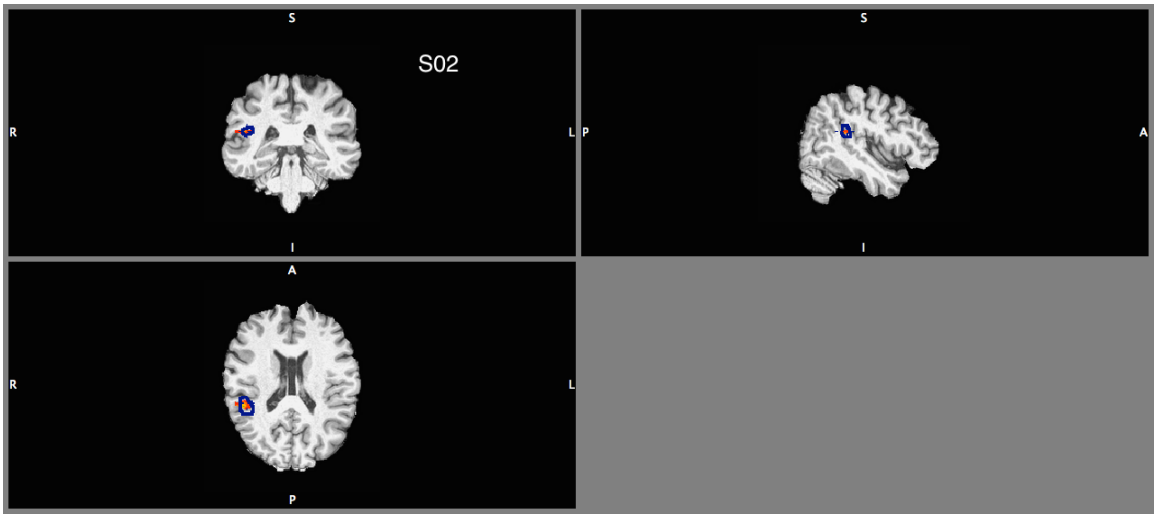

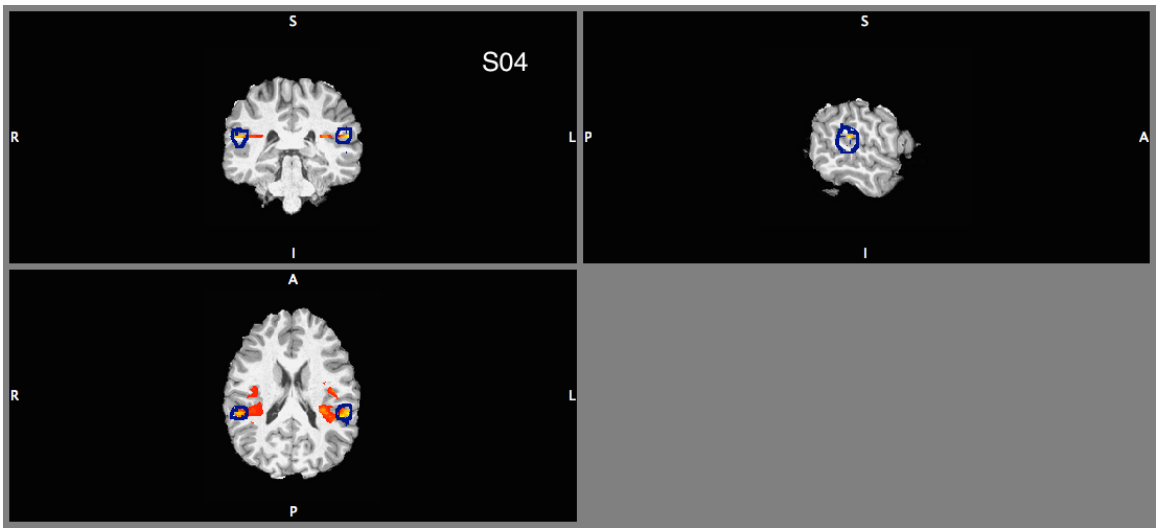

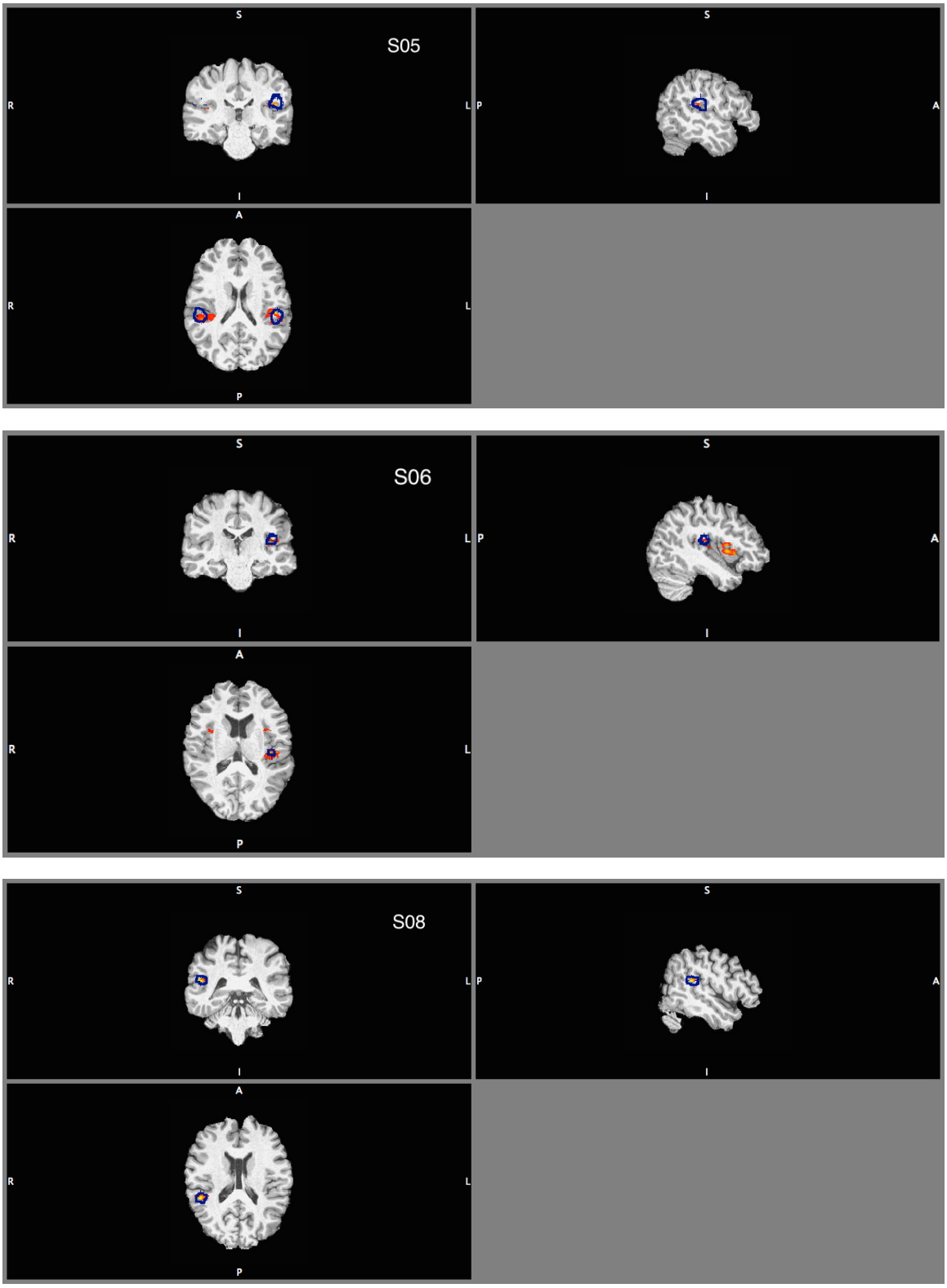

Figure 19. PIVC activity in subjects 2, 4, 5, 6 & 8 in Radial Oscillating > Radial Smooth contrast. The blue outline represents approximate locations of each participant's custom-made ROI. Red-yellow colour gradient represents above-threshold BOLD activity within looser masks (Table 4).

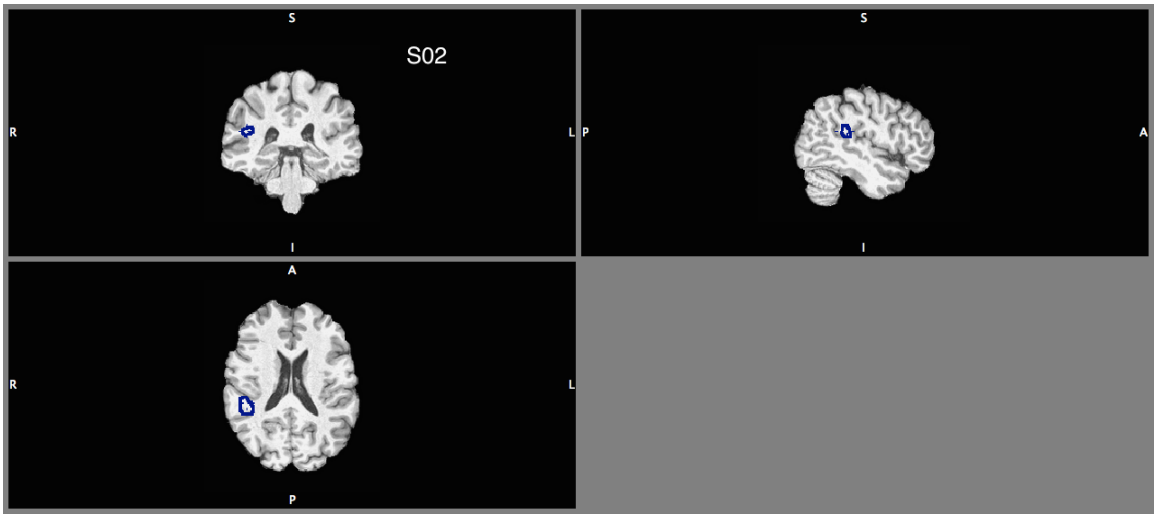
S02
S
R
L
I
S
P
A
I
A
R
L
P

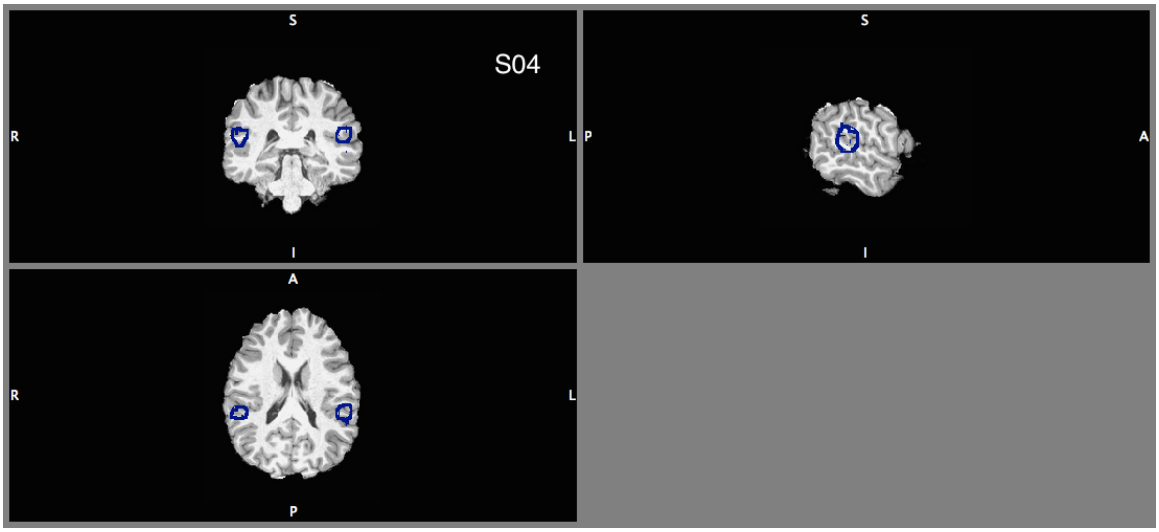
S04
S
R
L
I
S
P
A
I
A
R
L
P

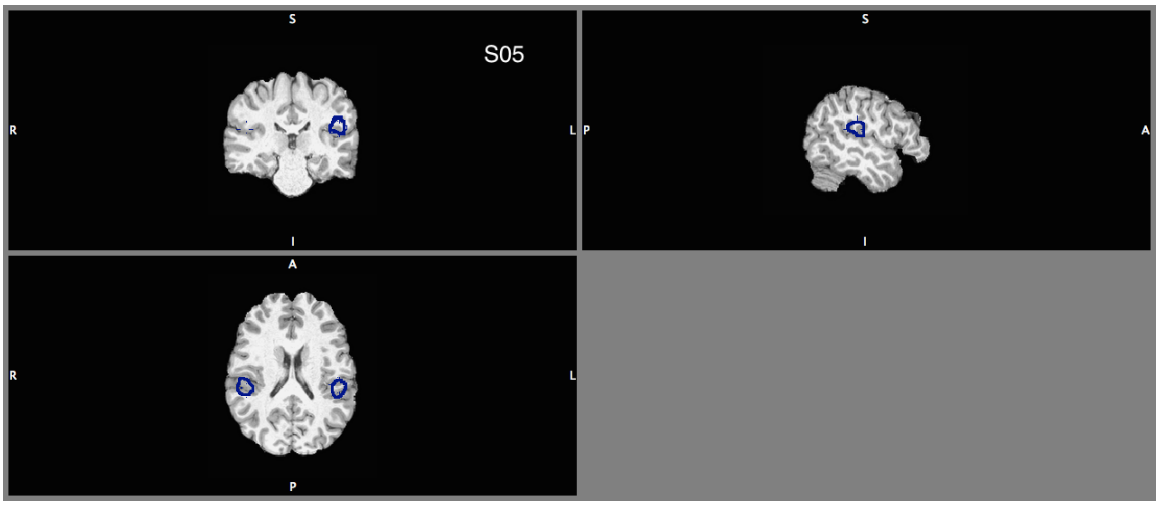
S05
S
R
L
I
S
P
A
I
A
R
L
P

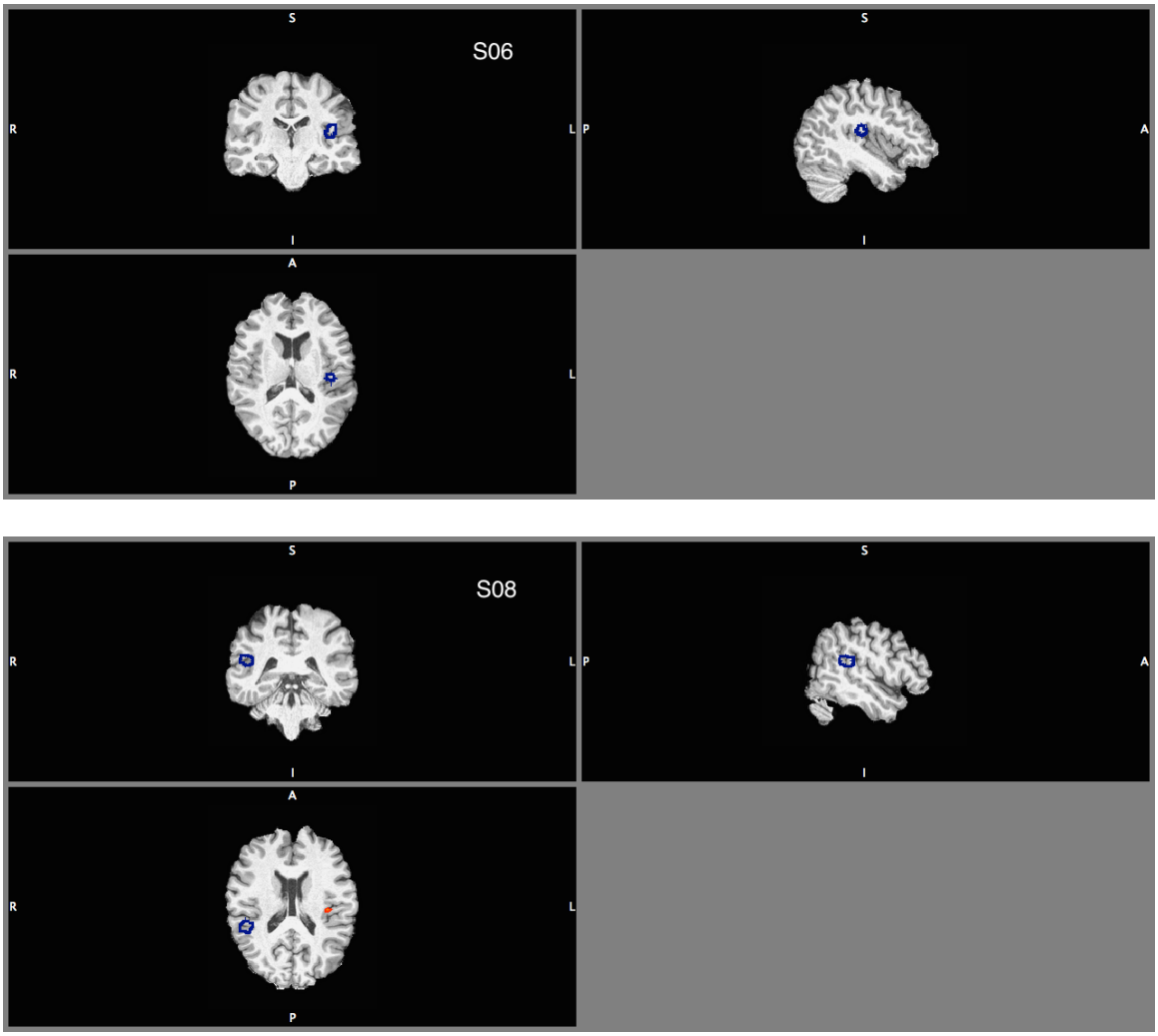

Figure 20. PIVC activity in subjects 2, 4, 5, 6 & 8 in Radial Smooth > Radial Oscillating contrast. Blue outline represents approximate location of each subject's custom-made ROI mask.

The result of this contrast is important as it points to a jitter effect represented in terms of BOLD activity. Assuming participants experienced vection in both conditions, (which ratings showed they did) this result points to a neural correlate for the stronger vection experienced during radial oscillating displays than in radial smooth displays. Surprisingly, other contrasts comparing vection inducing displays with non-vection inducing displays did not show significant differences in BOLD activity in PIVC. From

this result, I conclude that PIVC does not appear to be as strongly involved in vection as predicted and demonstrated in other neuroimaging vection studies.

CSv Activity

Cingulate sulcus visual area showed strong and consistent activity for the Radial Oscillating > Scrambled Smooth contrast in all 8 participants (Figure 21). Figure 22 shows the reverse of this contrast, and indicates that there was no CSv activity in scrambled smooth > radial oscillating contrast. The radial oscillating condition induced the strongest sensation of vection, whereas the scrambled smooth condition induced the weakest sensation of vection (or no vection - see section 3.1). Therefore, this contrast is hypothesized to be the clearest indicator of BOLD activity during vection. A limitation of this contrast is that it compares two conditions that differ in local motion properties, because there is an oscillating component in the radial oscillating condition that is absent in the scrambled smooth condition. Results show that in this Radial Oscillating > Scrambled Smooth contrast, $Z=4.03$, $p<0.049$, and occupies 1058 voxels in the left hemisphere on average. In the right hemisphere, $Z=3.52$, $p<0.049$ for 1455 voxels in CSv.

Radial Oscillating > Scrambled Smooth

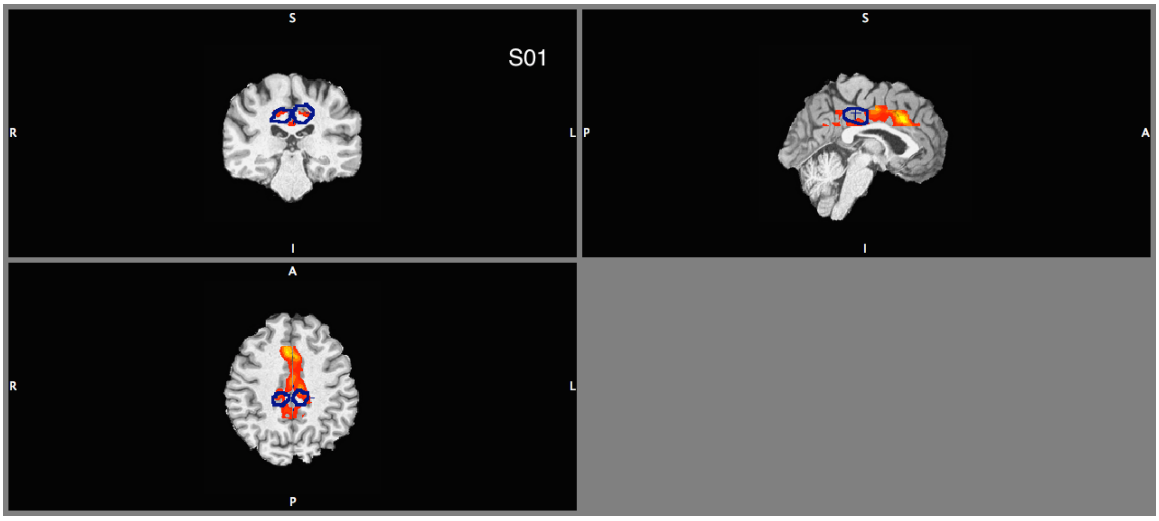
S01
S
R
L
I
P
A
A
R
L
P

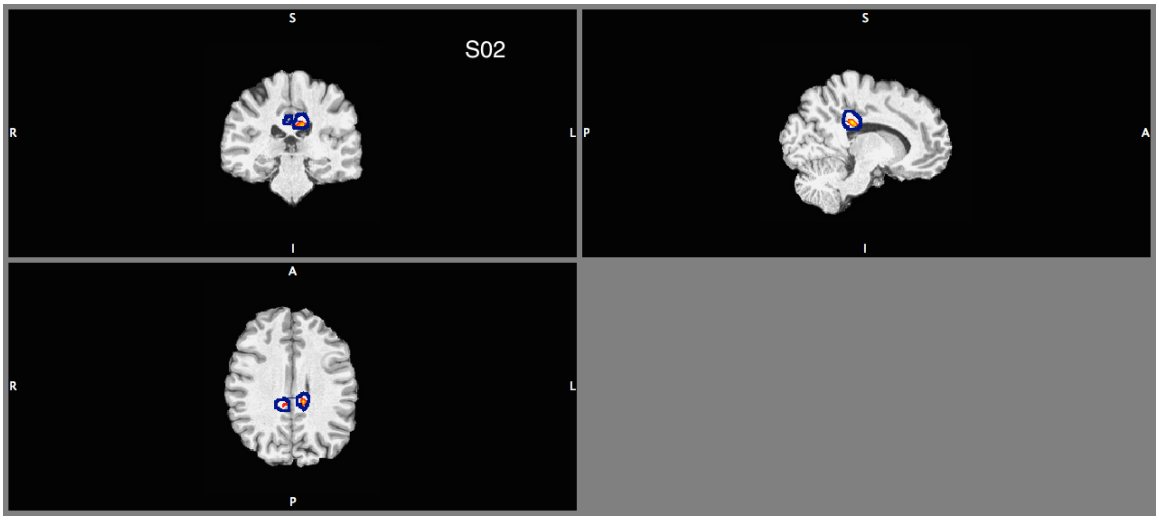
S02
S
R
L
I
P
A
A
R
L
P

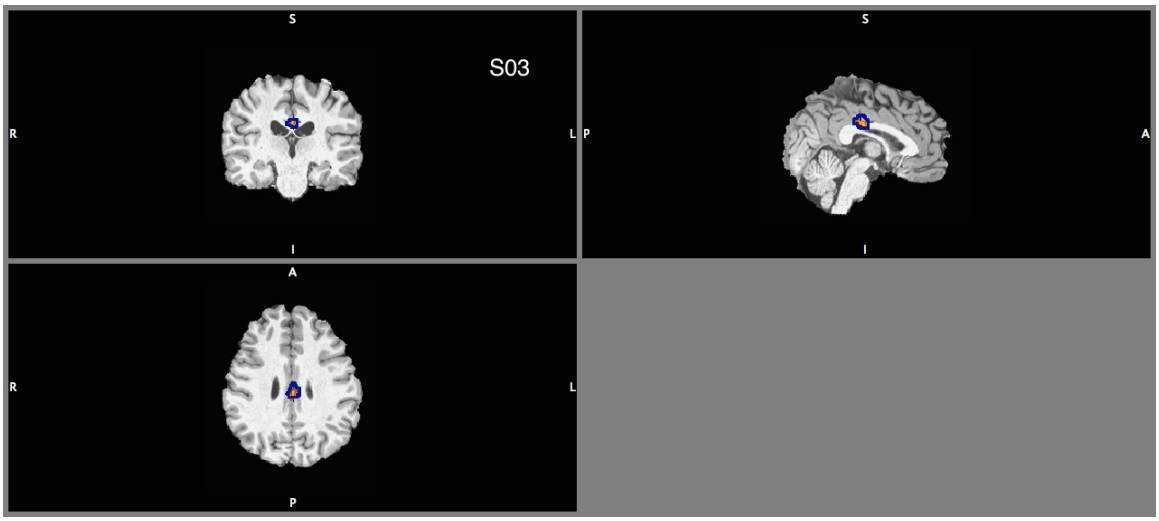
S03
S
R
L
I
P
A
A
R
L
P

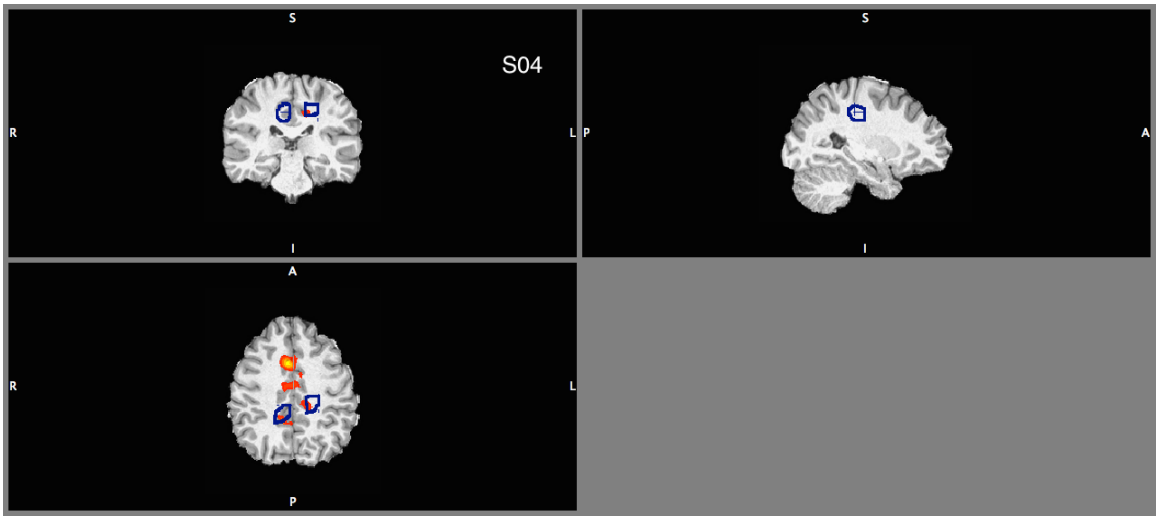
S04
S
R
L
I
S
P
A
I
A
R
L
P

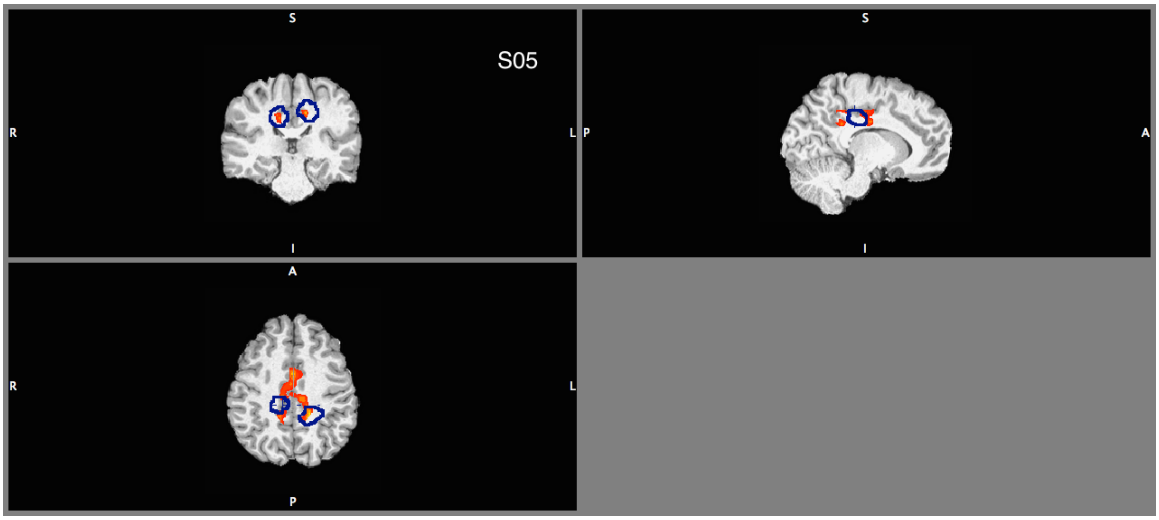
S05
S
R
L
I
S
P
A
I
A
R
L
P

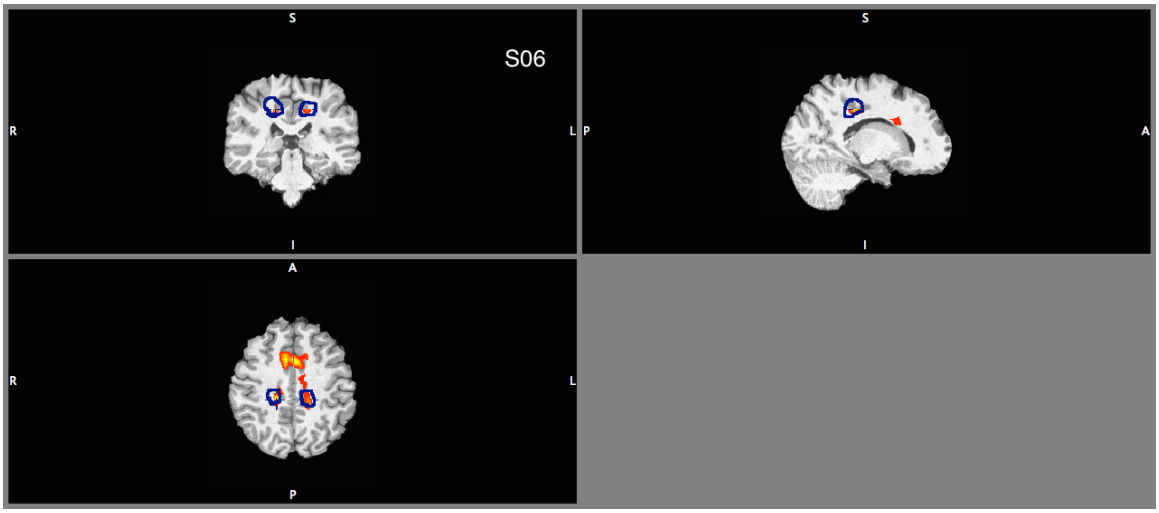

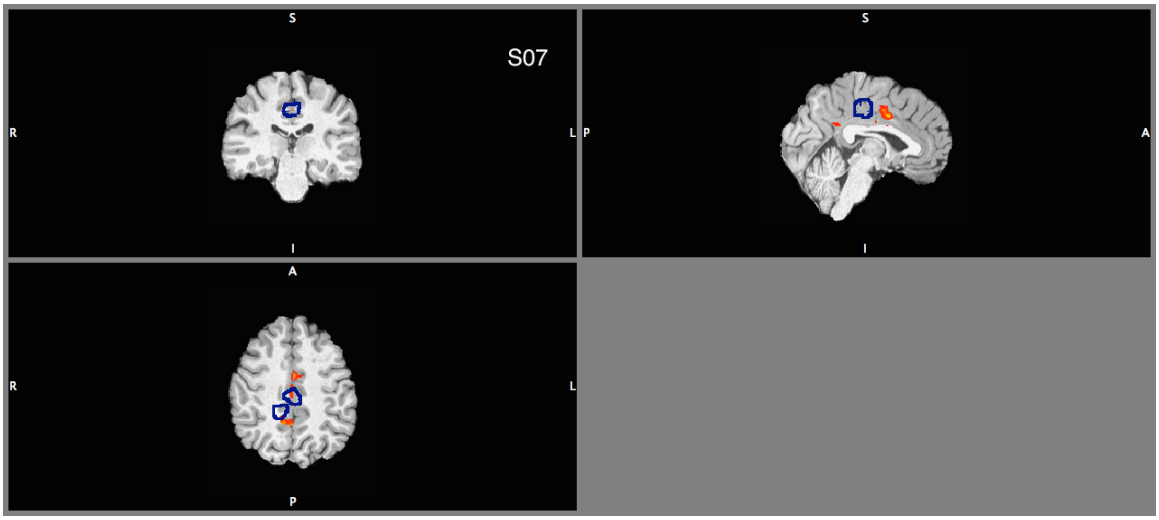

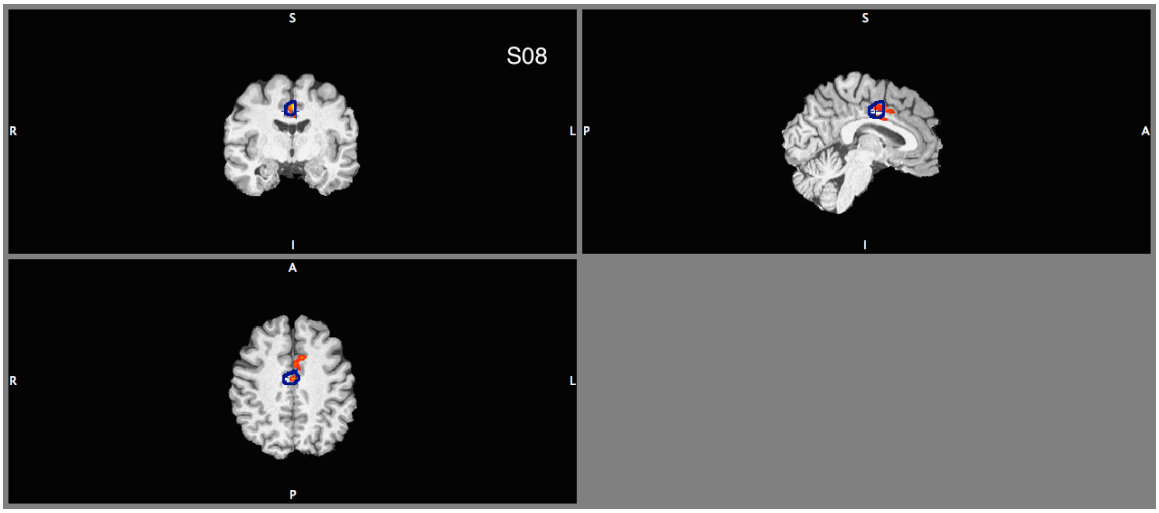

Figure 21. CSv activity in all subjects in Radial Oscillating > Scrambled Smooth contrast. The blue outline represents approximate localtion of ROI. Red-yellow colour gradient represents above-threshold BOLD activity. The blue

outline represents approximate localtion of subject's custom made mask. Red-yellow colour gradient represents above-threshold BOLD activity within larger mask (Table 4).

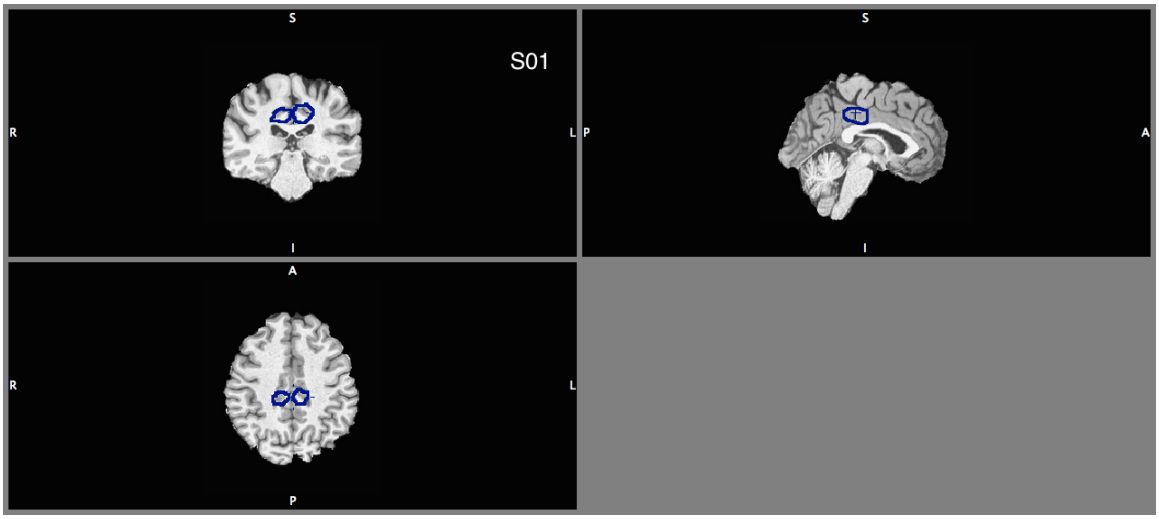

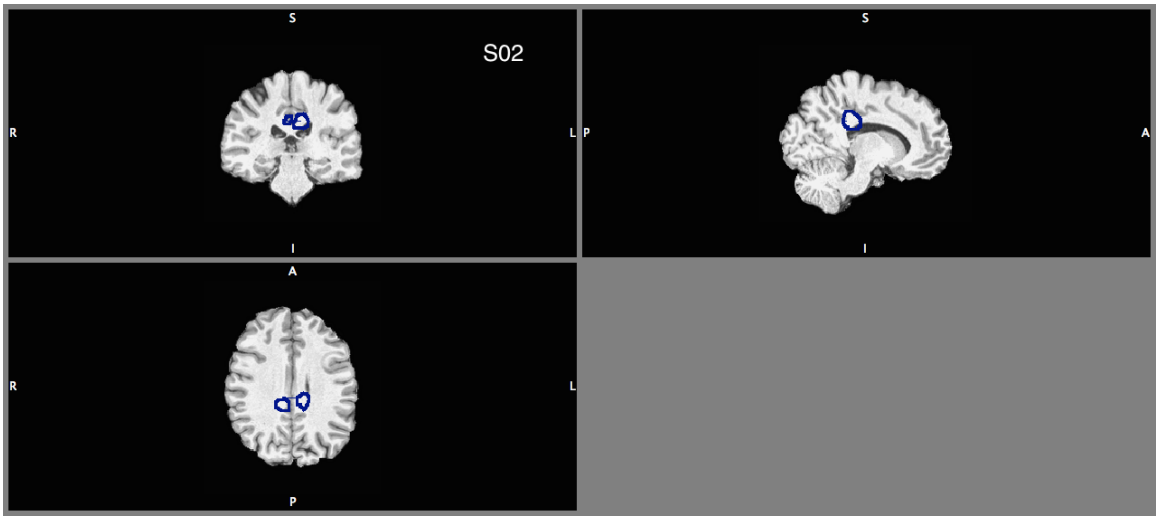

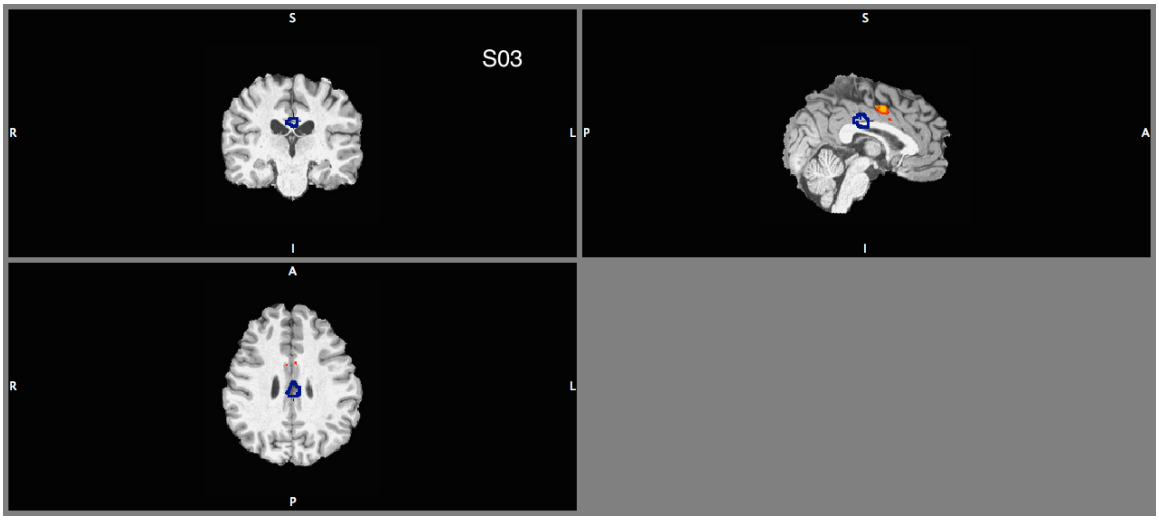
S03
S
R
L
I
P
A

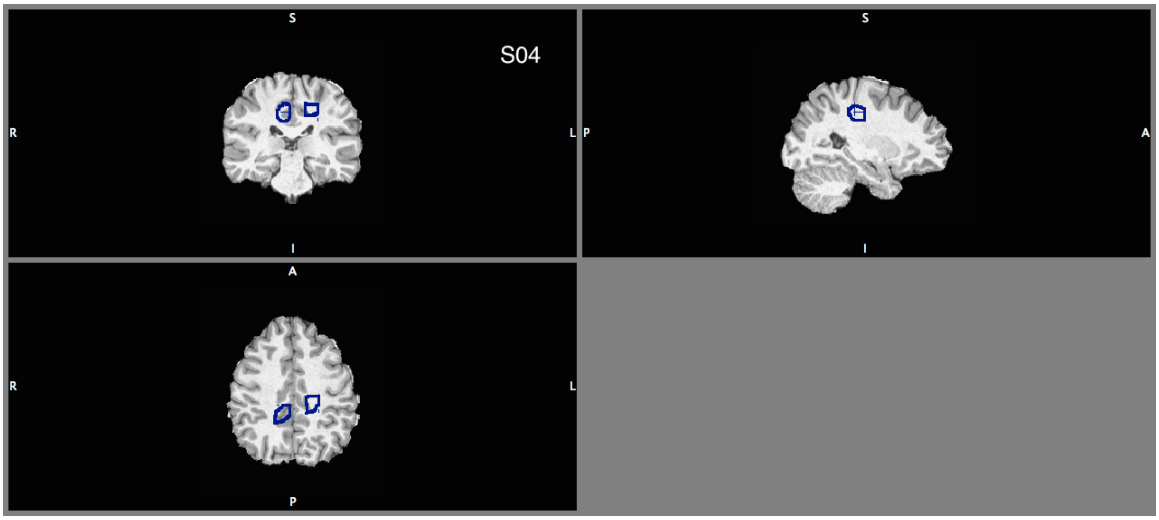
S04
S
R
L
I
P
A

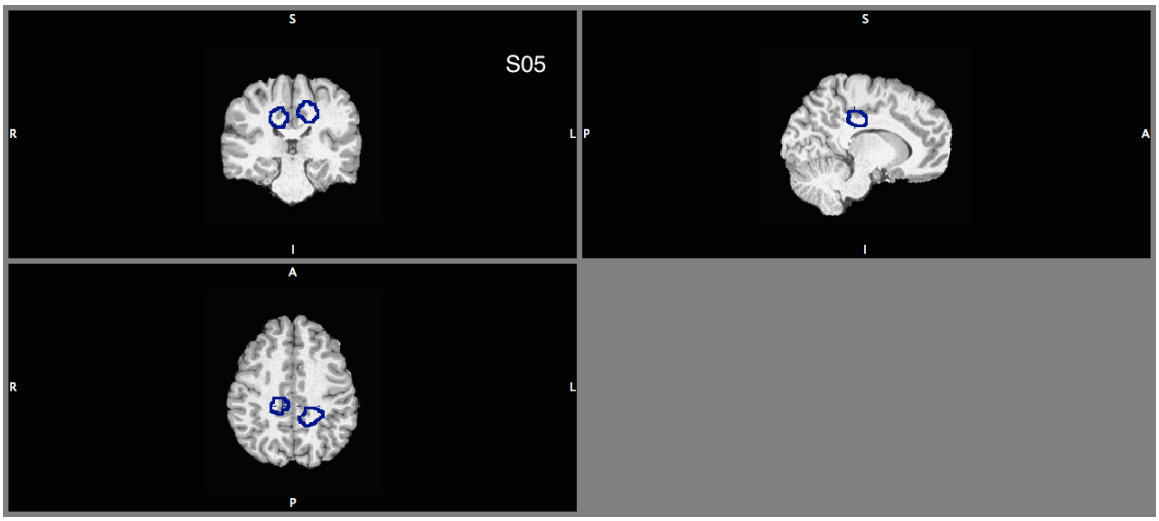
S05
S
R
L
I
P
A

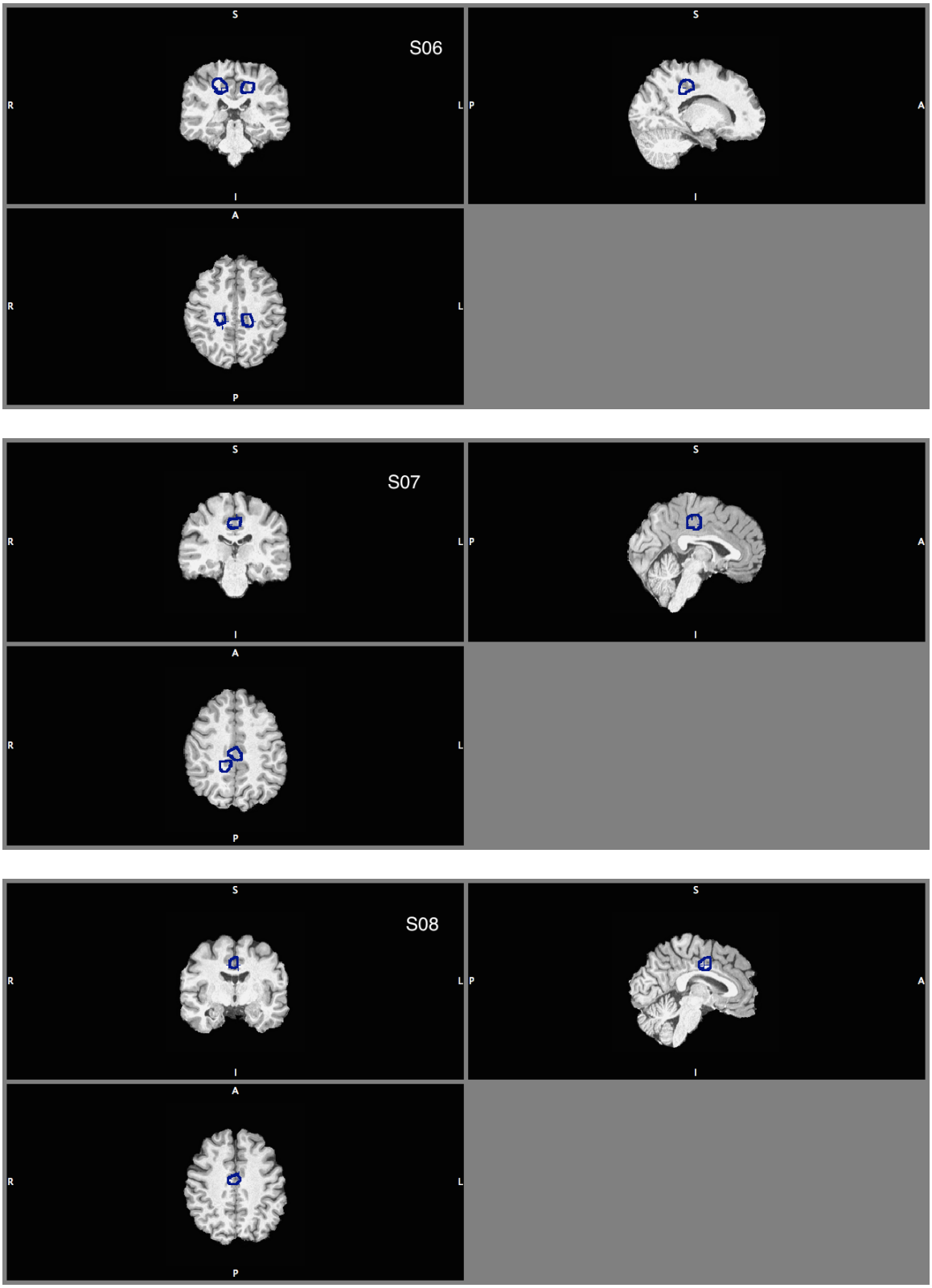

Figure 22. CSv activity in all subjects for the Scrambled Smooth >Radial Oscillating contrast.

In the *Radial Motion* > *Scrambled Motion* contrast, shown in Figure 23, there was preference for vection stimuli in 5 of 8 participants in area CSv. Figure 24 demonstrates the opposite of this contrast (Scrambled Motion > Radial Motion) in which there is no CSv activity. A significant change in BOLD activity would be expected in this contrast for vection sensitive areas. This is because this contrast combines both radial conditions hypothesized to induce strong vection perception compared to the combined scrambled motion conditions that do not induce strong vection. Illustrations representing BOLD activity for this contrast are presented below.

Radial Motion > Scrambled Motion

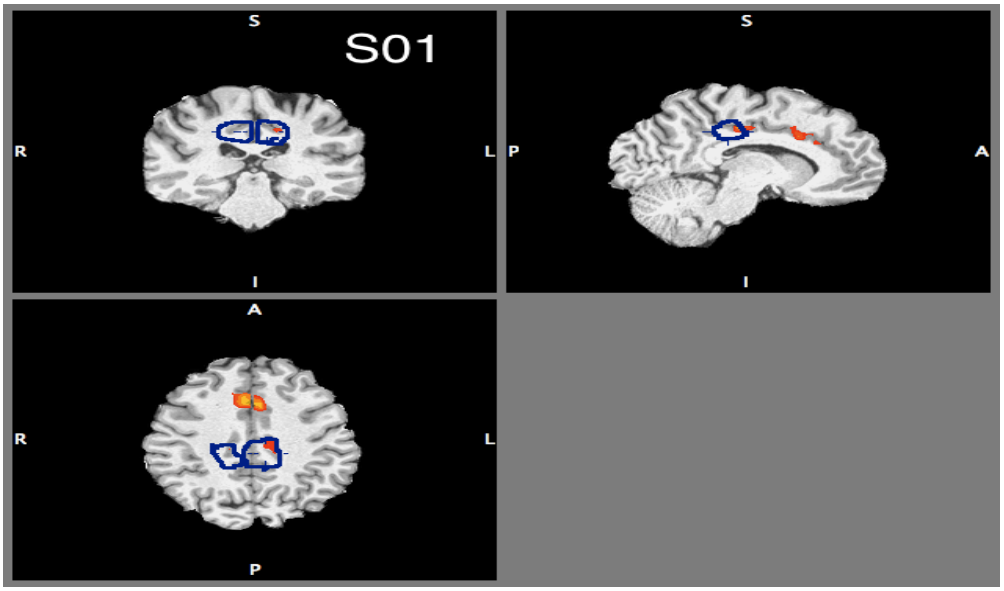

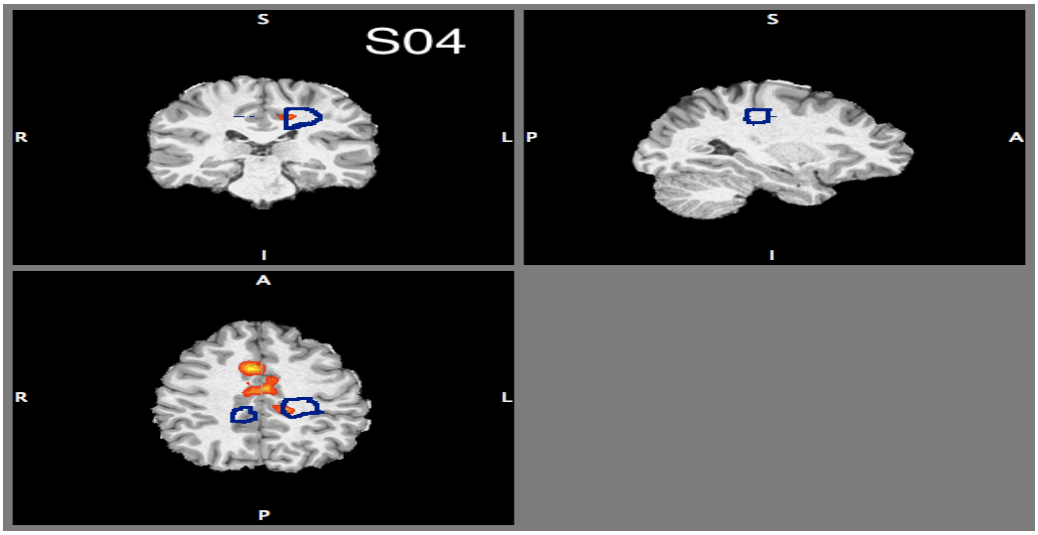
S04
S
R
L
I
S
P
A
I
A
R
L
P

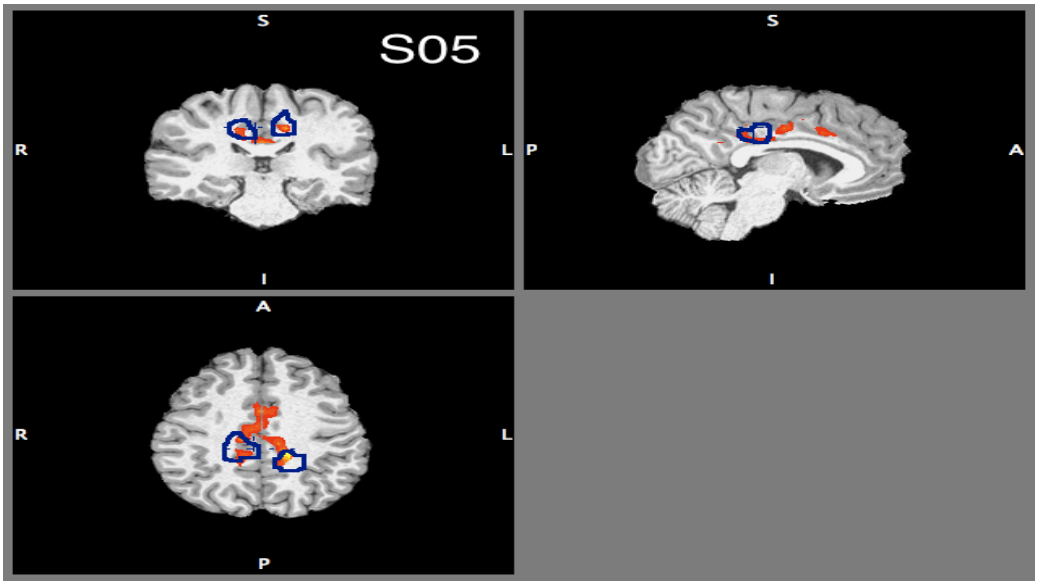
S05
S
R
L
I
S
P
A
I
A
R
L
P

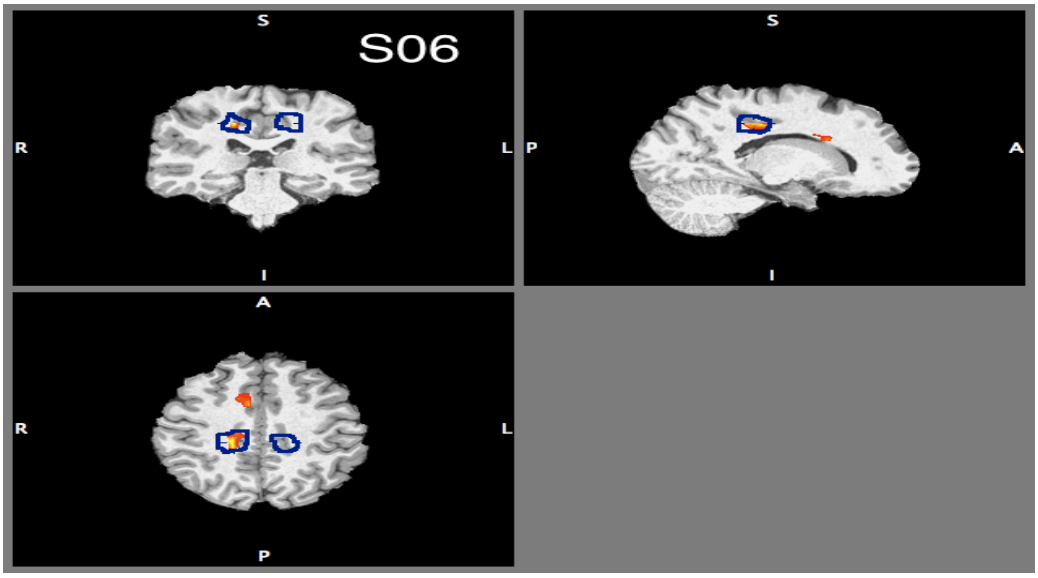
S06
S
R
L
I
S
P
A
I
A
R
L
P

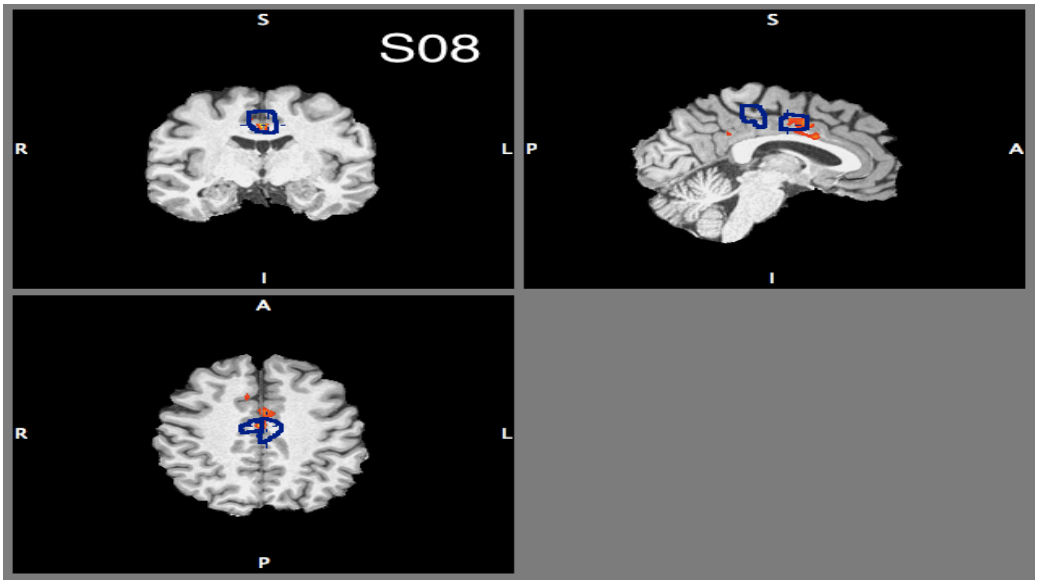

Figure 23. Radial Motion> Scrambled Motion contrast results for area CSv for 5 subjects with significant CSv activity.

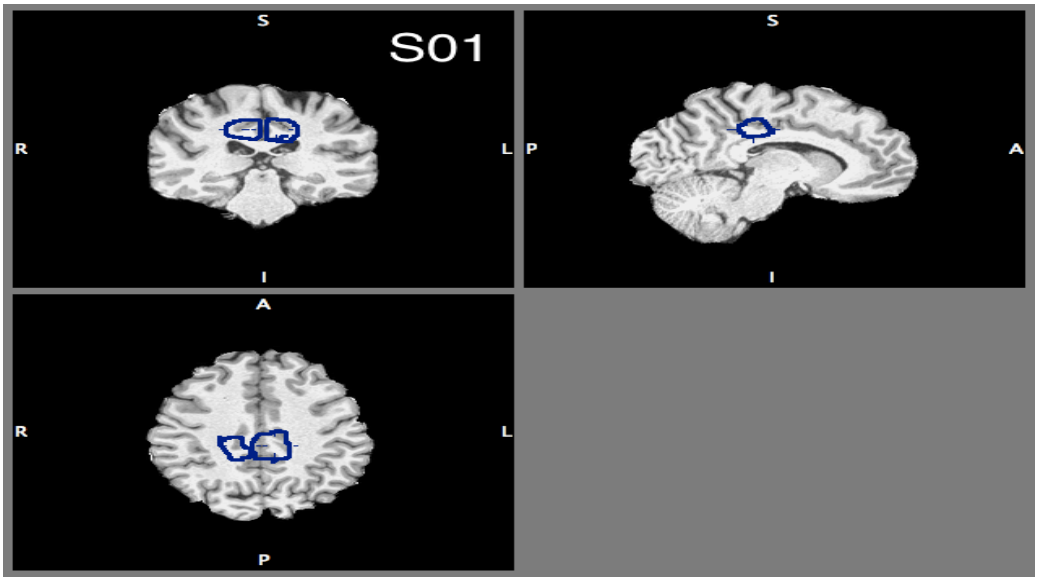

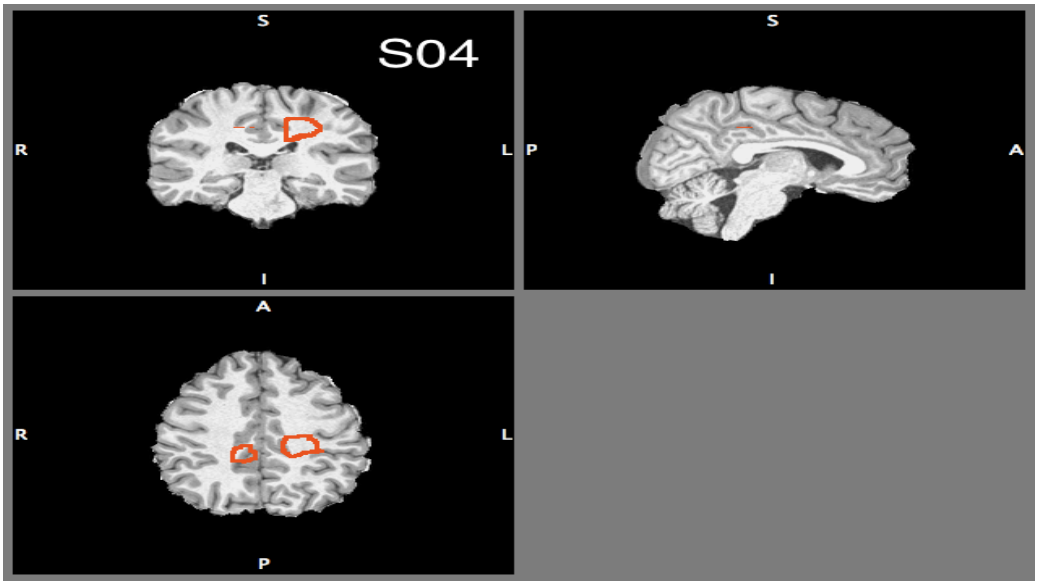
S04
S
R
L
I
S
P
A
I
A
R
L
P

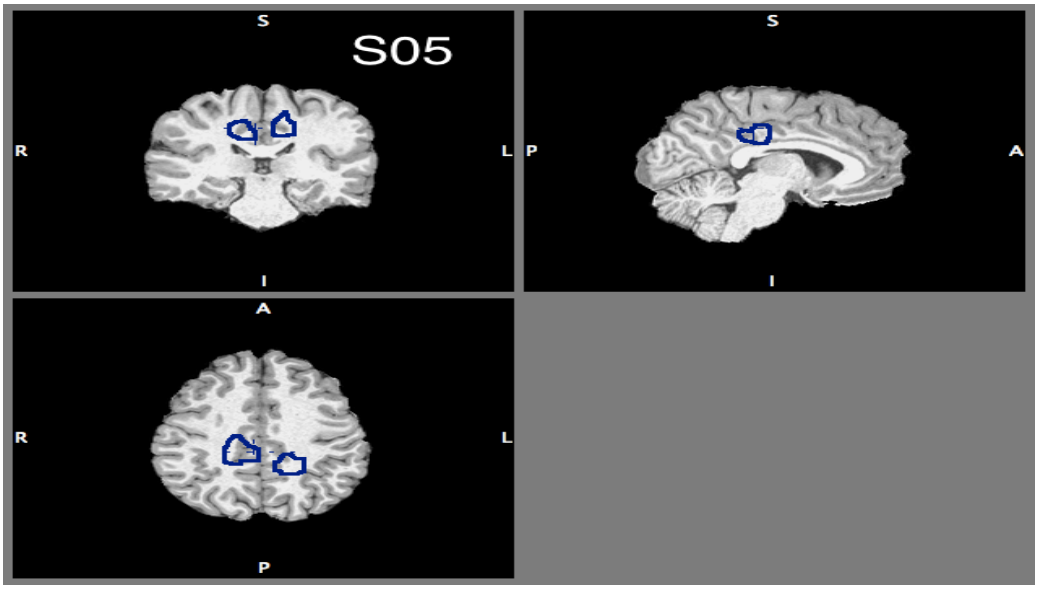
S05
S
R
L
I
S
P
A
I
A
R
L
P

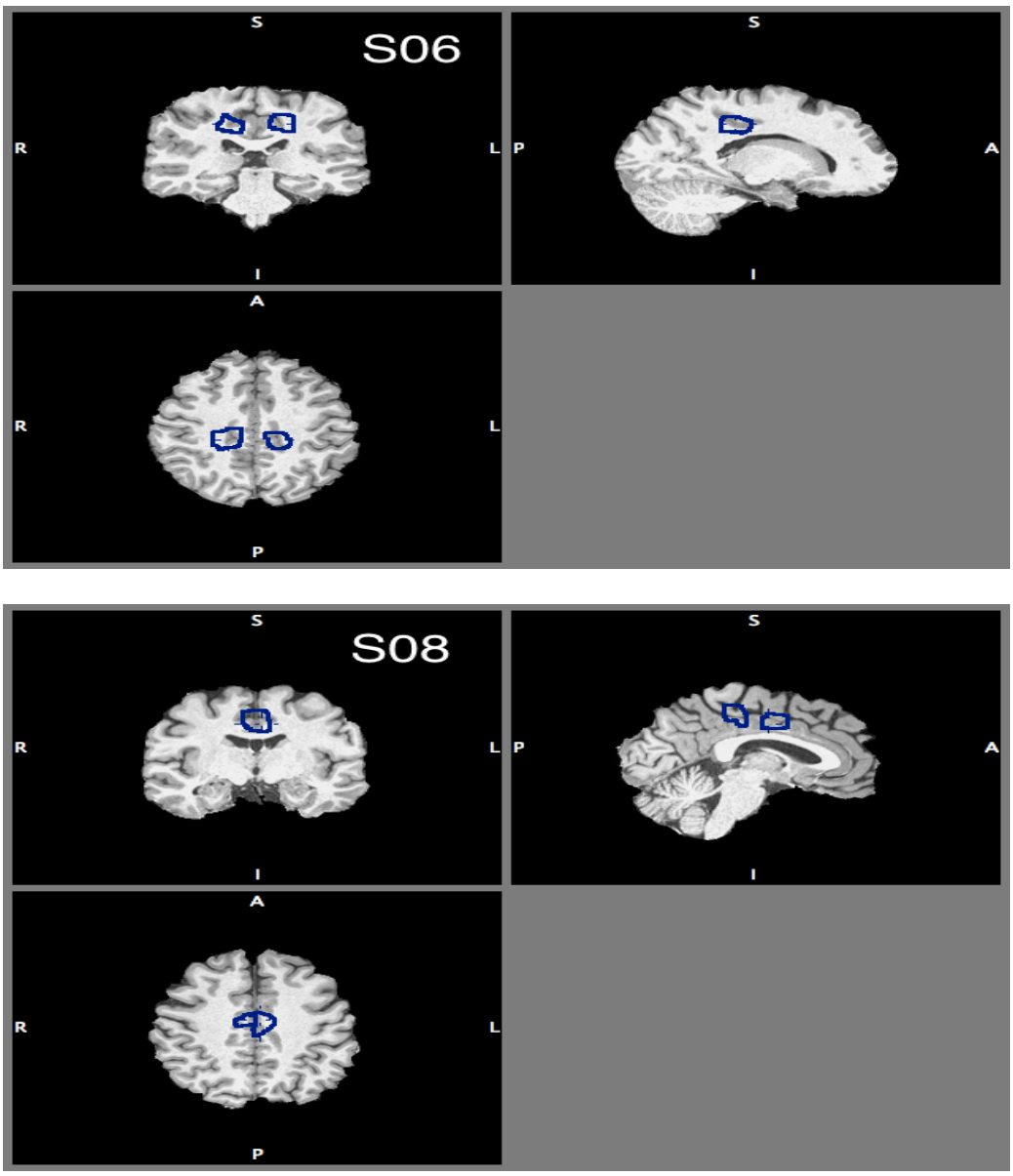

Figure 24. Scrambled Motion > Radial Motion contrast results for area CSv for 5 subjects with significant CSv activity.

Of major importance is CSv's strong response for the Radial Oscillating > Radial Smooth contrast. 7 of 8 participants showed significant activity when comparing Radial Oscillating to Radial Smooth conditions (Figure 25). Conversely, there is no CSv activity when comparing the radial smooth to the radial oscillating contrast (Figure 26). This is important because it relates to the hypothesized jitter effect. Moreover, this

contrast was significant in PIVC. Thus, from the results of the Radial Oscillating > Radial Smooth contrast, CSv demonstrates significant preference for the stronger vection display as did PIVC.

Radial Oscillating > Radial Smooth

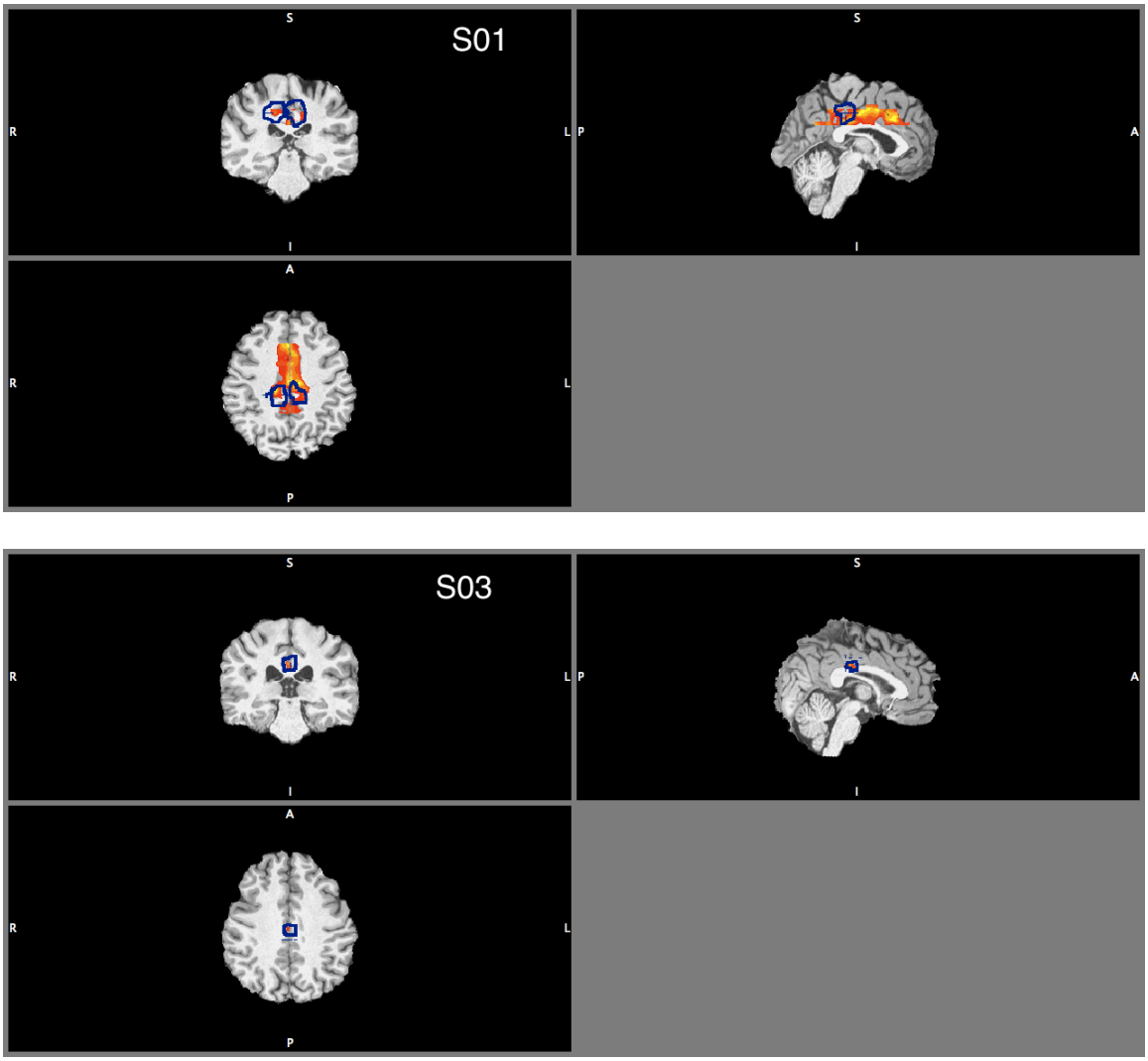

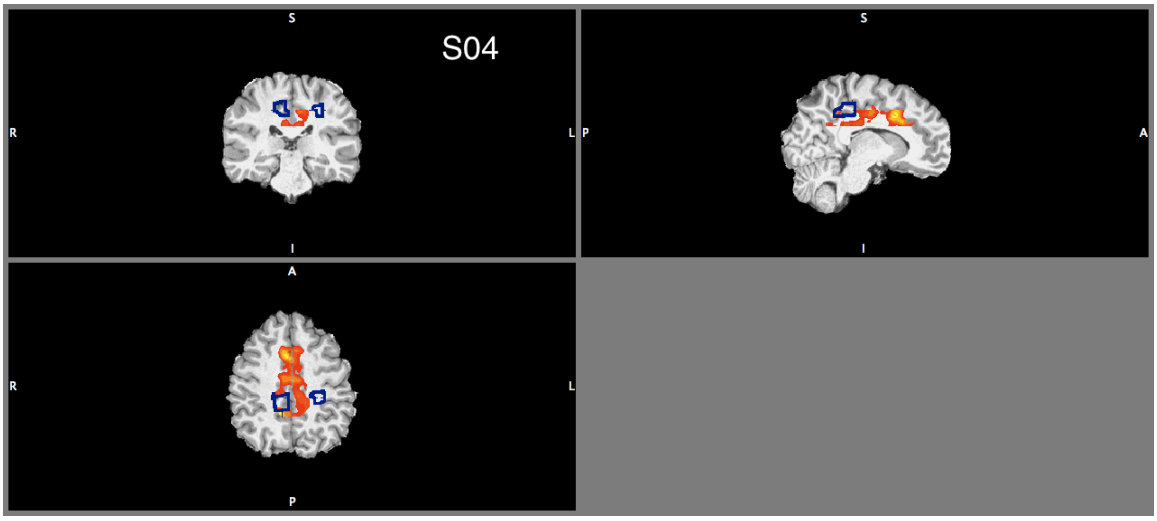
S04
S
R
L
I
P
A
A
R
L
P

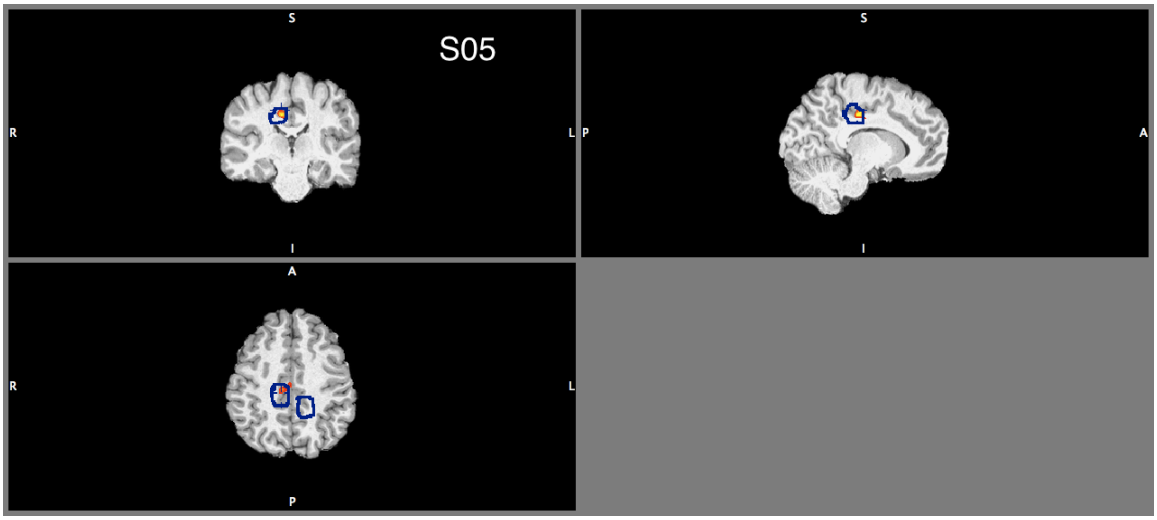
S05
S
R
L
I
P
A
A
R
L
P

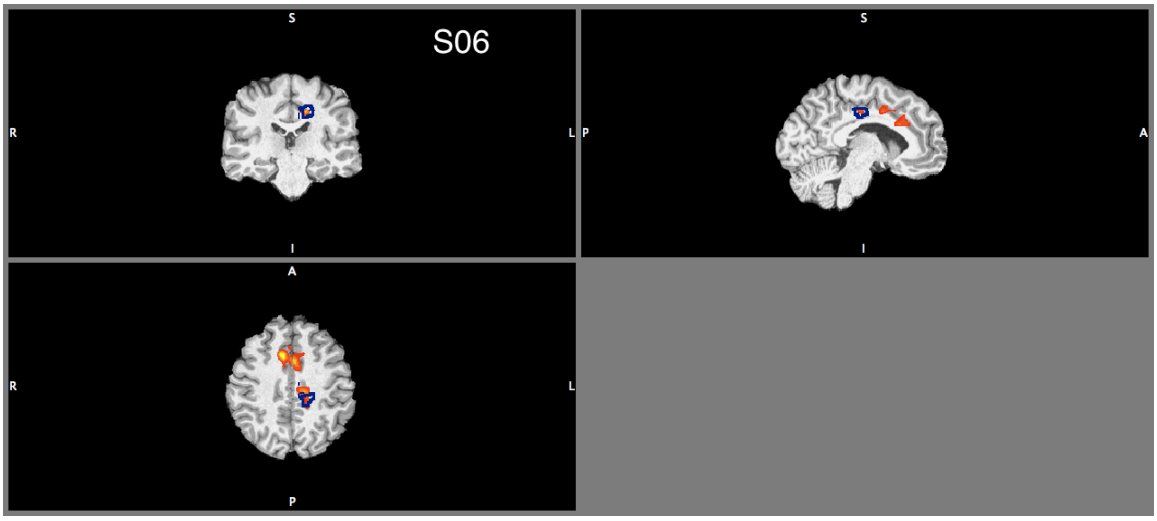
S06
S
R
L
I
P
A
A
R
L
P

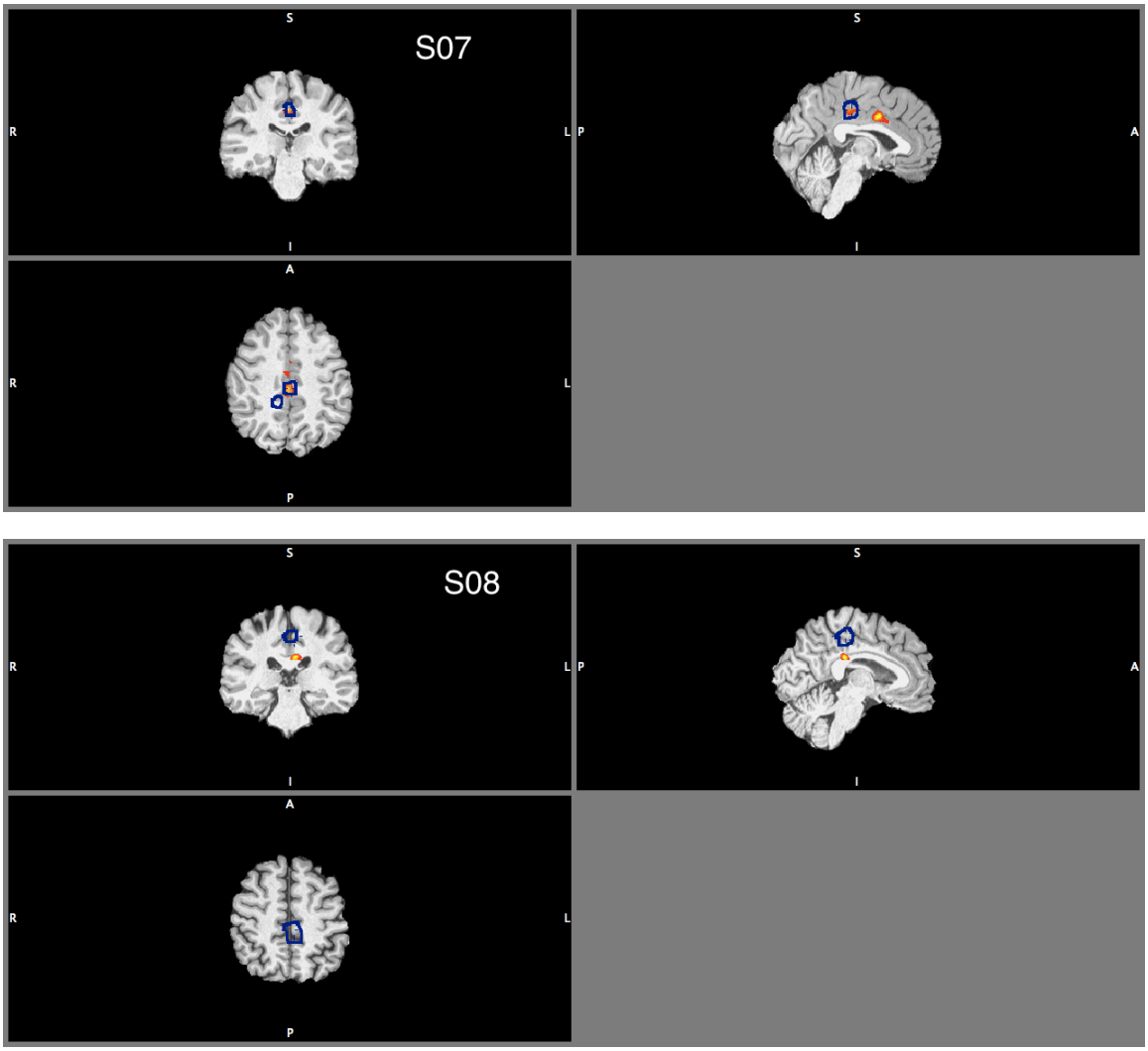

Figure 25. BOLD activity in Radial Oscillating > Radial Smooth contrast in CSv. These results indicate a jitter effect because CSv appears to distinguish a strong vection inducing stimulus from another.

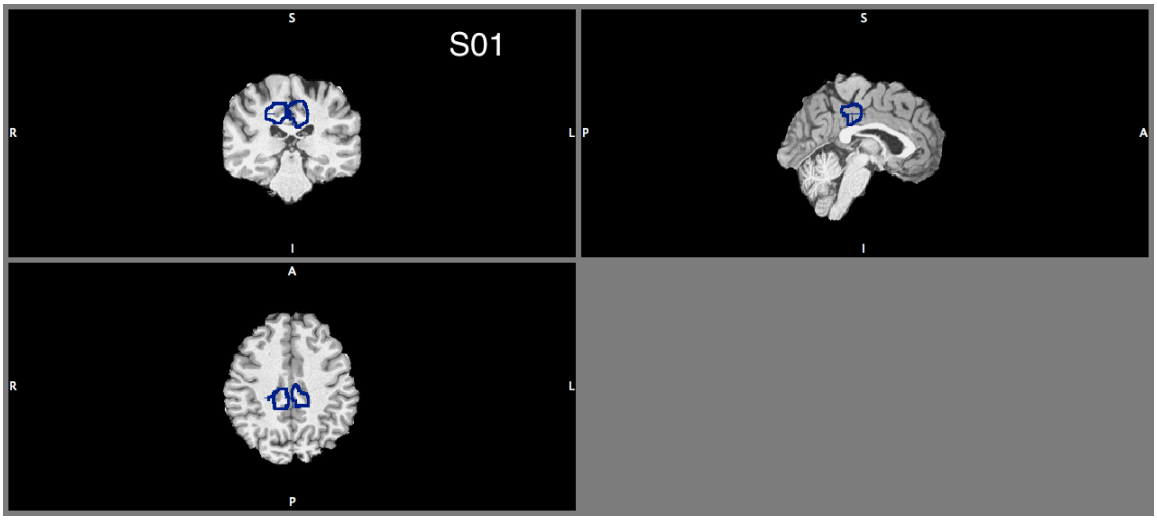
S01
S
R
L
I
P
A
A
R
L
P

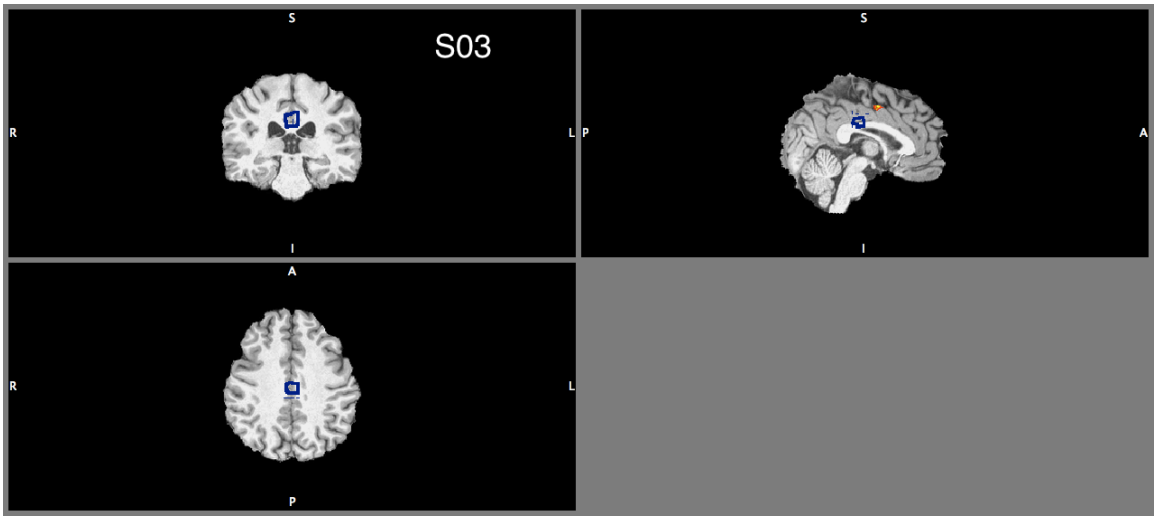
S03
S
R
L
I
P
A
A
R
L
P

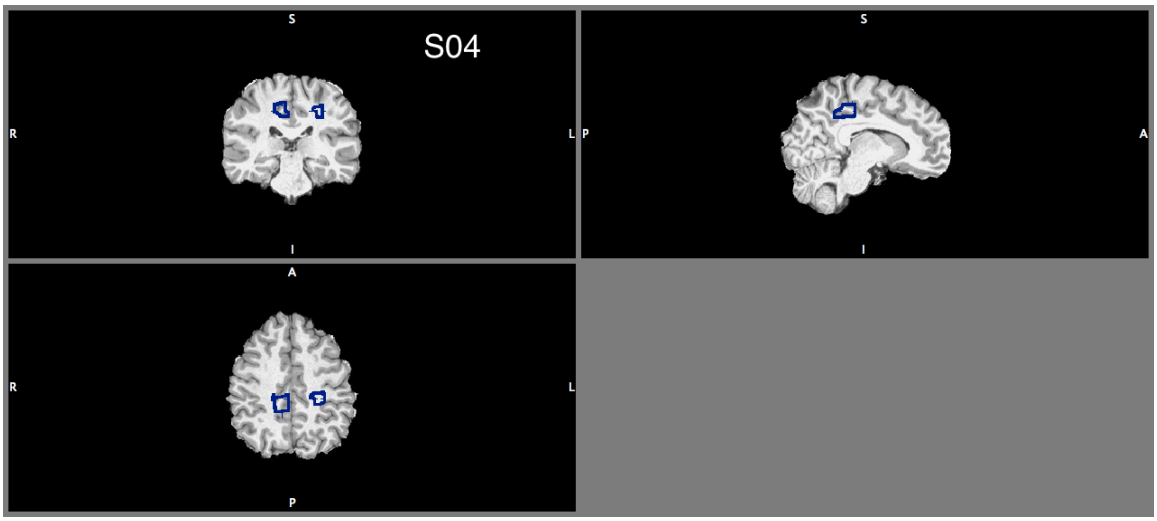
S04
S
R
L
I
P
A
A
R
L
P

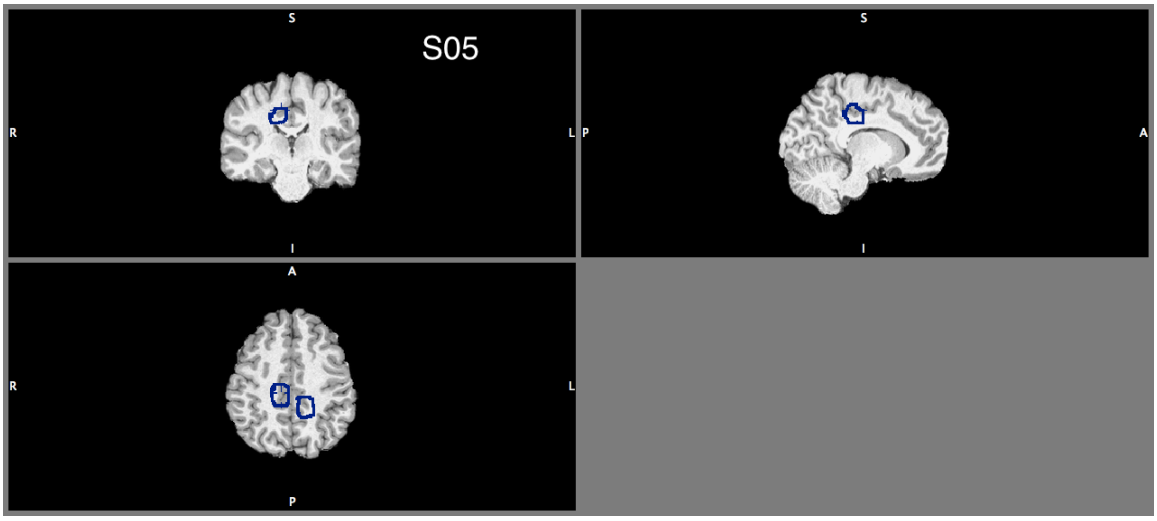
S05
S
R
L
I
S
P
A
I
A
R
L
P

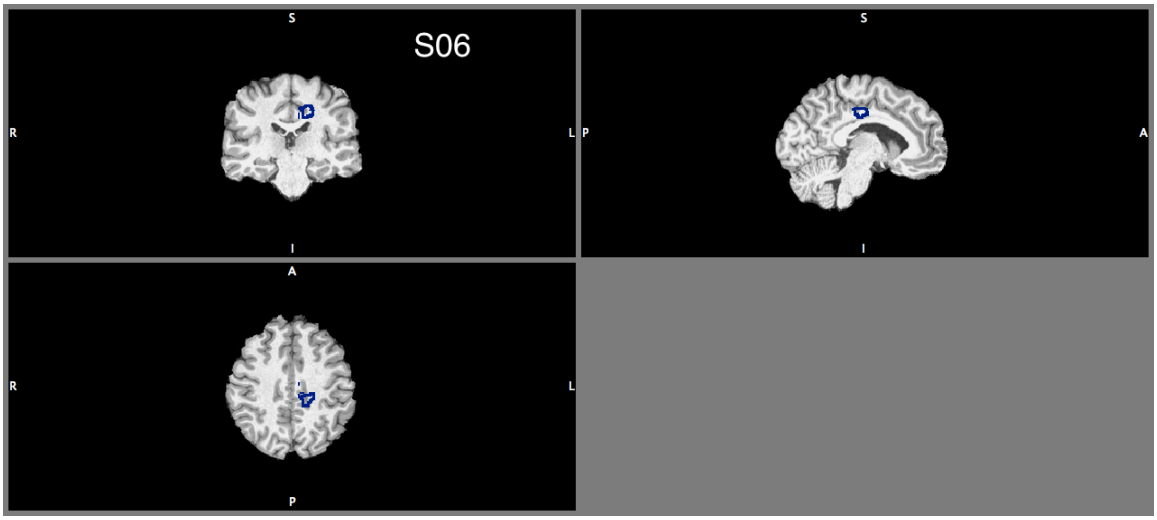
S06
S
R
L
I
S
P
A
I
A
R
L
P

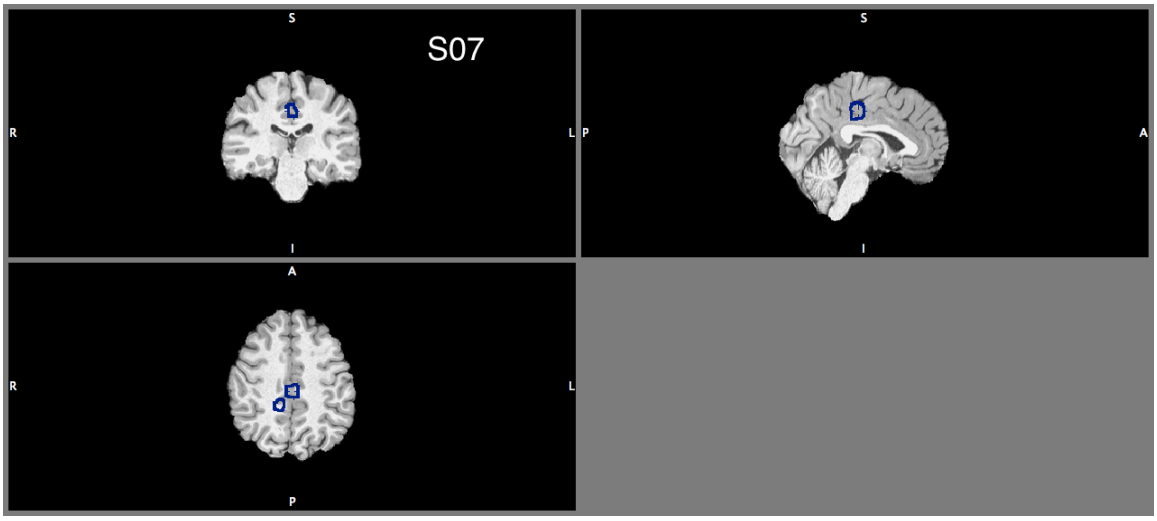
S07
S
R
L
I
S
P
A
I
A
R
L
P

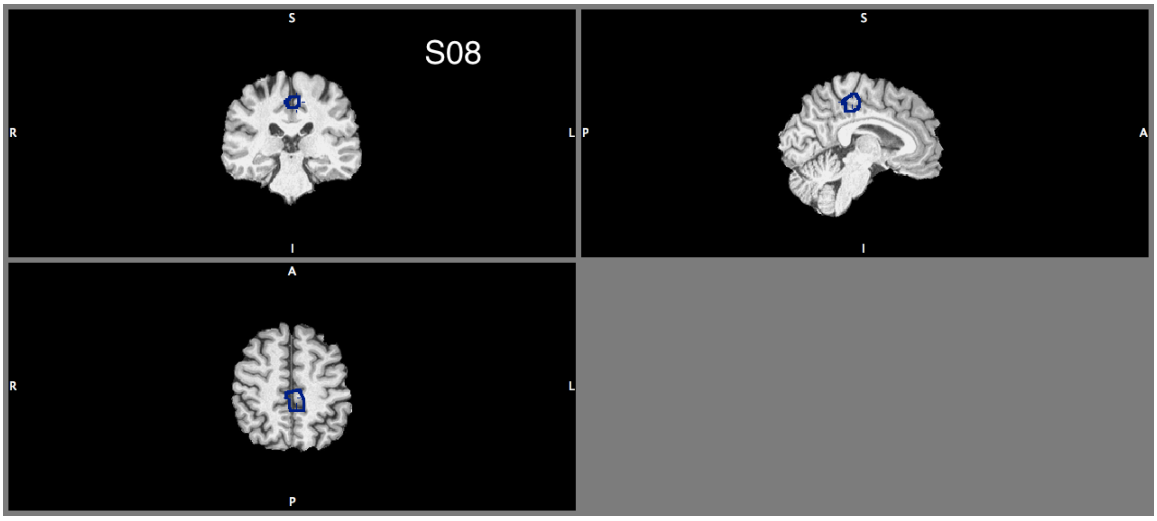

Figure 26. BOLD activity in Radial Smooth > Radial Oscillating contrast in CSv. These results suggest a correlation with behaviourally observed jitter effect because CSv apparently becomes active during oscillating radial displays but not for the radial smooth display.

Of note is that CSv was the only region that showed the hypothesized preference for oscillation in the Radial Oscillating > Scrambled Oscillating contrast, with 5 of 8 participants having significant Z-scores for this contrast and providing further evidence of CSv sensitivity to vection. This is because the intent of this contrast was to keep all factors other than vection perception constant. We hypothesized that if a brain region showed significant activity in this contrast, and in the Radial Smooth > Scrambled Smooth contrast, this would indicate a clear vection preference for the region. Despite not finding significance in the Radial Smooth > Scrambled Smooth contrast, CSv appears to be a brain region strongly sensitive to vection from radial optic flow stimuli based on our results.

VIP Activity

We obtained inconsistent results for area VIP, known for its involvement in egomotion compatible displays. This is because it showed increased activity for the

Radial Motion > *Scrambled Motion* contrast for 5 of 8 participants but aside from this contrast, it showed a slight preference for scrambled motion conditions over radial motion conditions. This is contrary to its hypothesized role in processing visual egomotion. It is possible that lateral intraparietal region (LIP) or medial intraparietal region (MIP) which are both object motion regions neighbouring VIP, were activated by the scrambled condition contrasts (Colby and Duhamel, 1991). However, contrary to previous findings we did not find evidence for VIP activation during vection-inducing stimuli.

V6 Activity

Findings for area V6 are also inconsistent because it responded strongly in the Radial Motion > Scrambled Motion contrast, but also to the Scrambled Oscillating > Radial Oscillating and Scrambled Smooth > Radial Smooth contrast. V6 activity in the Radial Motion > Scrambled Motion contrast is on the other hand consistent with its hypothesized role in wide-field optic flow stimulation (Pitzalis et al., 2006). The BOLD activity for this contrast is shown in figures 27 and 28. 7 of 8 participants had a significant Z-score within the V6 region for this contrast. In all, our findings on V6 differ from those discussed in the neuroimaging literature on V6 involvement in vection. Scrambled motion contrasts showing increased activity in V6 may be caused by coincidental localizing of region V6a - a visual object motion region located close to V6 (Pitzalis et al., 2013). Unlike for CSv and PIVC, custom-made masks were not made for V6. This is because no other regions were sufficiently responsive to vection displays.

Instead here, the blue outline represents region with highest activity within larger mask used (Table 4).

Radial Motion > Scrambled Motion

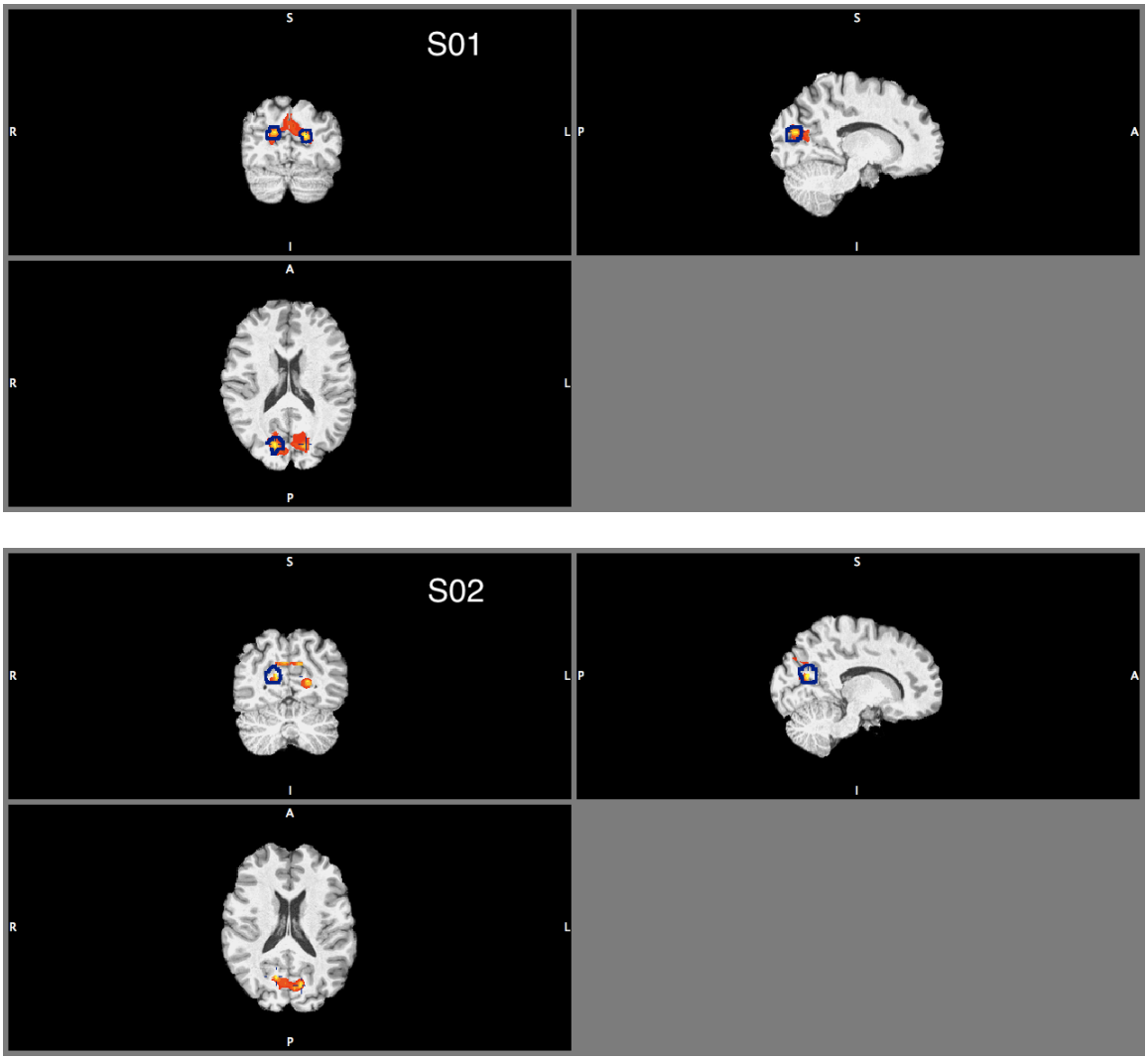

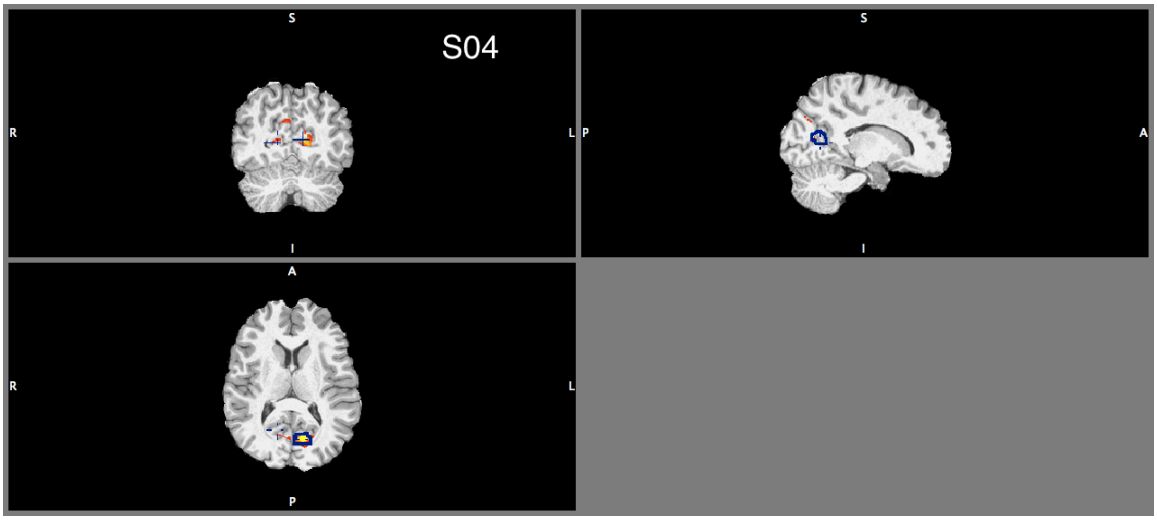
S04
S
R
L
I
S
P
A
I
A
R
L
P

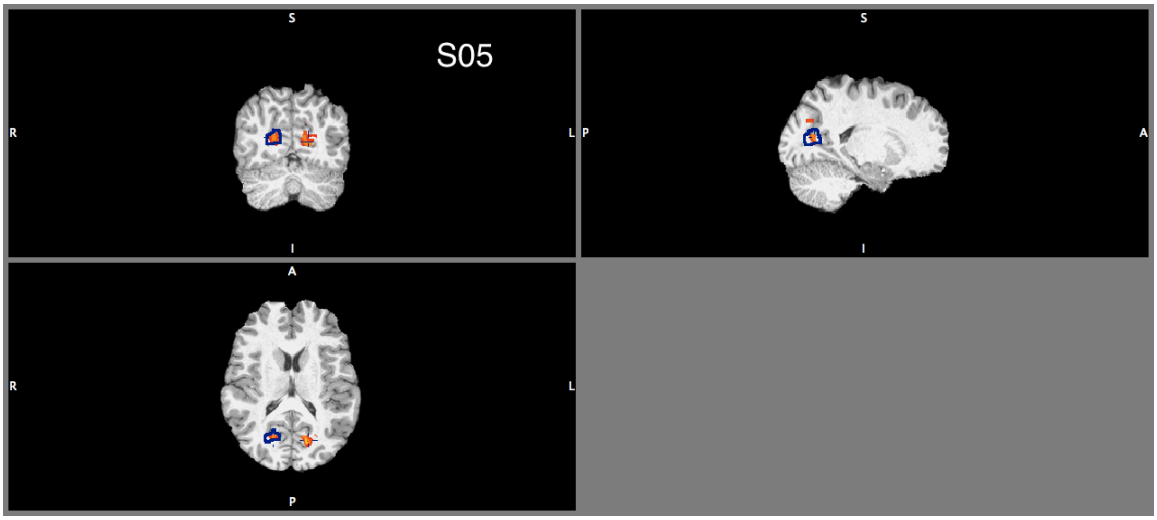
S05
S
R
L
I
S
P
A
I
A
R
L
P

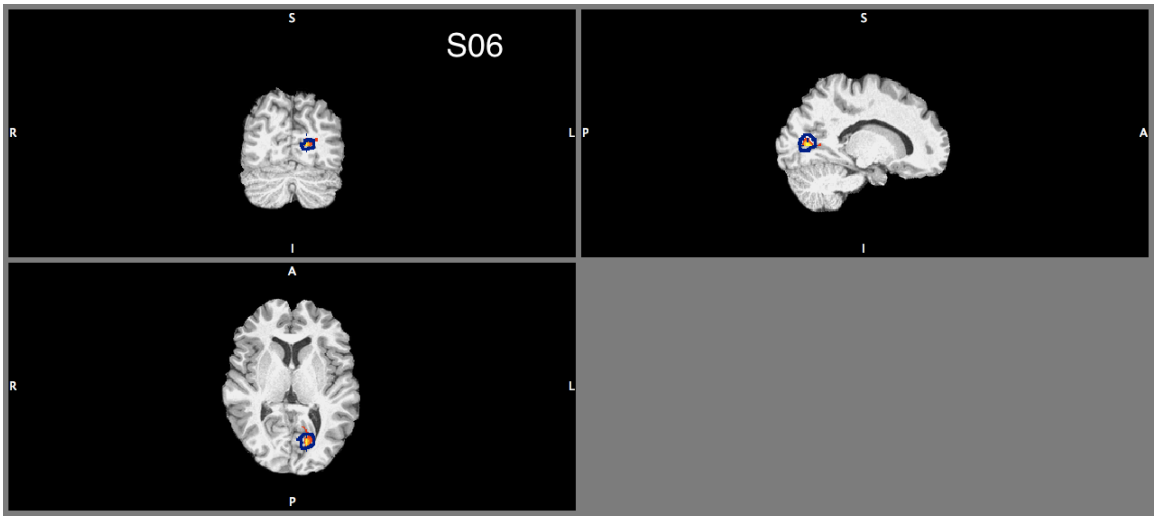
S06
S
R
L
I
S
P
A
I
A
R
L
P

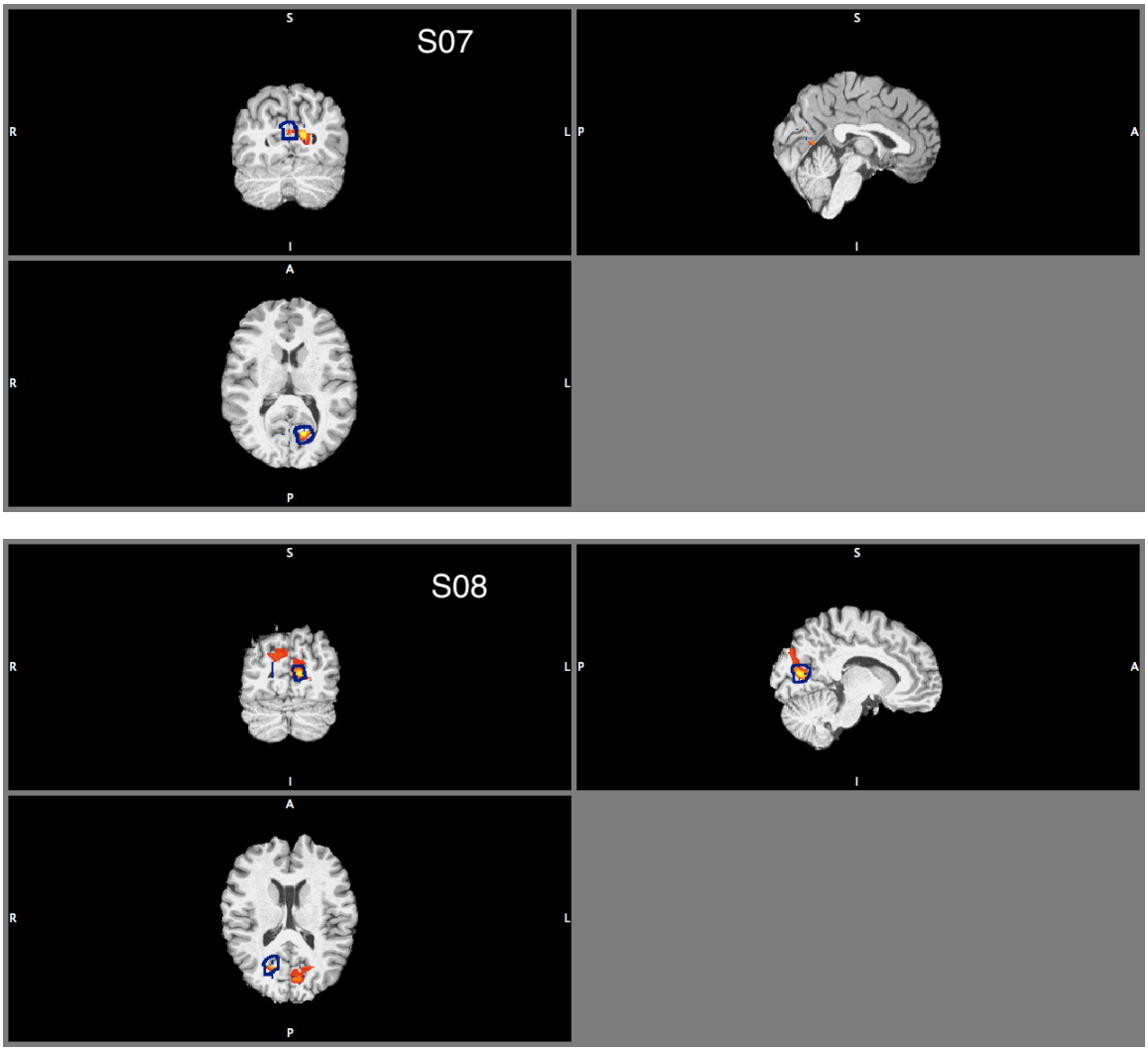

Figure 27. Figures depicting V6 activity in *Radial Motion > Scrambled Motion* contrast. Blue outline represents region with highest activity within larger mask used (Table 4). This is because custom made masks were not made for regions other than PIVC and CSv because no other regions were sufficiently responsive to vection displays.

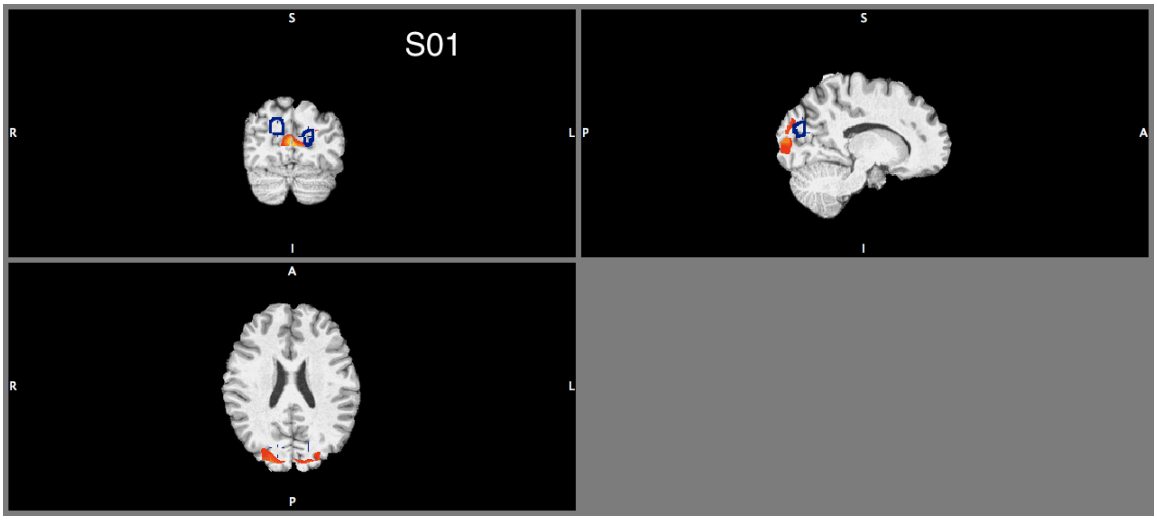
S01
S
R
L
I
P
A

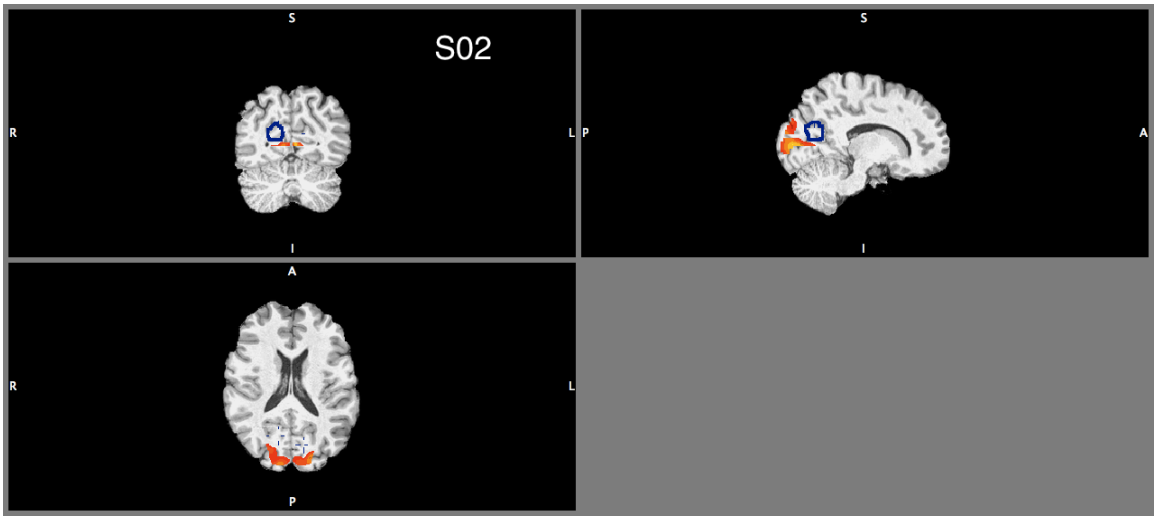
S02
S
R
L
I
P
A

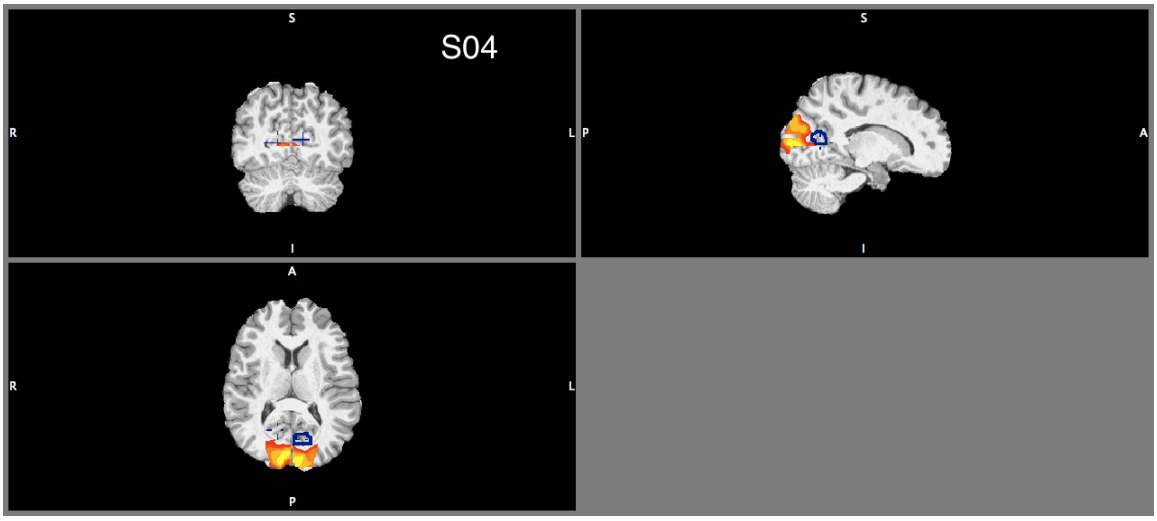
S04
S
R
L
I
P
A

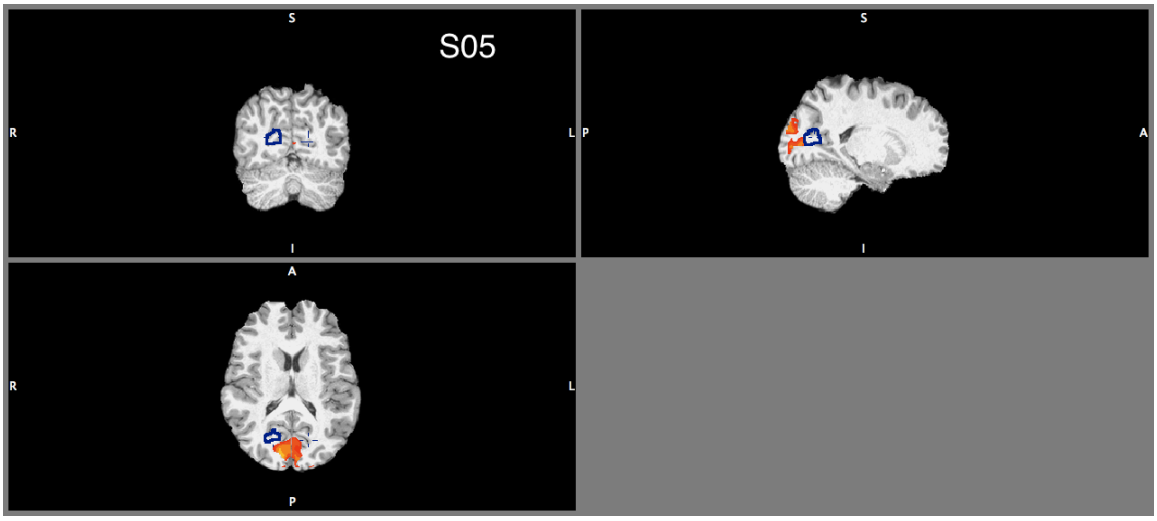
S05
S
R
L
I
P
A

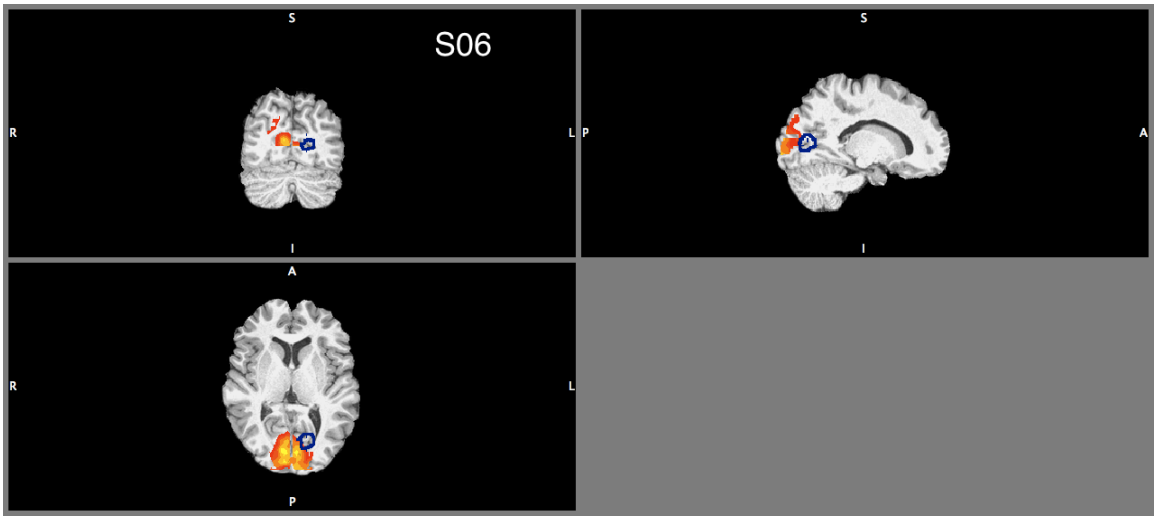
S06
S
R
L
I
P
A

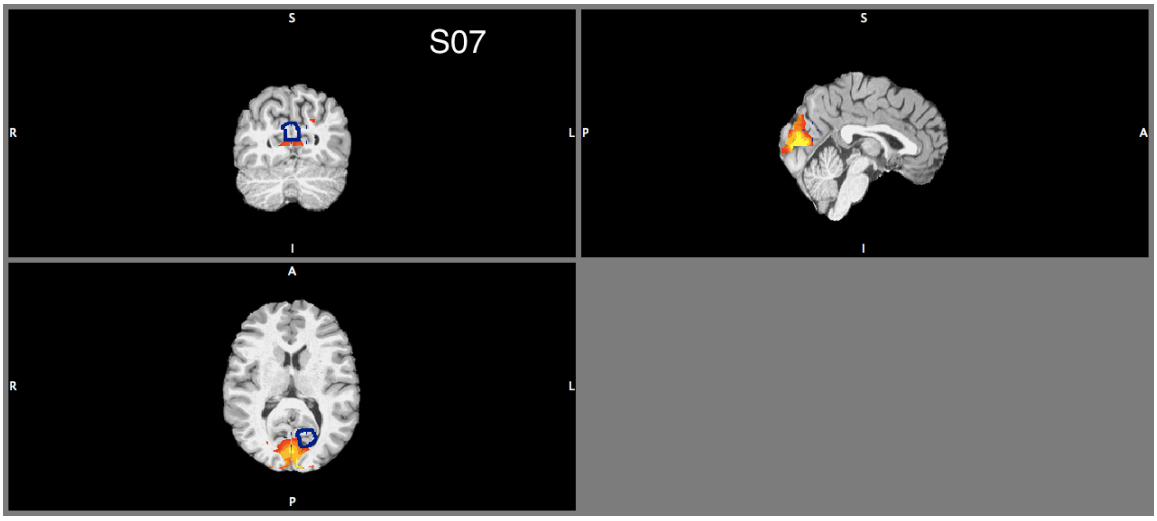
S07
S
R
L
I
P
A

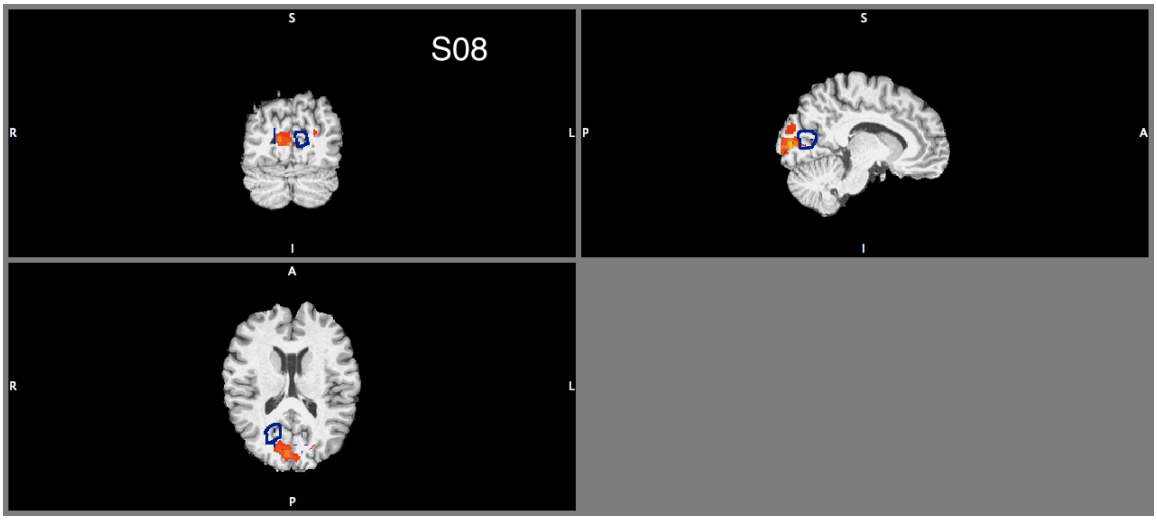

Figure 28. Figures depicting V6 activity in *Scrambled Motion* > *Radial Motion* contrast. Blue outline represents region with highest activity within larger mask used (Table 4). This is because custom made masks were not made for regions other than PIVC and CSv because no other regions were sufficiently responsive to vection displays.

Pc Activity

Precuneus motion area showed preferential activation in the Radial Oscillating > Scrambled Smooth comparison, but did not respond differentially for any other contrast, with 7 of 8 participants showing activity in this contrast. Consistent with literature presented on Pc, this area is active during vection inducing displays, but not as robustly as CSv. Results of this contrast are illustrated in figures 29 and 30 below where figure 29 illustrates findings of the radial oscillating > scrambled smooth contrast for Pc, and figure 30 the scrambled smooth > radial oscillating contrast. Results from figure 30 support reports of possible spatial updating involvement of Pc in vection. Specifically, Pc is involved in visual-spatial updating during vection – a cognitive aspect of self-motion processing. Just as in the V6 data presented in Figures 27 and 28, custom-made masks were not made for Pc. The blue outline represents region with highest activity within larger mask used (Table 4).

Radial Oscillating > Scrambled Smooth

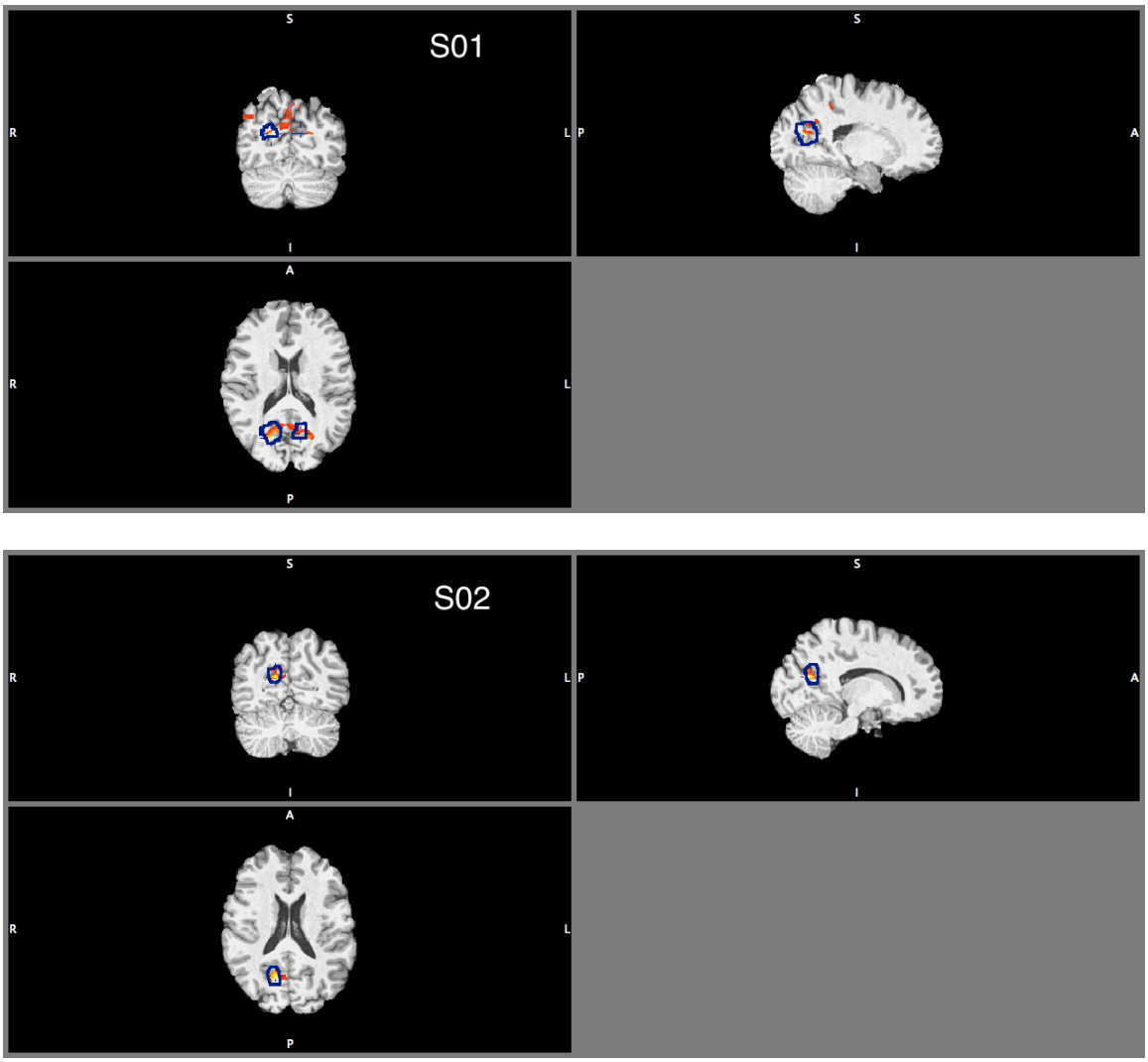

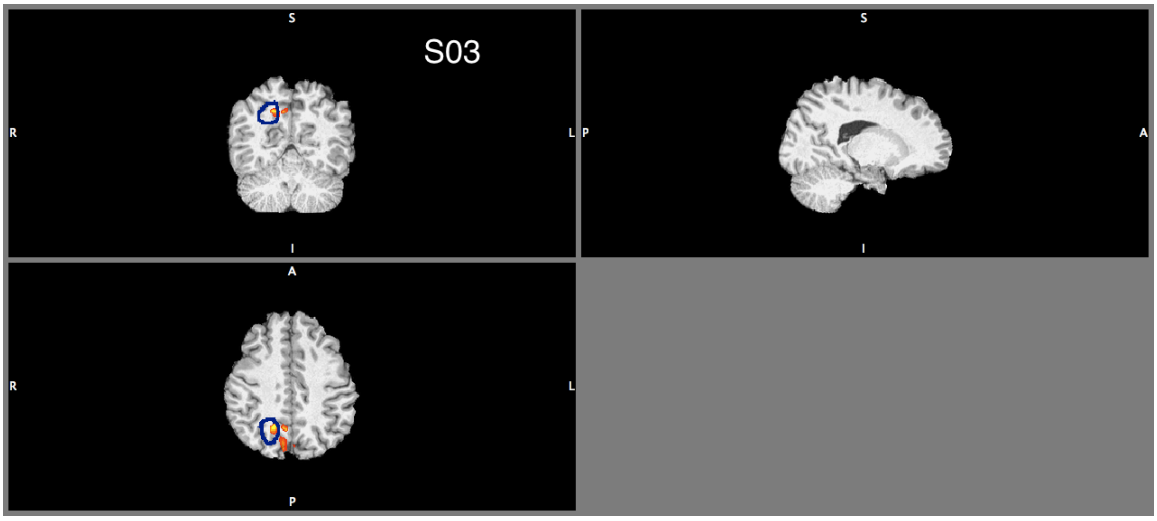
S03
S
R
L
I
P
A

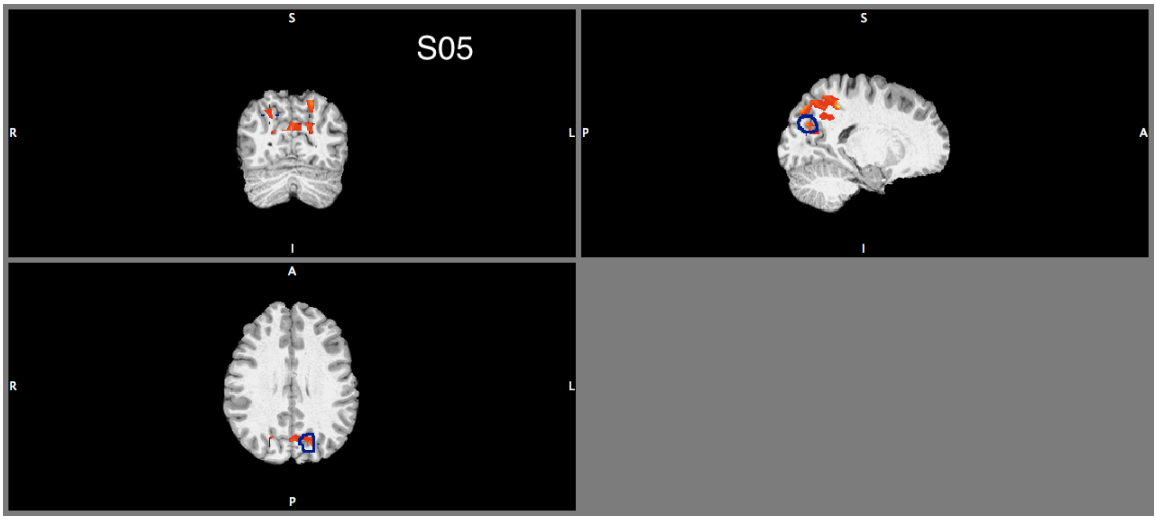
S05
S
R
L
I
P
A

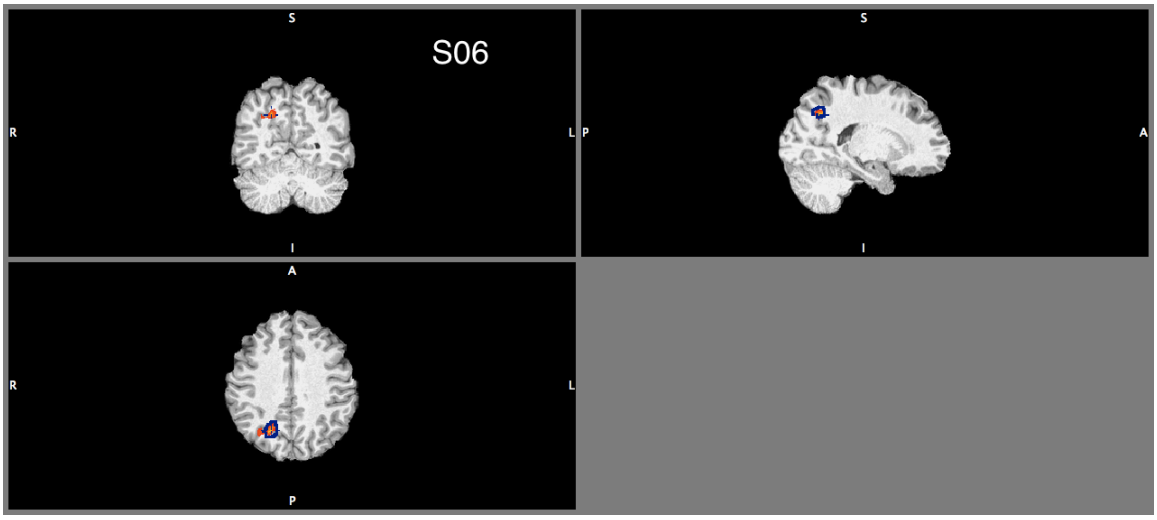
S06
S
R
L
I
P
A

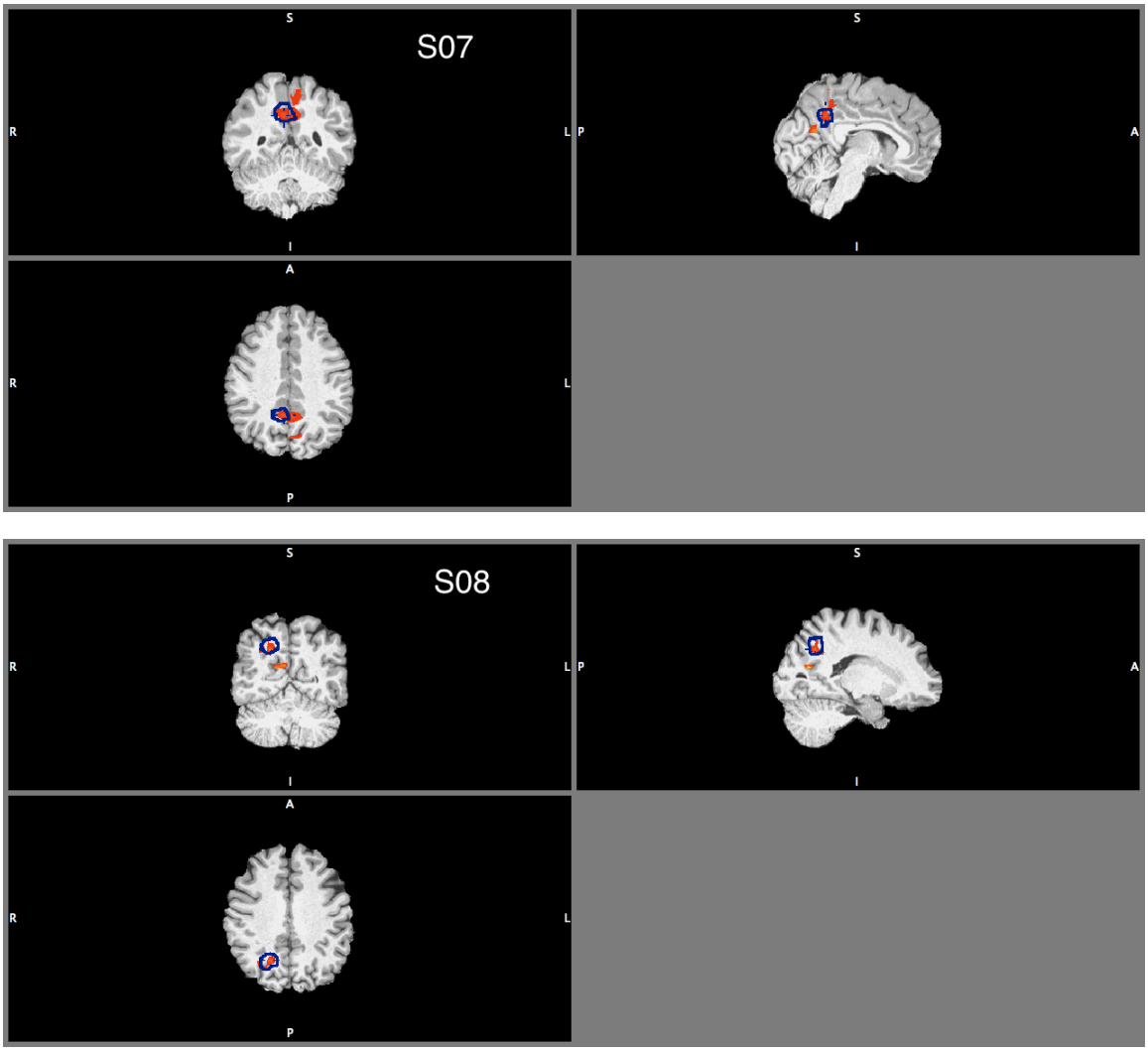

Figure 29. Precuneus activity during Radial Oscillating > Scrambled Smooth contrast. Results support reports of possible spatial updating involvement of Pc in vection. Blue outline represents region with highest activity within larger mask used (Table 4)

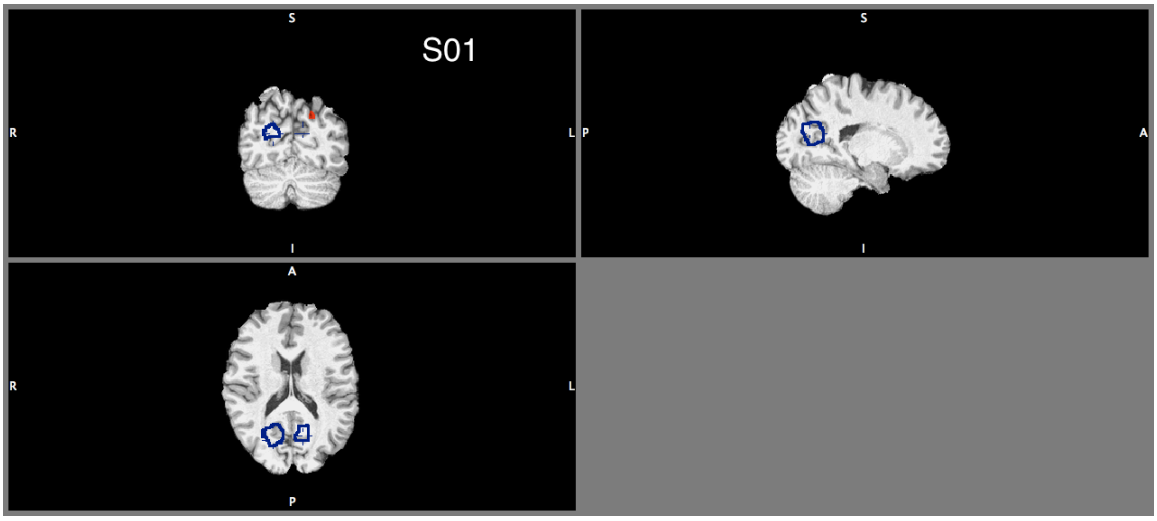
S01
S
R
L
I
P
A

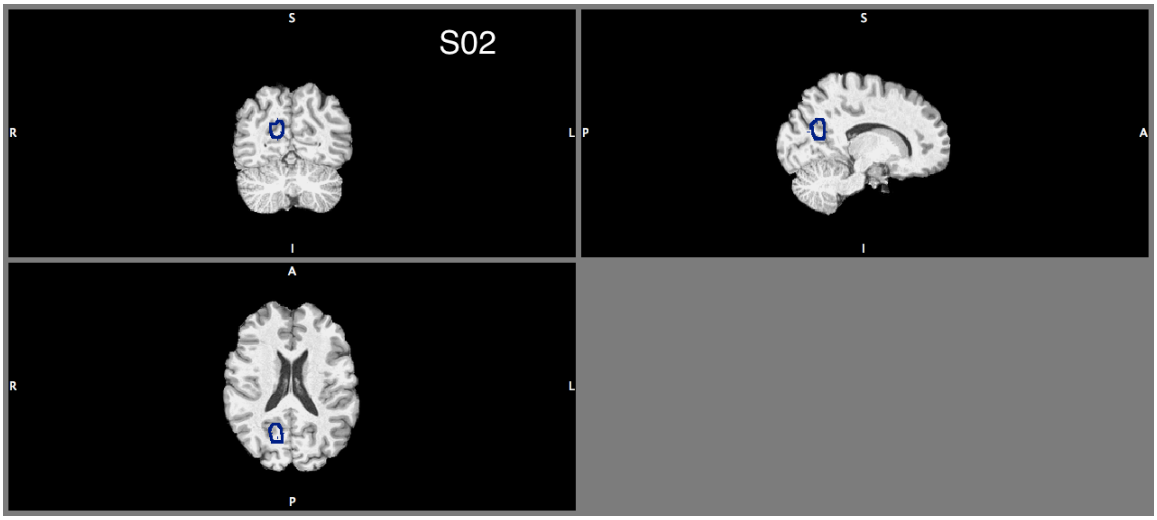
S02
S
R
L
I
P
A

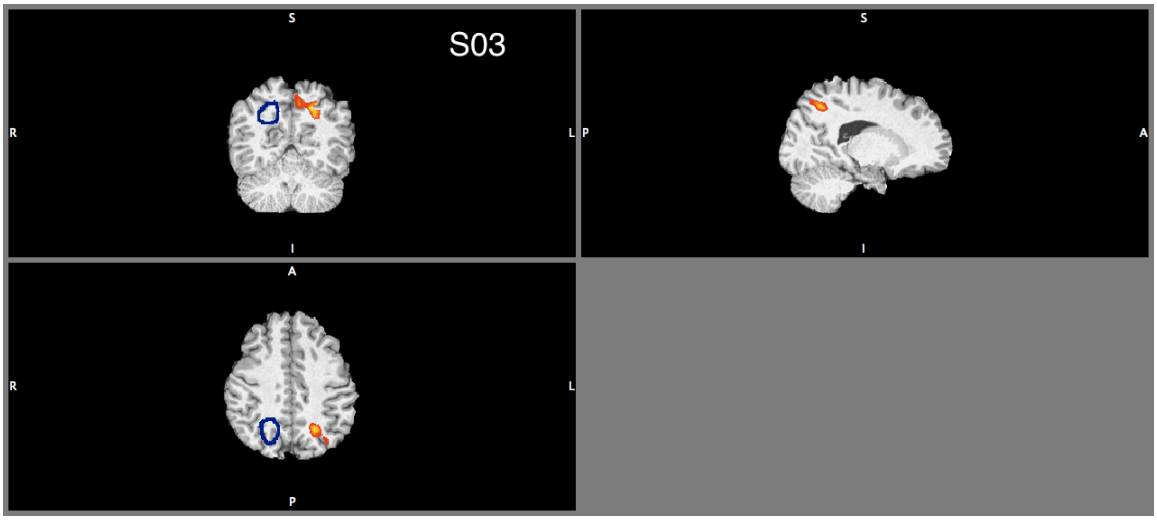
S03
S
R
L
I
P
A

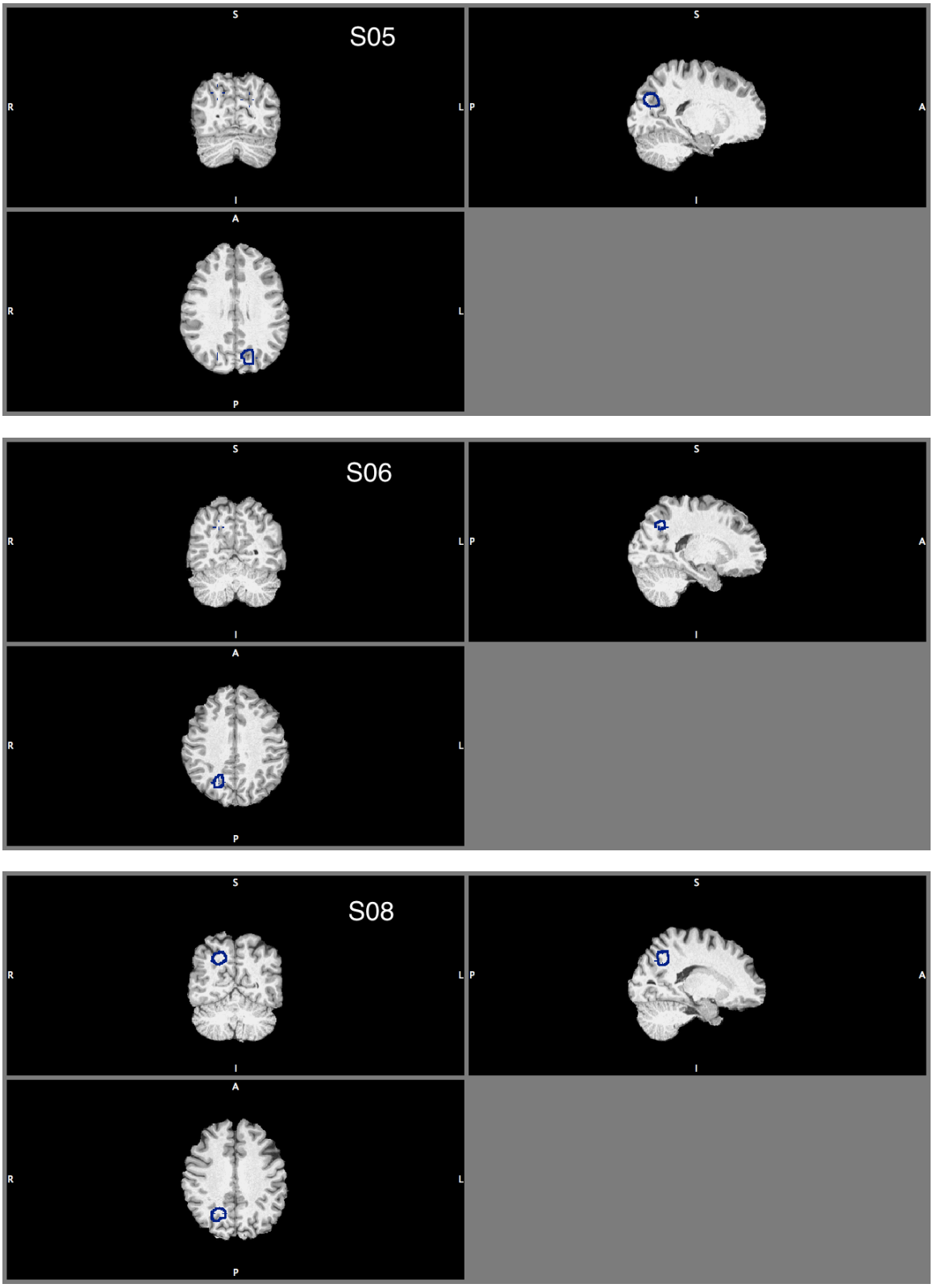

Figure 30. Precuneus activity during Scrambled Smooth > Radial Oscillating contrast.

MT+

Area MT+ showed strong preference for scrambled displays in two comparisons; Scrambled Smooth > Radial Smooth and Scrambled Oscillating > Radial Oscillating contrasts. 7 of 8 participants showed activity in both these contrasts. Excluding these two comparisons, MT+ showed no preferential activity for any of our planned contrasts. This result can be expected as it was stated earlier that MT+ is responsive to many types of coherent motion (Morrone et al., 2000). Though the scrambled conditions are segmented versions of the radial conditions, there is still local motion coherence in each of the 6 quadrants, but that motion coherence in the scrambled conditions is much lower than in the radial conditions.

3.4 - BOLD time series data for fMRI Vection Experiment

In the GLM conducted in FEAT for extracting Z-statistic data in section 3.3 it was revealed that there are significant differences between many contrasts of interest. However, a significant Z-score is insufficient in determining if there is vestibular inhibition or facilitation during vection trials. Though the sign of the contrast does indicate that one condition of the contrast has significantly increased activity relative to the other value, Z-scores do not indicate if there is inhibition or facilitation of BOLD signal occurring in a brain area. This is because a Z-score obtained from a contrast in FEAT is a relative difference between two conditions. Therefore, there are two possible outcomes that can result in a significant Z-score. First, BOLD decrease in one condition compared to the other even though both may have increase or decrease relative to baseline. Second, a significant Z-score can be observed if there is increase in BOLD signal associated with 1 condition, and a decrease in BOLD signal in another condition of a contrast relative to baseline. To determine which one of these possibilities occurs in PIVC and CSv during experimental trials, it is necessary to look at mean % BOLD signal change time series plots for each condition and observe if % BOLD increased or decreased over the course of a trial. Negative % BOLD signal change signifies decreased blood flow to a region (inhibition). Alternatively, a positive signal % change represents increased blood flow to a region (facilitation). In this section I present BOLD time series plots for each condition in functionally activated areas PIVC and CSv. Regions that were not strongly responsive to contrasts of interest such as MT, V6 and Pc had a 0 % signal change for each condition and in most contrasts, and for this reason are not included in this section.

Preprocessing of Time Series BOLD data

To analyze BOLD time series data for each cortical area, another set of masks were made. Masks were created for each individual based on coordinates of activation in the z-stat report and the number of voxels activated in all contrasts where the subject showed significant activity in the region. This allowed me to determine an exact location of the brain region of interest within the larger mask used in the previous z-score analysis. This new mask ensured that the functionally localized brain region of interest was covered in each subject.

Masks were drawn by hand in FSL View on top of a standard 1-mm MNI brain template. Lower-level, whole-brain FEAT analyses were loaded into FEAT Query, a tool that allows researchers to extract specific elements of the FEAT analysis, where each person's newly created ROI mask was re-run with their FEAT data. FEAT Query outputs BOLD signal values for each TR of a subject's lower-level run. These were converted to % BOLD signal change. % BOLD signal change data for each repeat of a condition was averaged by TR (10TR=20 sec, or the length of a trial). I then generated line graphs showing average % BOLD signal change by TR for the 4 conditions of each subject (Figures 31 and 32). % BOLD signal change was relative to the mean % signal change of the entire MRI run.

BOLD % Signal Change in PIVC

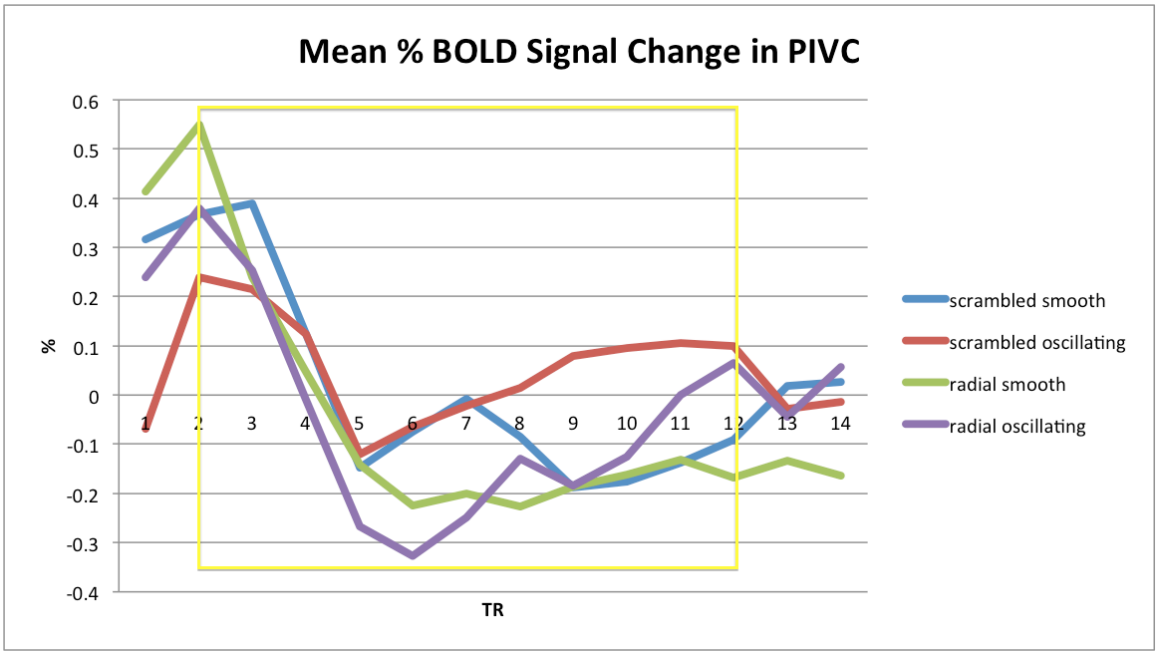

Figure 31. Mean BOLD signal % change for 5 subjects that showed significant z-scores in the *Radial Oscillating* > *Radial Smooth* contrast. % BOLD data recorded during trials within each of the 5 subjects' PIVC mask. The yellow box indicates the TRs occurring during the motion period of the video clips.

The line graph in Figure 31 shows average % BOLD signal change within each participant's PIVC mask over 10 TRs in all four conditions averaged across the five participants. Figure 31 shows an initial decrease in BOLD activity for all conditions. However, there is an increase or plateau in BOLD activity following the decrease. We can conclude that vestibular inhibition occurs in PIVC during all trials, including scrambled motion conditions. Interestingly, this inhibition is stronger (lower % signal change value) for radial smooth and radial oscillating than for scrambled smooth and scrambled oscillating conditions in Figure 31.

BOLD % Signal Change in CSv

CSv showed strong responses to vection displays in all contrasts of interest, as discussed in section 3.3. Figure 32 displays a line graph of average BOLD % signal change for each condition across participants at each TR. Similar to area PIVC, there

appears to be an initial decrease in BOLD signal. Unlike in PIVC, BOLD signal does not show a subsequent increase. This may be associated with higher sensitivity to vection in CSV than in PIVC, thus greater inhibition.

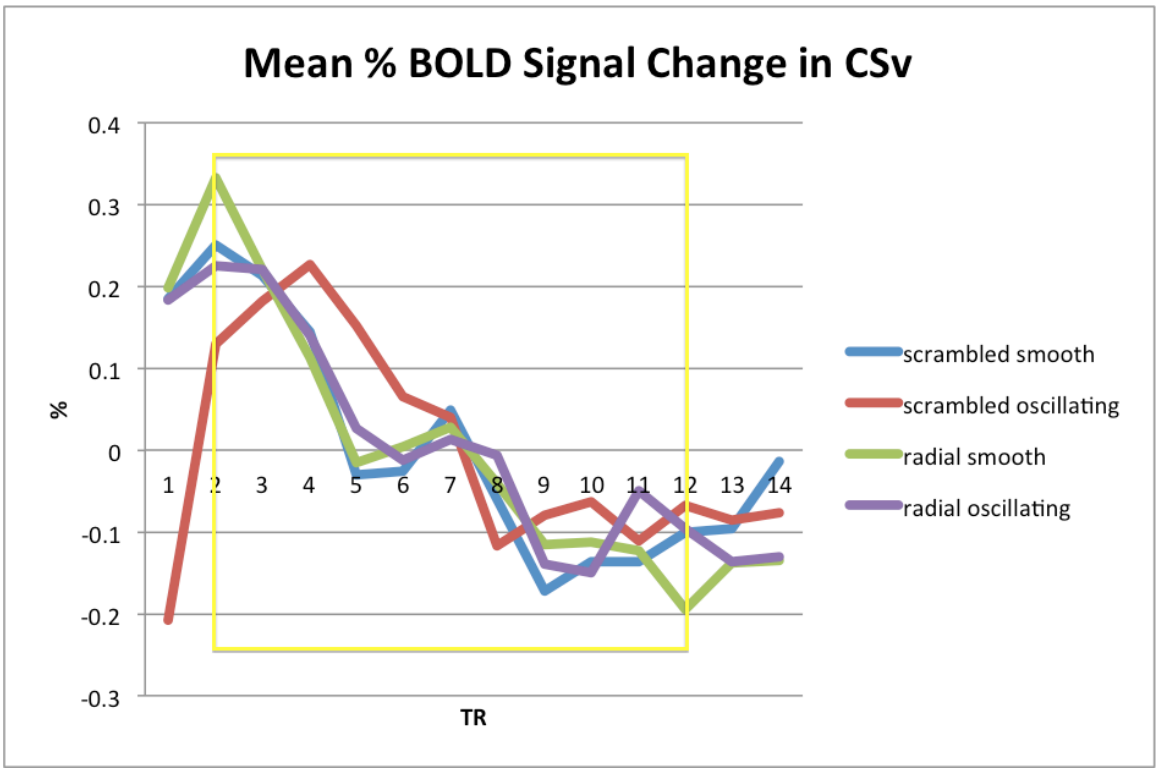

Figure 32. Mean BOLD % signal change within the CSv mask of 7 participants during trials.

We can confirm that there is a consistent decrease in % BOLD signal in these two regions during experimental trials and therefore our findings support Brandt's (1998) visual-vestibular reciprocal inhibition hypothesis. In PIVC, there was a stronger inhibition for radial smooth and radial oscillating conditions compared than in scrambled smooth and scrambled oscillating conditions (Figure 31). In CSv, % BOLD signal change decrease occurs in all conditions. This may highlight increased sensitivity of CSv to motion displays than of PIVC to motion displays.

4. Discussion

4.1 Psychophysical Measurement of Vection

Confirmation of participant experience of vection and its strength is an important measure to compare with changes in BOLD activity during vection. Magnitude estimation (Stevens, 1959) allows me to compare vection ratings across participants and different types of optic flow displays. Additionally, measures such as vection onset and duration are vital in understanding vection.

A main issue with the brain-imaging literature on self-motion is that vection is often not measured or is imprecisely measured. For instance, some mentioned studies do not measure vection, but assume the illusion is perceived, simply because participants were exposed to/attended to optic flow displays. Many experiments investigated self-motion without measuring vection (Cardin and Smith, 2010; Cardin and Smith, 2011; Cardin et al., 2012), but did not confirm it in the participants. Nishiike et al., (2002) instructed participants to raise their finger when the visual stimulus changed, not when vection was experienced, in their MEG vection experiment. Therefore, participant response was not based on perceived vection but on distinguishing between circles and squares. Also, finger motion undoubtedly activated cortical motor pathways related to motor control of the finger that may overlap with nearby cortical pathways associated with processing vection. Lastly, Nishiike and colleagues' method did not quantify vection.

On the other hand, Brandt and colleagues (1998) measured vection intensity using a scale ranging from 1 to 5. This approach gives an approximation of the extent of vection experienced, but this method poses some problems. First, the 1-5 rating scale method

assumes participants experience vection. Second, there is no modulus to which participants can compare the strength of one sensation of vection to another. This can create variability in responses because each participant will generate their own baseline to which they compare their sensation of vection. Third, because the 1-5 range is so limited, values assigned by participants may not be fully representative of their experience of vection and can pose problems for statistical analyses. Similarly, to Brandt's group, Pitzalis and colleagues (2013) measured vection sensation after each run in their fMRI experiment. However, here like the Brandt et al. (1998), there is no relative measure of vection, making the participant rating values ambiguous.

4.2 Brain Regions of Interest During Vection

Results in section 3.3 revealed that CSv responded most strongly to vection-eliciting stimuli, followed by PIVC. Some regions did not show any vection preference (MT+) and some showed preference for scrambled displays (VIP, V6). In this section I discuss my results in relation to the literature on these regions.

CSv

My results suggest that CSv plays a role in processing self-motion and vection. Evidence for CSv involvement in processing vection stems from our finding of significant CSv BOLD activity in the Radial Motion > Scrambled Motion contrast. This is similar to Wall and Smith's (2008) finding of CSv activity during coherent optic flow stimuli compared with 9 simultaneously presented miniature patches of the same display. Wall and Smith's 9-patch display was a scaled version of the full-field display whereas ours was a scrambled version of our full-field display. This finding directly signifies CSv preference for large-field stimulation compared with local motion stimuli.

Furthermore, CSv had higher activity in the Radial Oscillating > Radial Smooth contrast. This is a key finding because both are wide-field vection stimuli, but the oscillating display elicits higher vection ratings. The significant change in BOLD activity in the Radial Oscillating > Radial Smooth contrast suggests CSv preference during more compelling vection displays.

From this contrast alone it is difficult to determine if significant CSv activity results in stronger vection, or if it is due to changes in heading direction inherent in an oscillating display. What has led us to believe that CSv explicitly processes vection are

results from the Radial Oscillating > Scrambled Oscillating contrast. Because the scrambled motion preserves characteristics of the display including oscillation, and induces little to no vection, we can conclude that CSv activity is correlated with a compelling vection experience.

Recently, many authors (Fischer, et al., 2012; Billington, et al., 2013; Furlan et al., 2013) have reported strong links between CSv and VIP for processing self-motion in humans. CSv has an affinity for processing general components of vection such as wide-field optic flow, heading, or direction change and anticipated locomotion (Zhang and Bretten, 2011). According to Furlan and colleagues (2013), CSv activity increases during changes in heading direction. Reports by Smith (2014) suggest that CSv is involved in motor planning. Other reports suggest CSv is activated during vestibular processing arising from stimulation via GVS (Smith et al., 2012).

PIVC

We have functionally localized PIVC with the vection stimuli of Experiment 1 in the Radial Oscillating > Radial Smooth contrast and have shown that PIVC activity is reduced during vection (Figure 31). Based on our findings, we conclude that 1) PIVC is involved in vection processing but to a much lesser degree than reported previously. It was expected that there would be more significant BOLD activity for all comparisons with a vection > non-vection contrast than was actually found. 2) PIVC can be visually localized. This is assumed based on the significant PIVC activity in the Radial Oscillating > Radial Smooth contrast, indicating that PIVC activity demonstrates significant change in BOLD activity when correlated with a visual, self-motion inducing

stimulus. Most importantly, 3) PIVC shows a decrease in BOLD activity during vection. In section 3.4, Figure 31 shows a marked decrease in % BOLD signal change for radial conditions. This decrease in % BOLD signal change is not as strong during the scrambled, non-vection conditions which supports Brandt and colleagues (1998) visual-vestibular reciprocal inhibition hypothesis which predicts decreased blood flow to vestibular cortical regions during greater visual-vestibular conflict.

PIVC was at one time regarded as the principal cortical vestibular region for processing vection (Cardin and Smith, 2010). According to Cardin and Smith, PIVC bridges visual and vestibular cortical responses. For this reason it has been focal in the vection debate. PIVC has been functionally localized using vestibular stimuli in caloric irrigation (Suzuki et al., 2001; Fasold et al., 2002) as well as visually with egomotion compatible stimuli (Cardin and Smith, 2010). Ideally, PIVC should be localized using caloric irrigation as this is a more direct technique to stimulate vestibular cortical regions than the controversial and indirect visual methods.

Two studies have functionally localized PIVC using caloric irrigation in fMRI, and both report discrepant locations in terms of anatomical coordinate values (Suzuki et al., 2001; Fasold et al., 2002). Some studies have successfully identified insular regions corresponding to PIVC with visual stimuli similar to those of Cardin and Smith (2010; Beer et al., 2002; Kovacs et al., 2008; Indovina et al., 2014).

VIP

VIP did not show preference for vection in our contrasts and was more responsive to scrambled stimuli than to radial stimuli. This is surprising given that CSv - an area

linked to VIP activity – did show vection preference in our findings (Fischer, et al., 2012; Billington, et al., 2013; Furlan et al., 2013). However, it is important to note that these VIP-CSv ties are reported in heading estimation experiments as opposed to vection experiments specifically. It may be the case that VIP responds to stimulus features that elicit vection such as coherent flow and wide-field stimulation but not to the subjective experience of vection. Another likely possibility is that attempting to localize VIP, neighbouring regions LIP and MIP were functionally localized instead. This would be consistent with our finding of a supposed VIP preference for scrambled motion, as MIP and LIP are object-motion sensitive regions.

V6

We successfully localized area V6 in 6 of 7 participants in the localizer experiment (Experiment 2). The display involved varying spiral motion optic flow periods, creating wide-field motion - ideal for V6 activity (Pitzalis et al., 2013). This localizer was contrasted against periods of incoherent dot motion. In our vection experiment (Experiment 1), V6 showed activation only in the Radial Motion > Scrambled Motion contrast. Though this contrast has differences in physical characteristics of the displays it produces arguably the most robust vection contrasts in our experiment. There was no indication of reliable V6 preference for other radial > scrambled contrasts. Moreover, in our experiment V6 activity was quite unusual as there was more preference for scrambled conditions compared with radial motion conditions. This is unexpected because V6 reportedly responds to wide-field stimulation (Pitzalis, et al., 2013). Despite this unexpected finding, it is important to note that the majority of research on V6

involvement in vection does not explicitly measure vection with the exception of a recent Pitzalis and colleagues study (2013). It is also possible that V6 was mistaken for neighbouring V6a which is responsive to object motion and not self-motion (Pitzalis, 2013).

Pc

Pc is known for involvement in cognitive aspects of self-motion processing such as visual-spatial updating during self-motion. Pc showed activity for the Radial Oscillating > Scrambled Smooth contrast only. No other contrast supported Pc as a vection-related region. This is consistent with other findings on slight Pc involvement for vection, but not as a principal region for vection processing (Previc et al., 2000; Pitzalis et al., 2013). Therefore, it is plausible that Pc is involved in higher-level cognitive aspects of self-motion as opposed to self-motion perception (Wolbers et al., 2007; Wolbers et al., 2008).

MT+/MST+

In the localizer experiment, the MT+ complex was activated for all participants. We used Pitzalis and colleagues (2010) radial rings display to localize this area. Coherent motion patterns were contrasted against static frames. MST+ was separately localized but was only identified within four of seven participants. The literature suggests that MT+ is responsible for distinguishing between different types of motion patterns (Morrone et al., 2000). Thus it was robustly localized when coherent motion patterns were contrasted against static displays. However, our conditions in Experiment

1 were all defined by coherent motion patterns, therefore, MT activity was non-specific as it responded strongly to all types of motion patterns (radial or scrambled).

4.3 - Future Work

My thesis has highlighted the central role of CSv on vection. It is important that a robust functional localizer for CSv is developed to facilitate further studies. Smith et al., (2012) discuss a visual localizer of CSv. This localizer was very similar to our vection stimulus in that it contained a full-field large central optic flow display similar to our radial displays. This display was compared to a display with 9 identical smaller patches of the same full-field display. Conceptually this is similar to our scrambled displays as it is a local version of a large full-field display. However, our scrambled display divided the larger display whereas Smith and colleagues used scaled copies of their full-field displays. Thus, it is not clear if CSv responds to their localizer because of vection, or because of the wide-field display.

Further research should be conducted on localizing CSv using caloric irrigation as this will determine if CSv has stronger connections to cortical visual pathways, vestibular pathways or if it is a region that evenly processes or regulates both types of signals. If CSv does not respond to caloric stimulation, it can be concluded that CSv is a visually driven self-motion processing region. This finding, coupled with our reports of strong CSv involvement in vection processing would strongly suggest CSv's highly specialized role in visual self-motion processing. However, if there is a corresponding significant BOLD response in CSv to caloric stimulation, than this will suggest CSv is a polysensory region for self-motion processing as it responds to both visual stimuli such as our vection displays and vestibular stimuli. Smith et al. (2012) conducted a GVS experiment and reported corresponding coordinates for visual localization of CSv and vestibular localization of CSv. Though GVS is an imprecise and noisy vestibular stimulation

technique, this result suggests potential CSv involvement in vestibular processing and therefore its role as a polysensory region processing self-motion and vection. However, the specificity of caloric irrigation would appropriately confirm this.

To better understand anatomical location of CSv and connectivity with other visual, vestibular and motor processing regions, diffusion tensor analysis in MRI could be performed. Because we have identified general coordinates of CSv, diffusion tensor analysis can help determine this region's neural connectivity to VIP, PIVC, visual cortical regions and motor regions. Moreover, in understanding CSv location and function, new imaging techniques should be employed. BOLD imaging in MRI allows a good balance of structural and temporal resolution for functional localization. However, in improving temporal resolution for CSv response to a stimulus, EEG should be used for vection displays. This enhances temporal resolution by avoiding the inherent sluggishness of the BOLD response during fMRI.

In order to establish causal factors linking CSv to vection transcranial magnetic stimulation (TMS) can be applied to null signals to CSv when viewing and rating vection stimuli. In doing so, we can more precisely determine the role of CSv in vection. Specifically, if vection ratings decreased significantly during TMS disabling CSv activity, this would give us direct evidence of CSv involvement for perceiving vection. Moreover, TMS would give causal relations on CSv and vection as opposed to fMRI correlations. One caveat is that EEG and TMS may not be effective techniques for functionally localizing the deep centers in the cingulate sulcus, however, case studies on brain legions to the areas may give insight regarding the causal role of CSv on vection.

4.4 – Conclusion

My goals in this thesis were to first identify brain regions and their functions involved in vection processing, second to determine if there is inhibition or facilitation in these regions during vection, and third to investigate if there is a neural correlate to the behaviourally observed *jitter effect*. I identified CSv, and to a lesser extent PIVC as regions responsive to vection. Second, CSv showed a strong inhibition during all displays and PIVC was inhibited from BOLD activity only for vection conditions. PIVC inhibition occurred to a lesser extent than reported in the neuroimaging vection literature. These two findings allowed me to confidently conclude that vestibular inhibition occurs in vection sensitive regions during the illusion. Third, I was able to identify a neural correlate to the behavioral findings of a *jitter effect*. I found that the higher vection ratings during radial oscillating displays compared to radial smooth displays were accompanied by a significant z-score in the radial oscillating > radial smooth contrast in both CSv and PIVC. In all, the finding of inhibition during vection is an important result as it sheds light on our understanding of visual-vestibular integration and lends support for a visual dominance effect during sensory conflict with vestibular regions.

Bibliography

Allison, R. S., Zacher, J. E., Kirollos, R., Guterman, P. S., & Palmisano, S. (2012). Perception of smooth and perturbed vection in short-duration microgravity. Experimental Brain Research, 223(4), 479–87. doi:10.1007/s00221-012-3275-5

Antal, A., Baudewig.J., Paulus., W., and Dechent, P., (2008). The Posterior cingulate cortex and planum temporale/parietal operculum are activated by coherent visual motion. Visual Neuroscience, 25 17-26. doi: 10.10170S0952523808080024.

Balaban, C. D. (1983). A projection from nucleus reticularis tegmenti pontis of bechterew to the medial vestibular nucleus in rabbits. Exp Brain Research, 51, 304-309.

Beer, J., Blakemore, C., Previc, F.H., and Liotti, M. (2002). Areas of the human brain activated by ambient visual motion, indicating three kinds of self-motion. Exp Brain Research, 143, 78-88. doi: 10.1007/s00221-001-0947-y

Bense, S., Stephan, T., Yousry, T.A., Brandt, T., and Dieterich, M. (2001). Multisensory cortical signal increases and decreases during vestibular galvanic stimulation (fMRI). J Neurophysiology, 85, 886-899.

Billington, J., Wilkie, R. M., & Wann, J. P. (2013). Obstacle avoidance and smooth trajectory control: neural areas highlighted during improved locomotor performance. Frontiers in Behavioral Neuroscience, 7 (February), 9. doi:10.3389/fnbeh.2013.00009

Brandt, T., Bartenstein, P., Janek, A., & Dieterich, M. (1998). Reciprocal inhibitory visual-vestibular interaction. Visual motion stimulation deactivates the parieto-insular vestibular cortex. Brain : A Journal of Neurology, 121 (Pt 9, 1749–58.

Brandt, T., S.A., Brocke, J., and Roricht, S., (2001). In vivo assessment of human visual system connectivity with transcranial electrical stimulation during functional magnetic resonance imaging. Neuroimage, 14, 366-375.

Brandt, T., Deutschlander, A., Glasauer, S., Nolte, A., Bruckmann, H., Dietrich, M., and Stephan, T., (2005). Expectation of sensory stimulation modulates brain activation during visual motion stimulation. Annals New York Academy of Sciences, 1039, 325-336. doi: 10.1196/annals.1325.031

Bremmer, F., Schlack, a, Shah, N. J., Zafiris, O., Kubischik, M., Hoffmann, K., … Fink, G. R. (2001). Polymodal motion processing in posterior parietal and premotor cortex: a human fMRI study strongly implies equivalencies between humans and monkeys. Neuron, 29(1), 287–96. Retrieved from http://www.ncbi.nlm.nih.gov/pubmed/11182099

Brenner, E., Driesen, B., & Smeets, J. B. J. (2014). Precise timing when hitting falling balls. Frontiers in Human Neuroscience, 8, 342. Retrieved from http://www.pubmedcentral.nih.gov/articlerender.fcgi?artid=4033095&tool=pmcentrez&rendertype=abstract

Bottini, G., Sterzi, R., Paulesu, E., Vallar, G., Cappa., S.F., Erminio, F., and Irgenwer, H., Identification of the central vestibular projections in man: a positron emission tomography activation study. Exp Brain Res 99: 164 –169, 1994.

Bryan, A and Angelaki, D Optokinetic and Vestibular Responsiveness in the Macaque Rostral Vestibular and Fastigial Nuclei *Journal of Neurophysiology* 101(2): 714-720. 2009

Calabro, F. J., & Vaina, L. M. (2012). Interaction of cortical networks mediating object motion detection by moving observers. Experimental Brain Research, 221(2), 177–89.

Cardin, V., Hemsworth, L., & Smith, A. T. (2012). Adaptation to heading direction dissociates the roles of human MST and V6 in the processing of optic flow. Journal of Neurophysiology, 108(3), 794–801. doi:10.1152/jn.00002.2012

Cardin, V., & Smith, A. T. (2010). Sensitivity of human visual and vestibular cortical regions to egomotion-compatible visual stimulation. Cerebral Cortex (New York, N.Y. : 1991), 20(8), 1964–73. doi:10.1093/cercor/bhp268

Cardin, V., & Smith, A. T. (2011). Sensitivity of human visual cortical area V6 to stereoscopic depth gradients associated with self-motion. Journal of Neurophysiology, 106(3), 1240–9. doi:10.1152/jn.01120.2010

Cavanna, A. E., & Trimble, M. R. (2006). The precuneus: a review of its functional anatomy and behavioural correlates. Brain : A Journal of Neurology, 129(Pt 3), 564–83. doi:10.1093/brain/awl004

Ciavarro, M. (2013, May 7). The role of medial parieto occipital cortex in visuospatial attention and reach planning: electrophysiological studies in human and non-human primates. Retrieved from http://amsdottorato.unibo.it/5930/1/Ciavarro_Marco_tesi.pdf

Cohen, B. and Raphan, T. (2004). Springer handbook of auditory research: Vol. 19/ The Physiology of the Vestibuloocular Reflex (VOR) (pp.235-265)

Colby, C. L. and Duhamel, J. R., Heterogeneity of extrastriate visual areas and multiple parietal areas in the macaque monkey. Neuropsychologia 29: 487–515, 1991.

Deutschlander, A., Bense, S., Stephan, T., Schwaiger M., Brandt, T., and Dietrich, M., (2002). Sensory systems interactions during simultaneous vestibular and visual stimulation in PEt Human Brain Mapping, 16, 92-103. doi 10.1002/hbm.10030

Deutschlander, A., Bense, S., Stephan, T., Schwaiger, T., Dieterich, M, and Brandt, T., (2004). Rollvection vesrus linear vection: comparison of brain activations in PEt Human Brain Mapping, 21 (3), 143-153.

Dieterich, M, Bense, S., Stephan, T., Yousry, T.A., and Brandt, T., (2003). fMRI signal increases and decreases in cortical areas during small-field optokinetic stimulation and central fixation. Exp Brain Research, 148, 117-127.

Dieterich, M., Bucher, S.F., Seelos, K.C., Brandt, T., (1998). Horizontal or vertical optokinetic stimulation activates visual motion-sensitive ocular-motor and vestibular cortex areas with right hemispheric dominance. An fMRI study. Brain,121 (8), 1479-1495.

Duffy, C. J. (1998). MST Neurons Respond to Optic Flow and Translational Movement. J Neurophysiol, 80(4), 1816–1827. Retrieved from http://jn.physiology.org/content/80/4/1816.short

Duffy, C. J., & Wurtz, R. H. (1991). Sensitivity of MST neurons to optic flow stimuli. I. A continuum of response selectivity to large-field stimuli. Journal of Neurophysiology, 65(6), 1329–45. Retrieved from http://jn.physiology.org/content/65/6/1329.abstract

Duhamel, J., Colby, C. L., Goldberg, M. E., Rizzolatti, G., Cattaneo, L., Fabbri-destro, M., … Haggard, P. (2014). Ventral Intraparietal Area of the Macaque : Congruent Visual and Somatic Response Properties Ventral Intraparietal Area of the Macaque : Congruent Visual and Somatic Response Properties, 126–136.

Dukelow, S. P., DeSouza, J. F. X., Culham, J. C., van den Berg, A. V., Menon, R. S., & Vilis, T. (2001). Distinguishing Subregions of the Human MT+ Complex Using Visual Fields and Pursuit Eye Movements. J Neurophysiol, 86(4), 1991–2000. Retrieved from http://jn.physiology.org/content/86/4/1991.short

Eickhoff, S. B., Weiss, P. H., Amunts, K., Fink, G. R., & Zilles, K. (2006). Identifying human parieto-insular vestibular cortex using fMRI and cytoarchitectonic mapping. Human Brain Mapping, 27(7), 611–21. doi:10.1002/hbm.20205

Fasold, O., von Brevern, M., Kuhberg, M., Ploner, C. J., Villringer, A., Lempert, T., & Wenzel, R. (2002). Human Vestibular Cortex as Identified with Caloric Stimulation in Functional Magnetic Resonance Imaging. NeuroImage, 17(3), 1384–1393. doi:10.1006/nimg.2002.1241

Fischer, E., Bülthoff, H. H., Logothetis, N. K., & Bartels, A. (2012). Visual motion responses in the posterior cingulate sulcus: a comparison to V5/MT and MST. Cerebral Cortex (New York, N.Y. : 1991), 22(4), 865–76. doi:10.1093/cercor/bhr154

Furlan, M., Wann, J. P., & Smith, A. T. (2013). A Representation of Changing Heading Direction in Human Cortical Areas pVIP and CSv. Cerebral Cortex (New York, N.Y. : 1991). doi:10.1093/cercor/bht132

Galletti, C., Gamberini, M., Kutz, D. F., Fattori, P., Luppino, G., & Matelli, M. (2001). The cortical connections of area V6: an occipito-parietal network processing visual information. The European Journal of Neuroscience, 13(8), 1572–88. Retrieved from http://www.ncbi.nlm.nih.gov/pubmed/11328351

Gibson, J.J., (1966). The senses considered as perceptual systems. Houghton Mifflin, Boston, USA.

Guldin, W. O., & Grüsser, O.-J. (1998). Is there a vestibular cortex? Trends in Neurosciences, 21(6), 254–259. Retrieved from http://www.sciencedirect.com/science/article/pii/S0166223697012113

Howard, I. (1982). Human visual orientation. Retrieved from http://scholar.google.com/scholar?cluster=8398096640091320600&hl=en&oi=scholarr#0

Huk, A. C., & Heeger, D. J. (2002). Pattern-motion responses in human visual cortex. Nature Neuroscience, 5(1), 72–5. Retrieved from http://dx.doi.org/10.1038/nn774

Indovina, I., Maffei, V., Pauwels, K., Macaluso, E., Orban, G.A., and Lacquaniti, F., (2013). Simulated self-motion in a visual gravity field: Sensitivity to vertical and horizontal heading in the human brain. NeuroImage, 71, 114-124.

Kovacs, G., Raabe, M., Greenlee, M.W., (2008). Neural correlates of visually induced self-motion illusion in depth. Cerebral Cortex, 18, 1779-1787.

Lishman, J. R., & Lee, D. N. (1973). The autonomy of visual kinaesthesis. Perception, 2(3), 287–94. Retrieved from http://www.ncbi.nlm.nih.gov/pubmed/4546578

Mach, E. (1875). Grundlinien der Lehre von den Bewegungsempfindungen (p. 127). Engelmann. Retrieved from http://books.google.com/books?hl=en&lr=&id=VTMXAAAAYAAJ&pgis=1

Morrone, M. C., Tosetti, M., Montanaro, D., Fiorentini, A., Cioni, G., & Burr, D. C. (2000). A cortical area that responds specifically to optic flow, revealed by fMRI. Nature Neuroscience, 3(12), 1322–8. Retrieved from http://dx.doi.org/10.1038/81860

Nakamura, S. (2010). Additional oscillation can facilitate visually induced self-motion perception: the effects of its coherence and amplitude gradient. Perception, 39(3), 320–9. Retrieved from http://www.ncbi.nlm.nih.gov/pubmed/20465169

Nakamura, S. (2013). Separate presentation of additional accelerating motion does not enhance visually induced self-motion perception. Multisensory Research, 26(3), 277–85. Retrieved from http://www.ncbi.nlm.nih.gov/pubmed/23964479

Nishiike, S., Nakagawa, S., Nakagawa, A., Uno, A., Tonoike, M., Takeda, N., & Kubo, T. (2002). Magnetic cortical responses evoked by visual linear forward acceleration. Neuroreport, 13(14), 1805–8. Retrieved from http://www.ncbi.nlm.nih.gov/pubmed/12395128

Oman, C.H., (1982). A heuristic mathematical model for the dynamics of sensory conflict and motion sickness hearing in classical musicians. Acta Oto-laryngologica 94 (392), 4-44.

Palmisano, S., Allison, R. S., & Pekin, F. (2008). Accelerating self-motion displays produce more compelling vection in depth. Perception, 37(1), 22–33. Retrieved from http://www.ncbi.nlm.nih.gov/pubmed/18399245

Palmisano, S., & Chan, A. Y. C. (2004). Jitter and size effects on vection are immune to experimental instructions and demands. Perception, 33(8), 987–1000. Retrieved from http://www.ncbi.nlm.nih.gov/pubmed/15521696

Palmisano, S., Gillam, B. J., & Blackburn, S. G. (2000). Global-perspective jitter improves vection in central vision. Perception, 29(1), 57–67. Retrieved from http://www.ncbi.nlm.nih.gov/pubmed/10820591

Palmisano, S., Kim, J., (2009). Effects of gaze on vection from jittering, oscillating, and purely radial optic flow. Attention, Perception and Psychophysics, 71 (8), 1842-1853.

Pitzalis, S., Fattori, P., & Galletti, C. (2012). The functional role of the medial motion area V6. Frontiers in Behavioral Neuroscience, 6, 91. Retrieved from http://www.pubmedcentral.nih.gov/articlerender.fcgi?artid=3546310&tool=pmcentrez&rendertype=abstract

Pitzalis, S., Galletti, C., Huang, R.-S., Patria, F., Committeri, G., Galati, G., … Sereno, M. I. (2006). Wide-field retinotopy defines human cortical visual area v6. The Journal of Neuroscience : The Official Journal of the Society for Neuroscience, 26(30), 7962–73. doi:10.1523/JNEUROSCI.0178-06.2006

Pitzalis, S., Sdoia, S., Bultrini, A., Committeri, G., Di Russo, F., Fattori, P., … Galati, G. (2013). Selectivity to translational egomotion in human brain motion areas. PloS One, 8(4), e60241. Retrieved from http://dx.plos.org/10.1371/journal.pone.0060241

Pitzalis, S., Sereno, M. I., Committeri, G., Fattori, P., Galati, G., Patria, F., & Galletti, C. (2010). Human v6: the medial motion area. Cerebral Cortex (New York, N.Y. : 1991), 20(2), 411–24. Retrieved from http://cercor.oxfordjournals.org/content/20/2/411.short

Previc, F.H., Liotti, M., Blakemore, C., Beer, J., and Fox, P., (2000). Functional imaging of brain areas involved in the processing of coherent and incoherent wide field-of-view visual motion. Exp Brain Reseach, 131, 393-405.

Previc, F. H., & Ercoline, W. R. (Eds.). (2004). Spatial disorientation in aviation (Vol. 203). Aiaa.Reason, J. T. (1978). Motion sickness adaptation: a neural mismatch model. Journal of the Royal Society of Medicine, 71(11), 819–29. Retrieved from http://www.pubmedcentral.nih.gov/articlerender.fcgi?artid=1436193&tool=pmcentrez&rendertype=abstract

Reason, J, T. (1978). Motion Sickness Adaptation. Journal of the Royal Society of Medicine, vol 71, 819-829.

Regan, D. (1997). Visual factors in hitting and catching. Journal of Sports Sciences, 15(6), 533–58. Retrieved from http://dx.doi.org/10.1080/026404197366985

Riccio, G. E., & Stoffregen, T. A. (1991). An ecological Theory of Motion Sickness and Postural Instability. Ecological Psychology, 3(3), 195–240. Retrieved from http://dx.doi.org/10.1207/s15326969eco0303_2

Robinson, D.A. (1977). Vestibular and optokinetic symbiosis: an example of explaining by modeling. In Baker, R. & Berthoz, A. (Eds), Control of gaze by brain stem neurons (pp. 49–58). Amsterdam, New York: Elsevier North-Holland.

Rodman, H. R., & Albright, T. D. (1989). Single-unit analysis of pattern-motion selective properties in the middle temporal visual area (MT). Experimental Brain Research, 75(1). Retrieved from http://link.springer.com/10.1007/BF00248530

Schaafsma, S. J., & Duysens, J. (1996). Neurons in the ventral intraparietal area of awake macaque monkey closely resemble neurons in the dorsal part of the medial superior temporal area in their responses to optic flow patterns. Journal of Neurophysiology, 76(6), 4056–68. Retrieved from http://www.ncbi.nlm.nih.gov/pubmed/8985900

Schneider, K. a, Richter, M. C., & Kastner, S. (2004). Retinotopic organization and functional subdivisions of the human lateral geniculate nucleus: a high-resolution functional magnetic resonance imaging study. The Journal of Neuroscience : The Official Journal of the Society for Neuroscience, 24(41), 8975–85. doi:10.1523/JNEUROSCI.2413-04.2004

Smith, A.T., (2014). The functions and connections of the Cingulate Sulcus Visual Area (CSv). The 10th annual asia-pacific conference on vision. July 19-22, 2014, Takamatsu, Kagawa, Japan.

Smith, A. T., & Wall, M. B. (2008). Sensitivity of human visual cortical areas to the stereoscopic depth of a moving stimulus. Journal of Vision, 8(10), 1.1–12. Retrieved from http://www.journalofvision.org/content/8/10/1.short

Smith, A. T., Wall, M. B., & Thilo, K. V. (2012). Vestibular inputs to human motion-sensitive visual cortex. Cerebral Cortex (New York, N.Y. : 1991), 22(5), 1068–77. doi:10.1093/cercor/bhr179

Stevens, S. S. (1959). Cross-modality validation of subjective scales for loudness, vibration, and electric shock. Journal of Experimental Psychology, 57(4), 201.

Suzuki, M., Kitano, H., Ito, R., Kitanishi, T., Yazawa, Y., Ogawa, T., ... & Kitajima, K. (2001). Cortical and subcortical vestibular response to caloric stimulation detected by functional magnetic resonance imaging. Cognitive Brain Research, 12(3), 441-449.

Teller, D. Y., & Movshon, J. A. (1986). Visual development. Vision Research, 26(9), 1483–1506. Retrieved from http://www.sciencedirect.com/science/article/pii/0042698986901690

Tootell, R. B., Reppas, J. B., Kwong, K. K., Malach, R., Born, R. T., Brady, T. J., … Belliveau, J. W. (1995). Functional analysis of human MT and related visual cortical areas using magnetic resonance imaging. The Journal of Neuroscience : The Official Journal of the Society for Neuroscience, 15(4), 3215–30. Retrieved from http://www.ncbi.nlm.nih.gov/pubmed/7722658

von Helmholtz, H. (1867/1925). Physiological Optics, Vol. 3, 3rd edn. The Optical Society of America, Menasha, WI.

Von Pföstl, V., Stenbacka, L., Vanni, S., Parkkonen, L., Galletti, C., & Fattori, P. (2009). Motion sensitivity of human V6: a magnetoencephalography study. NeuroImage, 45(4), 1253–63. doi:10.1016/j.neuroimage.2008.12.058

Waespe W, and Henn V. Neuronal activity in the vestibular nuclei of the alert monkey during vestibular and optokinetic stimulation. *Exp Brain Res* 27: 523-538, 1977

Wall, M. B., & Smith, A. T. (2008). The representation of egomotion in the human brain. Current Biology : CB, 18(3), 191–4. Retrieved from http://www.ncbi.nlm.nih.gov/pubmed/18221876

Watson, J. D., Myers, R., Frackowiak, R. S., Hajnal, J. V, Woods, R. P., Mazziotta, J. C., Zeki, S. (1993). Area V5 of the human brain: evidence from a combined study using positron emission tomography and magnetic resonance imaging. Cerebral Cortex, 3(2), 79–94. Retrieved from http://www.ncbi.nlm.nih.gov/pubmed/8490322

Worsley, K. J., Evans, A. C., Marrett, S., & Neelin, P. (1992). A three-dimensional statistical analysis for CBF activation studies in human brain. Journal of Cerebral Blood Flow and Metabolism, 12, 900-900.

Winkler, A. M., Ridgway, G. R., Webster, M. A., Smith, S. M., & Nichols, T. E. (2014). Permutation inference for the general linear model. NeuroImage, 92, 381–97. Retrieved from http://www.sciencedirect.com/science/article/pii/S1053811914000913

Wolbers, T., Hegarty, M., Büchel, C., & Loomis, J. M. (2008). Spatial updating: how the brain keeps track of changing object locations during observer motion. Nature Neuroscience, 11(10), 1223–30. doi:10.1038/nn.2189

Wolbers, T., Wiener, J. M., Mallot, H. A, & Büchel, C. (2007). Differential recruitment of the hippocampus, medial prefrontal cortex, and the human motion complex during path integration in humans. The Journal of Neuroscience : The Official Journal of the Society for Neuroscience, 27(35), 9408–16. doi:10.1523/JNEUROSCI.2146-07.2007

Worseley, K.J., Evans, A.C., Marrett, S. & Neelin, P. (1992). A three-dimensional statistical analysis for CBF activation studies in human brain. Journal of Cerebral Blood Flow and Metabolism, 12 (6), 900-918.

Wutte, M. G., Smith, M. T., Flanagin, V. L., & Wolbers, T. (2011). Physiological Signal Variability in hMT+ Reflects Performance on a Direction Discrimination Task. Frontiers in Psychology, 2, 185. Retrieved from http://www.pubmedcentral.nih.gov/articlerender.fcgi?artid=3151615&tool=pmcentrez&rendertype=abstract

Zacharias, G. L. and Young, R.L., (1981). Influence of combined visual and vestibular cues on human perception and control of horizontal rotation. Experimental Brain Research 9, 159–171.

Zeki, S., Kennard, C., Watson, J. D. G., Lueck, C. J., & Frackowiak, R. S. J. (1991). Cortex of Functional Specialization in Human Visual, 17(March).